Department of Physics and Astronomy
University of Heidelberg

Leptonic CP violation in the minimal type-I seesaw model

Bottom-up phenomenology & top-down model building

Master Thesis in Physics
submitted by

Thomas Rink
born in Marburg (Germany)

2017

Acknowledgements

I would like to thank my supervisor Prof Dr Manfred Lindner for the possibility to contribute to his research group, as well as my co-supervisor and collaborator, Dr Kai Schmitz, for his support and the opportunity to work with him. Further, I am grateful for the proof-reading of Moritz Platscher and Tobias Schierhuber with respect to physical, as well as Karsten Mosny and Katharina Eidam regarding linguistic aspects. Most important, I thank my parents, Silke and Helmut Rink, for their support over the entire time of my studies.

Abstract

This work deals with a minimal realization of the type-I seesaw model with only two right-handed Majorana neutrinos, which is investigated from two perspectives; bottom-up and top-down. In a data-driven approach, the manifestation of certain hierarchies in the neutrino Yukawa matrix is analyzed in the context of realizable approximate two-zero textures. A general method for the investigation of Yukawa structures is developed and applied to the minimal seesaw model. Besides a robustness study of the obtained results, theoretical error bars are assigned to this model's predictions. In a top-down ansatz, a high-energy embedding of the minimal seesaw model is built that exhibits minimal degrees of freedom. A minimal $SU(5)$ Froggatt-Nielsen flavor model is chosen and assuming approximate exchange symmetries in the heavy neutrino sector helps to reduce the model's free parameter. Demanding consistency with electroweak naturalness and leptogenesis leads to a most minimal type-I seesaw model, that emerges from a high-energy theory and predicts at the same time all measured neutrino observables.

Zusammenfassung

Die vorliegende Arbeit beschäftigt sich mit einer minimalen Variante des Typ-I-Seesaw-Mechanismus mit nur zwei rechtshändigen Majorana-Neutrinos, welche im Folgenden aus zwei Perspektiven, bottom-up and top-down, untersucht wird. In einem experimentell motivierten Ansatz wird zunächst die Ausprägung bestimmter Hierarchien innerhalb der Neutrino-Yukawa-Matrix im Hinblick auf approximative Zwei-Nulltexturen analysiert. Dazu wurde eine allgemeine Methode zur Untersuchung von Yukawastrukturen entwickelt und am Beispiel des minimalen Seesaw-Modells getestet. Neben einer Stabilitätsanalyse der gewonnenen Ergebnisse konnten den Modellvorhersagen theoretische Fehlerbalken zugewiesen werden. In einem top-down Ansatz wurde eine Einbettung des minimalen Seesaw-Modells in eine Hochenergie-Theorie konstruiert, welche eine minimale Anzahl von Freiheitsgeraden besitzt. Durch Modifikation eines $SU(5)$-Froggatt-Nielsen-Flavor-Modells und der Annahme approximativer Austauschsymmetrien des schweren Neutrinosektors konnte eine starke Reduktion der freien Modellparameter erreicht werden. Zusätzliche Forderungen nach moderaten Higgsmassenkorrekturen und erfolgreicher Leptogenese führen zur minimalsten Realisierung des Type-I-Seesaw-Modells, welche auf einer Hochenergie-Theorie gründet und zugleich mit allen gemessenen Neutrino-Observablen übereinstimmt.

This master thesis has been carried out at the
Max Planck Institute for Nuclear Physics Heidelberg
under the supervision of
Prof Dr Manfred Lindner and Dr Kai Schmitz.

Contents

List of Figures

List of Tables

Acronyms

$0\nu\beta\beta$	neutrinoless double β decay
BAU	baryon asymmetry of the Universe
BSM	physics beyond the standard model
CIP	Casas-Ibarra parametrization
CKM	Cabibbo-Kobayashi-Maskawa
$\not{CP}$	CP violation
DOF	degree of freedom
EWPT	electroweak phase transition
FN	Froggatt-Nielsen
GUT	grand unified theory
IH	inverted hierarchy
LCC	Lorentz-covariant conjugate
LH	left-handed
LNV	lepton number violation
LO	leading-order
NH	normal hierarchy
PMNS	Pontecorvo-Maki-Nakagawa-Sakata
RGE	renormalization group equation
RH	right-handed
SSB	spontaneous symmetry breaking
SM	standard model of particle physics
UV	ultraviolet
VEV	vacuum expectation value

1. Introduction

Almost ninety years after their first postulation through Wolfgang Pauli in 1930 [1], neutrinos are more topical than ever, as discoveries related to them led to four nobel prices within the last thirty years [2]. Moreover, the nobel price in 2015 [3] for the detection of neutrino oscillations [4–6] and the associated proof of their massiveness clearly confirmed that they provide new phenomena that are not incorporated in the current standard model of particle physics (SM).

Instead of joy about having some direction towards "new" physics beyond the standard model (BSM), particle physics is immediately confronted with further questions. There is no conceptual reason why neutrinos are so much lighter than all other SM particles[1] and, furthermore, it is still unclear if they are massive Dirac or Majorana fermions. We still do not know enough about neutrino properties, although they are with a number density of $n = 336\,\mathrm{cm}^{-3}$ nine orders of magnitude more abundant than usual atoms in our Universe [9]. For example, oscillation experiments measured very precisely their mass-squared differences and mixing angles [8], yet it is unknown which kind of mass-ordering neutrinos exhibit [10] as the sign of the atmospheric mass-squared difference remains undetected. A lot of effort is spend on experiments that try to measure still unknown quantities of this very elusive particle species, e.g. experiments like GERDA [11] search for signatures from neutrinoless double β decay ($0\nu\beta\beta$), which could reveal the neutrino to be of Majorana type. Further, β decay experiments like KATRIN [12] aim to measure the neutrino's absolute mass and current oscillation experiments, e.g. Noνa [13] and T2K [14], reach growing sensitivity, indicating a future detection of leptonic CP violation ($\not{CP}$). One has to keep in mind, that a lot of work has already been accomplished since their first detection in 1956 [15]. For instance, sun-monitoring through solar neutrinos [16, 17] has become standard as well as neutrino beam technology [18].

Also on theoretical side, neutrino physics provides huge opportunities as it connects the largest scales of cosmology with the smallest ones associated with particle physics. Over the decades, various models have been invented to explain the neutrinos' mass as they are currently just implemented as massless left-handed (LH) Weyl fermions in the SM. As already the simplest extension, i.e. the introduction of right-handed (RH) neutrinos ν_R and application of the Higgs mechanism, suffers from unnaturally small Yukawa coupling, different approaches have emerged to tackle the problem of neutrino mass generation. All such attempts can be mainly grouped into two classes, tree-level [19–30] and loop-level genera-

[1] Although the absolute neutrino mass scale is still unknown, we already know from current limits, e.g. [7], and their measured mass-squared differences [8] that they are orders of magnitude lighter than all other SM particles.

tion [31–36]. Where the first class tries to explain the lightness of SM neutrinos by the massiveness of some other new particle, the second group of models assumes massless neutrinos, whose masses are generated through radiative corrections to their propagators at higher order in perturbation theory. Both classes can be easily embedded in broader theoretical frameworks like grand unified theories (GUTs) or left-right-symmetric models, such that literature provides a great number of neutrino mass models; see [37]. Not only their mass makes theory interesting, but also other processes can be explained by neutrinos. The baryon asymmetry of the Universe (BAU), i.e. the imbalance of matter and antimatter in the early Universe, which explains the existence of matter today, can be understood through CP violating decays of some heavy neutrinos, usually known as leptogenesis [38], and has become a field of vast studies, see review [39]. Further, the role of heavy neutrinos shortly after the big bang has also been discussed, e.g. to explain the origin of inflation [40].

The problem, theoretical neutrino physics has to tackle, is the lack of predictions. Although there exist many successful neutrino mass models, most of them rely on some high-energy origin, which is not accessible through low-energy neutrino experiments. Hence, there is no possibility to distinguish them and moreover, due to embedding in some broader context, they are usually accompanied by various degrees of freedom (DOFs), making predictions even harder. In the next years, another low-energy neutrino observable, the Dirac CP phase δ, is expected to be measured by experiments and theory is at draw to invent strategies or benchmarks that help constraining the vast number of models. Common approaches to obtain small parameter spaces are, e.g. the assumption and introduction of additional symmetries or minimal number of necessary DOFs. Thereby, one hopes to arrive at some minimal model that may be in agreement with current experimental data, such that typical benchmark scenarios for future measurements are obtained.

This thesis deals with one particular example of such minimal models, i.e. the minimal type-I seesaw model with only two RH neutrinos [41–46]. By assuming further symmetries, leading to certain zeros within the model's neutrino Yukawa matrix, one is able to reduce its parameter space in a way that clear predictions are obtained, e.g. for CP phases. In the following, this minimal realization of the type-I seesaw scenario is approached from two different directions; bottom-up and top-down. Motivated by future experimental measurements, we investigate what can be inferred for the UV region if a certain CP phase is measured. Especially, the model's capability to agree with experiment is studied in cases, where the general assumptions of zero-entries in the underlying Yukawa matrix are slightly relaxed, allowing us to assign theoretical error bars to previous predictions.

In a second investigation, we embed the type-I seesaw with only two RH neutrinos in a special ultraviolet (UV) model [47], i.e. a Froggatt-Nielsen (FN) mechanism [48] implemented in a minimal $SU(5)$ GUT [49], and search for corresponding minimal realizations, that can still accommodate for all measured observables. A minimal benchmark scenario, testable with upcoming data sets, is formulated by assuming (approximate) exchange symmetries within the heavy neutrino sector and consistency with theoretical demands like electroweak naturalness and suc-

cessful leptogenesis. Both approaches are mainly based on the references [50] and [51].[2] This thesis is structured in the following way:
Chapter 2 introduces the subject of massive neutrinos. Besides phenomenological consequences like neutrino oscillations, the generic type-I seesaw mechanism is presented with a special parametrization of its parameter space. Chapter 3 deals with a minimal realization and a newly developed method to gain more knowledge from future progress in oscillation measurements. Taking this particular model, we show how structures within the neutrino Yukawa matrix can be assessed by application of a self-defined hierarchy parameter. In chapter 4, we construct a minimal UV realization of the presented model that agrees with all currently measured neutrino observables. By embedding into a minimal $SU(5)$ FN model and assuming certain discrete symmetries in the heavy neutrino sector, we are able to successively reduce our model's parameter space. Finally, we conclude our investigations with the summary of main results in chapter 5.

[2] While the first reference is already accepted for publication in JHEP, the second one is currently under peer-review.

2. Theory and phenomenology of massive neutrinos

The detection of neutrino oscillations and the associated explanation through their mass[1] is one of the strongest indicators that there exists some physics beyond the current standard model. Hence, the origin of neutrino masses and related phenomenology is one of the biggest questions in particle physics. The current chapter deals with the simplest mechanism of neutrino mass generation, the type-I seesaw mechanism [19–22], and gives an overview of phenomenological consequences as well as current scientific knowledge. Further, variations of the seesaw framework as well as other neutrino mass mechanisms are discussed and additionally the high-energy scenario of leptogenesis [38, 39, 52] is covered, which is going to be important for later purposes. Before diving into the seesaw framework, the properties of Majorana fermions [53] are derived from the Dirac perspective.

2.1. Dirac and Majorana fields

The type-I seesaw mechanism requires the existence of RH Majorana neutrinos to explain the origin of small neutrino masses in a very natural way. In the following, this special type of fermion field is constructed from scratch and differences between Dirac and Majorana mass terms are pointed out.[2] Before doing so, the basic concepts of Dirac fields are repeated.

2.1.1. Dirac fields

Dirac fields are one important ingredient in the theoretical understanding of Nature, since they describe the relativistic motion of spin-$\frac{1}{2}$ particles, which make up almost all matter fields in our visible Universe.[3] Although one can directly derive the spin-$\frac{1}{2}$ representation of the Poincaré group from basic principles, we refer to the standard literature [54, 56, 57] and take it for granted that we need so-called spinors to construct solutions of the Dirac equation. With "spinor", we generally mean elements of the vector space, on which the spin-$\frac{1}{2}$ representation acts and from which solutions of the Dirac equation can be constructed. We start

[1] The detection of oscillations alone does not proof the neutrino's massiveness, as also other processes could invoke flavor changes. Their mass is a sufficient but not necessary condition.

[2] A more formal introduction into this subject can be found in chapter 10 and 11 of [54] or, with special focus on Majorana fields, in [55].

[3] As we will cover in the following, the neutrino occupies a special role within the SM, since it could also be a Majorana fermion.

by assuming that the Dirac Lagrangian, from which the Dirac equation can be deduced via variation principle, has already been found,

$$\mathcal{L}_{Dirac} = \bar{\psi}_D \left(i\partial\!\!\!/ - m_D \right) \psi_D \,, \tag{2.1}$$

with the conventional Feynman slash notation $\partial\!\!\!/ \equiv \gamma^\mu \partial_\mu$ and the Dirac-conjugated field $\bar{\psi} \equiv \psi^\dagger \gamma^0$. We encounter a set of four (4×4) matrices γ^μ, that span the so-called spinor space. The γ-matrices obey special properties, among others the anti-commutator relation $\{\gamma^\mu, \gamma^\nu\} = 2g^{\mu\nu}$, which is usually known as Clifford algebra. Any set of matrices, that fulfills this property, can be used as basis for the spinor space and is related to all other possible realizations by a unitary transformation, $\gamma^\mu = U\tilde{\gamma}^\mu U^\dagger$. For the Dirac field, a special representation of the Clifford algebra, the *Dirac* representation, is chosen, which has the following structure,

$$\gamma^0 = \begin{pmatrix} \mathbb{1}_2 & 0 \\ 0 & -\mathbb{1}_2 \end{pmatrix} , \qquad \gamma^i = \begin{pmatrix} 0 & \sigma^i \\ -\sigma^i & 0 \end{pmatrix} , \tag{2.2}$$

with the Pauli-matrices σ^i and $i = 1, 2, 3$ that are given in the appendix A. Having a closer look on the chosen basis, one recognizes that these are block-diagonal and therefore reducible.

The vector space of four-dimensional Dirac spinors can be divided into two separate spaces of left- and right-handed chiral components, ψ_L and ψ_R; or stated differently, the Dirac spinor forms a "doublet" of two-dimensional left- and right-handed Weyl spinors $\Psi_{L/R}$, which can be projected out with the corresponding projection operators $\mathcal{P}_{L/R} = \frac{1}{2}(1 \mp \gamma^5)$[4]. This property is reflected in the following representation:

$$\psi = \psi_L + \psi_R = \begin{pmatrix} \Psi_L \\ \Psi_R \end{pmatrix} , \quad \psi_L \equiv \mathcal{P}_L \psi = \begin{pmatrix} \Psi_L \\ 0 \end{pmatrix} , \quad \psi_R = \mathcal{P}_R \psi = \begin{pmatrix} 0 \\ \Psi_R \end{pmatrix} , \tag{2.3}$$

with the four-component and two-component Weyl fields, $\psi_{L/R}$ and $\Psi_{L/R}$ respectively. Since we will not work in two-component notation, we will use the term Weyl field for $\psi_{L/R}$ and $\Psi_{L/R}$ synonymously. Hence, the Dirac field as general solution of the Dirac equation is composed of two independent Weyl fermions; the LH component ψ_L and the RH one ψ_R. In this sense, Weyl fields can be considered as fundamental building blocks of more complex fermionic fields.

Since the SM is by construction a chiral theory, it is formulated in terms of left- and right-handed chiral fermion fields. Combining (2.1) with (2.3) leads to the chiral Dirac Lagrangian,

$$\mathcal{L}_{Dirac} = \bar{\psi}_L i\partial\!\!\!/ \psi_L + \bar{\psi}_R i\partial\!\!\!/ \psi_R - m_D \left(\bar{\psi}_R \psi_L + \text{h.c.} \right) . \tag{2.4}$$

Further, the Dirac mass term is invariant under global and local $U(1)$ transformations and hence conserves all charges associated with it, e.g. electric charge, lepton- and baryon number. A special thing to notice is that the mass term mixes

[4] Left- and right-handed chiral states are related to the two different eigenvalues of $\gamma^5 \equiv i\gamma^0\gamma^1\gamma^2\gamma^3$. See appendix A for properties of projectors $\mathcal{P}_{L/R}$ and γ^5.

the two different chiral states. Viewed from an interacting perspective, such terms implicate a chirality flip, whereas the kinetic terms are blind to chirality. However, within the SM framework, direct mass terms like the ones above, are forbidden by the $SU(2)_L \times U(1)_Y$ gauge group as they are not invariant under the corresponding transformation and would spoil gauge invariance. At this point, the the Higgs mechanism becomes important as it breaks $SU(2)_L \times U(1)_Y$ down to $U(1)_Q$, while generating fermion mass terms at the same time through Yukawa interactions with each SM fermion. The resulting fermionic mass terms are proportional to the Higgs VEV $v_{EW} \equiv \langle \phi^0 \rangle$ and the corresponding Yukawa coupling y_f, $m_f = v_{EW} y_f$. As a beautiful side-effect also the vector bosons, $W^{\pm}_{\mu}$ and Z_{μ}, obtain their masses while the photon A_{μ} remains massless[5].

2.1.2. Majorana fields

In the following, we try to shed some light on Majorana fermions and approach them from the familiar Dirac perspective.

The Dirac field has been constructed as a general solution of the Dirac equation and is assumed to be complex. Since any set of γ-matrices can be used to span the spinor space, one can also look for simpler solutions, i.e. real fields [58]. These can be obtained by choosing a set of completely imaginary matrices, which is referred to their inventor as *Majorana* representation [53],

$$\begin{aligned} \gamma^0 &= \begin{pmatrix} 0 & \sigma^2 \\ \sigma^2 & 0 \end{pmatrix}, & \gamma^1 &= \begin{pmatrix} i\sigma^3 & 0 \\ 0 & i\sigma^3 \end{pmatrix}, \\ \gamma^2 &= \begin{pmatrix} 0 & -\sigma^2 \\ \sigma^2 & 0 \end{pmatrix}, & \gamma^3 &= \begin{pmatrix} -i\sigma^1 & 0 \\ 0 & -i\sigma^1 \end{pmatrix}. \end{aligned} \tag{2.5}$$

The solutions of the Dirac equation are now real and fulfill the so-called Majorana condition,

$$\psi_M \stackrel{!}{=} \psi_M^C \,, \tag{2.6}$$

with the Lorentz-covariant conjugate (LCC), $\psi^C \equiv \gamma_0 C \psi^*$. The charge-conjugation operator in the familiar Dirac basis, $C \equiv i\gamma_2\gamma_0$, obeys the following properties:

$$C^\dagger = C^{-1} = C^T = -C \,. \tag{2.7}$$

As the Majorana condition (2.6) imposes further constraints on the spinor space, the corresponding Majorana fermion is equivalent to only one Weyl field of definite chirality. This seems unusual, as we are used to the notion of Dirac particles. One always has to keep in mind that Dirac particles are constructed with two independent Weyl spinors and as we need RH and LH components for a mass term, the generic choice is to identify them with both spinors, ψ_L and ψ_R. The

[5] For more details about the Higgs mechanism, see the literature, e.g. [54, 56, 57]. Since the Higgs mechanism is just of minor importance in this work, we will not go into mathematical details. Only the phenomenological consequences are commented on when necessary.

situation is different for Majorana fermions, where we only have one Weyl spinor. Since we need both chirality components to construct a mass term, we can use the knowledge that a Lorentz-covariant conjugated LH Weyl spinor transforms as a RH component and vice versa. There exist some ambiguity in this construction as both chirality Weyl-component prove equally well; thus, we list both possibilities,

1. LH Weyl spinor - $\psi_R = (\psi_L)^C$:

$$\psi_M = \psi_L + \eta\,(\psi_L)^C = \begin{pmatrix} \Psi_L \\ i\sigma_2 \Psi_L^* \end{pmatrix} \tag{2.8}$$

2. RH Weyl spinor - $\psi_L = (\psi_R)^C$:

$$\psi_M = \psi_R + \eta\,(\psi_R)^C = \begin{pmatrix} i\sigma_2 \Psi_R^* \\ \Psi_R \end{pmatrix}. \tag{2.9}$$

An additional factor η is introduced to accommodate for a potentially occurring phase through charge conjugation; the Majorana particle's CP-properties can be adjusted by selecting $\eta = \pm 1$ for even and odd CP-parity respectively. One can easily proof that both cases fulfill (2.6) by using the following spinor properties under charge conjugation. For our concerns, the action of C on chiral components is important,[6]

$$(\psi_L)^C = \left(\psi^C\right)_R, \quad (\psi_R)^C = \left(\psi^C\right)_L, \quad \overline{\psi^C} = \psi^T C = -\psi^T C^{-1}. \tag{2.10}$$

The corresponding Majorana Lagrangian has similar structure as the Dirac one (2.1), but with an additional factor of $\frac{1}{2}$ due to the reduced number of DOFs,

$$\mathcal{L}_{Majorana} = \frac{1}{2}\bar{\psi}_M \left(i\partial\!\!\!/ - m_M\right)\psi_M\,. \tag{2.11}$$

Since we are interested in chiral fields, the Majorana mass term is expanded in terms of the above field definition; again, it is arbitrary which chirality is chosen for the underlying Weyl fermion. Conventionally, left-handed fields are used, yielding

$$\begin{aligned} \mathcal{L}_{Majorana} &= \bar{\psi}_L i\partial\!\!\!/ \psi_L - \frac{m_M}{2}\left(\bar{\psi}_L^C \psi_L + \text{h.c.}\right) \\ &= \bar{\psi}_L i\partial\!\!\!/ \psi_L + \frac{m_M}{2}\left(\psi_L^T C^{-1} \psi_L + \text{h.c.}\right), \end{aligned} \tag{2.12}$$

As already indicated by the Majorana condition (2.6), Majorana particles are their own antiparticles and, thus, must not be charged. The Majorana mass term reflects this statement as it cannot be invariant under any $U(1)$ charge. More precisely, massive Majorana fermions induce lepton number violation (LNV) by two units, which yields important phenomenological consequences like $0\nu\beta\beta$ [59, 60] or the possibility of baryogenesis through leptogenesis [38, 39]. When speaking about RH Majorana neutrinos, we mean Majorana fermion, that are constructed from RH Weyl spinors and hence rely on the second definition of (2.9).

[6] Proof, see appendix A.

2.2. Neutrino mixing and oscillations

Now the general statements about Dirac and Majorana fields are extended to the case of three neutrino generations. As already mentioned in the introduction, it is still unclear whether neutrinos are of Dirac or Majorana nature and observations of neutrino oscillations points towards some mass generation mechanism beyond the current knowledge. In this section some basic low-energy phenomenology of massive neutrinos and the current experimental status are presented in order to set the stage for our analysis in chapter 3.

2.2.1. Generation mixing

By extending the Dirac and Majorana mass terms in (2.1) and (2.11) to three generations and diagonalizing the corresponding mass matrices, leptonic mixing matrices are obtained, similar to the Cabibbo-Kobayashi-Maskawa (CKM) matrix U_{CKM} of the quark sector [61, 62]. Such mixing matrices reflect the mismatches between mass and weak eigenstates and have important phenomenological consequences. The small neutrino mass in combination with their weak interacting nature makes the observations of flavor oscillations possible over large distances. The difference between Dirac and Majorana neutrinos in their mixing properties is topic of this subsection.

Dirac neutrino mixing

Although the SM does not contain RH neutrinos ν_R^α, for the moment we just assume their existence such that a fermionic mass term according to (2.1) is possible. At first, we discuss the case of Dirac neutrinos to further contrast differences to the following Majorana case. This will allow us to understand the origin of neutrino oscillations and can also be seen to be fully analogous to the derivation of the CKM matrix in the quark sector. First of all, the Dirac mass term of (2.4) has to be generalized to all three neutrino flavors, $\alpha, \beta = (e,\, \mu,\, \tau)$, leading to the following expression

$$\mathcal{L}^D_{mass} = -\bar{\nu}_R^\alpha m_{\alpha\beta} \nu_L^\beta + \text{h.c.}\,. \tag{2.13}$$

In the following, we also keep track of the charged lepton masses and the charged weak current since we expect the leptonic equivalent of the CKM matrix to appear due to the simultaneous diagonalization of both matrices. The interacting of the Lagrangian is usually given in weak eigenstates, hence, exhibits diagonal form,

$$\mathcal{L}^D_{mixing} = -\bar{\nu}_R^\alpha m_{\alpha\beta} \nu_L^\beta - \bar{l}_R^\alpha m^l_{\alpha\beta} l_L^\beta + \frac{g}{\sqrt{2}} \left(W^+_\mu \bar{\nu}_L^\alpha \gamma^\mu l_L^\alpha + h.c. \right) \tag{2.14}$$

with the weak eigenstates $\nu^\alpha_{L/R} = (\nu^e, \nu^\mu, \nu^\tau)_{L/R}$ and $l^\alpha_{L/R} = (e, \mu, \tau)_{L/R}$. As a next step, both mass matrices are diagonalized by unitary transformations, such that all quantities are now expressed in terms of mass eigenstates; indicated by

a primed. This is done with the following transformations, whereby each chiral fermion is transformed individually:

$$\begin{aligned} \nu_L^\alpha &= U_{\alpha i}^\nu \nu_L^{\prime i} \qquad & \nu_R^\alpha &= V_{\alpha i}^\nu \nu_R^{\prime i} \\ l_L^\alpha &= U_{\alpha i}^l l_L^{\prime i} \qquad & l_R^\alpha &= V_{\alpha i}^l l_R^{\prime i}, \end{aligned} \tag{2.15}$$

with the flavor index $\alpha = e,\ \mu,\ \tau$ and the mass basis index $i = 1,\ 2,\ 3$. Transition to the mass eigenstate basis of charged and neutral leptons gives rise to a mixing matrix in the Lagrangian's charged current,

$$\begin{aligned} \mathcal{L}_{mixing}^D &= -\bar{l}_R^{\prime i} V_{i\alpha}^{l\dagger} m_{\alpha\beta}^l U_{\beta j}^l l_L^{\prime j} - \bar{\nu}_R^{\prime i} V_{i\alpha}^{\nu\dagger} m_{\alpha\beta}^\nu U_{\beta j}^\nu \nu_L^{\prime j} + \frac{g}{\sqrt{2}} \left(W_\mu^+ \bar{\nu}_L^{\prime i} U_{i\alpha}^{\nu\dagger} U_{\alpha j}^e \gamma^\mu l_L^{\prime j} + \text{h.c.} \right) \\ &= -\bar{l}_R^i D_i^l l_L^i - \bar{\nu}_R^i D_i^\nu \nu_L^i + \frac{g}{\sqrt{2}} \left(W_\mu^+ \bar{\nu}_L^i U_{PMNS}^\dagger \gamma^\mu l_L^j + \text{h.c.} \right), \end{aligned} \tag{2.16}$$

where we omitted the dash for mass eigenstates in the last line to avoid clutter. After diagonalization both mass matrices are in general complex, but due to the freedom of choosing arbitrary field phases, the corresponding mass eigenstates can be selected in such a way that the mass eigenvalues become real and non-negative. This leaves us with a diagonal mass and a complex mixing matrix, incorporating the mismatches between weak and mass eigenstates of both, charged and neutral, lepton fields. The leptonic equivalent to the CKM matrix is commonly called Pontecorvo-Maki-Nakagawa-Sakata (PMNS) matrix U_{PMNS} [59,63] and has a very special meaning for low-energy neutrino phenomenology that we will comment on in a second. The whole parameter space of the leptonic SM sector, augmented with right-handed neutrinos, is summarized by the following matrices,

$$\begin{aligned} D^l &\equiv V^{l\dagger} m^l U^l = \text{diag}(m_e, m_\mu, m_\tau) \\ D^\nu &\equiv V^{\nu\dagger} m^\nu U^\nu = \text{diag}(m_{\nu_e}, m_{\nu_\mu}, m_{\nu_\tau}), \end{aligned} \tag{2.17}$$

assuming $U_{PMNS}^\dagger \equiv U^{\nu\dagger} U^l$. In contrast to quarks, which are usually detected as mass eigenstates or equivalently the mass eigenstate of the confined particle containing it, neutrinos can only be measures through weak interactions. The is based on the fact, that charge and mass eigenstates coincide. This implies, that instead of the propagating mass eigenstate $\nu^{'}$, neutrinos manifest themselves only through their weak eigenstate, e.g. ν_e, which is a superposition of all mass eigenstates according to (2.15). These propagate with different group velocities depending on their masses and thus lead to changing phases differences among them. As a consequence the probability to find a certain flavor eigenstate changes with time and distance. Since charged leptons are usually measured in the mass basis, we can define the charged lepton fields as directly mass eigenstates and immediately set m^l to diagonal form. If we want to correct this in the performed derivation, we only need to set $U^l = V^l = \mathbb{1}$. As a consequence, the neutrino mixing matrix coincides with the PMNS matrix $U^\nu = U_{PMNS}$ and, thus, leptonic mixing can be investigated through neutrino flavor conversion, commonly known as neutrino oscillations.

Majorana neutrino mixing

Now the generation mixing of Majorana neutrinos is presented and compared to the procedure for Dirac neutrinos. Since the general idea is the same and is deviation is almost identical, just formal differences to the former case are highlighted and in addition a special parameter choice of Majorana neutrinos with degenerate masses is discussed. The generalized Majorana mass term (2.12) has the form

$$\mathcal{L}^{M}_{mass} = -\frac{1}{2}\nu_L^{aT} C^{-1} m_{\alpha\beta} \nu_L^{\beta} + \text{h.c.} \tag{2.18}$$

again α and β are flavor indices. First of all, it has to be noticed that a general Majorana matrix always has to be symmetric $m_{\alpha\beta} = m_{\beta\alpha}$, for a proof see appendix C. Now we perform the same steps as for Dirac neutrino. With the familiar unitary transformations (2.15), we go into the mass basis such that the mass matrices are again diagonal. The choice of left- or right-handed Weyl fermions to build the Majorana fermion (2.9) only affects nomenclature of the neutrino's transformation matrix ($U \to V$). We obtain almost the same Lagrangian, but with slightly different transformation matrices that will have important consequences in the following,

$$\begin{aligned}
\mathcal{L}^{M}_{mixing} &= -\bar{l}_R^i V^{l\dagger}_{i\alpha} m^l_{\alpha\beta} U^l_{\beta j} l_L^{\prime j} - \nu_L^{\prime iT} C^{-1} U^{\nu T}_{\alpha i} m^{\nu}_{\alpha\beta} U^{\nu}_{\beta j} \nu_L^{\prime j} \\
&\quad + \frac{g}{\sqrt{2}} \left(W^+_{\mu} \nu_L^{\prime iT} C^{-1} U^{\nu}_{i\alpha} U^{e}_{\alpha j} \gamma^{\mu} l_L^{\prime j} + \text{h.c.} \right) \\
&= -\bar{l}_R^i D^l_i l^i_L - \nu_L^{iT} C^{-1} D^{\nu}_i \nu^i_L + \frac{g}{\sqrt{2}} \left(W^+_{\mu} \nu_L^{iT} C^{-1} U^{\dagger}_{PMNS} \gamma^{\mu} l_L^j + \text{h.c.} \right) .
\end{aligned} \tag{2.19}$$

Equivalently, the SM lepton sector with Majorana neutrinos can be described by the following quantities,

$$\begin{aligned}
D^l &\equiv V^{l\dagger} m^l U^l = \text{diag}(m_e, m_\mu, m_\tau), \\
D^{\nu} &\equiv U^{\nu T} m^{\nu} U^{\nu} = \text{diag}(m_{\nu_e}, m_{\nu_\mu}, m_{\nu_\tau}) ,
\end{aligned} \tag{2.20}$$

with $U^{\dagger}_{PMNS} \equiv U^{\nu T} U^l$. By taking the charged lepton basis to be diagonal from the beginning, the PMNS matrix U_{PMNS} is only determined by the neutrino transformation matrix $U_{PMNS} \to (U^{\nu})^*$ which will influence the leptonic later on.

Pseudo-Dirac neutrinos A special set-up of Majorana neutrinos arrangement is achieved, when the generalized mass matrix exhibits the following structure,

$$m_{\alpha\beta} = \begin{pmatrix} 0 & \times \\ \times & 0 \end{pmatrix} . \tag{2.21}$$

Such a mass terms is called to be of pseudo-Dirac nature and it arises if the two chiral components of a Dirac spinor are assigned to different flavors. In this context, it corresponds to two Majorana components having different CP properties and being degenerate in mass. The name relates to the fact that one Dirac field is equivalent to two Majorana field of same mass but different CP parity, which makes experimental differentiation between both cases very difficult [64].

2.2.2. CP phases within mixing matrices

This subsection deals with the phases contained in the neutrino mixing matrix, which could potentially lead to $\not{CP}$ and how they emerge in the two different neutrino mass cases. This procedure follows chapter 8.3 of [37] and gives some intuition, where and how occurring complex phases are absorbed.

The (3×3) neutrino mixing matrix U is unitary and, therefore, has nine real DOFs[7] which can be described by three angles and six phases. It can be parametrized in the following way:

$$U = e^{i\alpha} e^{i\beta_1 \lambda_3} e^{i\gamma_1 \lambda_8} \tilde{U} e^{i\beta_2 \lambda_3} e^{i\gamma_2 \lambda_8} \tag{2.22}$$

with the two Gell-Mann matrices $\lambda_{3,8}$ and the (3×3)-matrix $\tilde{U}$ containing the three mixing angles and one phase. The latter is usually expressed equivalently to the CKM matrix of the quark sector

$$\tilde{U} = \begin{pmatrix} c_{12}c_{13} & s_{12}c_{13} & s_{13}e^{-i\delta} \\ -s_{12}c_{23} - c_{12}s_{23}s_{13}e^{i\delta} & c_{12}c_{23} - s_{12}s_{23}s_{13}e^{i\delta} & s_{23}c_{13} \\ s_{12}s_{23} - c_{12}c_{23}s_{13}e^{i\delta} & -c_{12}s_{23} - s_{12}c_{23}s_{13}e^{i\delta} & c_{23}c_{13} \end{pmatrix}, \tag{2.23}$$

with the usual conventions $c_{ij} \equiv \cos\theta_{ij}$, $s_{ij} \equiv \sin\theta_{ij}$ and the phase $\delta \in [0, 2\pi)$. As a next step, the emergence of potential CP violating phases in Dirac and Majorana mixing matrices is discussed. The general assumption is that there are still unphysical phases contained in U that can be eliminated by appropriate field redefinition. The main focus lies on the weak interaction-part of the SM-Lagrangian, as it contain the leptonic mixing matrices as well as fermionic field,

$$\mathcal{L}_{weak} \supset W_\mu^+ \left(\bar{\nu}'^1, \bar{\nu}'^2, \bar{\nu}'^3\right)_L e^{-i\gamma_2\lambda_8} e^{-i\beta_2\lambda_3} \tilde{U}^\dagger e^{-i\gamma_1\lambda_8} e^{-i\beta_1\lambda_3} e^{-i\alpha} \gamma^\mu \begin{pmatrix} e' \\ \mu' \\ \tau' \end{pmatrix}_L . \tag{2.24}$$

Dirac neutrinos

In the Dirac neutrino case the phase factors containing β_2, λ_3 can be eliminated by an appropriate phase rotation of the individual neutrino fields ν^α. An additional rotation of the charged lepton fields leads to an absorption of the phases α, β_1 and γ_1 that restores the Lagrangian in its conventional form; the only difference is the exchange of U by $\tilde{U}$. Now, all freedom in "field re-phasing" is used and we arrive at the minimal number of DOFs; three mixing angles θ_{12}, θ_{23}, θ_{13} and one phase δ. Since δ is the only remaining phase in the Dirac case, it is commonly called *Dirac phase* and equivalent to the one appearing in the quark mixing matrix U_{CKM} [61].

Majorana neutrinos

At a first look, one might think that the procedure of phase absorption for (2.24) is the same besides a transposed instead of a "daggered" field. The problem arises not

[7] Simple proof: $3 \times 3 = 9$ complex entries correspond to 18 real DOFs The condition $UU^\dagger = \mathbb{1}$ yields three real constraints for the diagonal entries and three complex constrains for the off-diagonal ones $\rightarrow 18 - 3 - (2 \times 3) = 9$ real parameters.

number of ...	**Dirac**	**Majorana**
angles θ_{ij}	$\frac{1}{2}n(n-1)$	$\frac{1}{2}n(n-1)$
phases	$\frac{1}{2}(n-1)(n-2)$	$\frac{1}{2}n(n-1)$
$\hookrightarrow$ Dirac-type	all	$\frac{1}{2}(n-1)(n-2)$
$\hookrightarrow$ Majorana-type	0	$n-1$

Table 2.1.: Number of angles and phases of the leptonic mixing matrix for Dirac and Majorana neutrinos [66, 67].

here, but in the Majorana mass term (2.18), containing two times the same mixing matrix. Thus, the phases β_2 and γ_2 cannot be removed by any field redefinition and still contribute to U as so-called *Majorana phases*. Similar to the Dirac case, the remaining phase factors can be absorbed into the charged lepton fields and the Dirac phase δ remains in $\tilde{U}$. Hence, the Majorana mixing matrix contains three instead of only one phase, which is often parametrized in the following way

$$U = \tilde{U} \times \mathrm{diag}(1, e^{i\sigma}, e^{i\tau}). \tag{2.25}$$

The special form of the Majorana mass term (2.11) leads to addition of the individual Majorana phases, bisecting the domain of possible Majorana phases, $\sigma, \tau \in [0, \pi)$. For some purposes it is useful to shift both Majorana phases into the neutrino mass matrix. This can be done by appropriate redefinition of the neutrino fields according to

$$\nu_L^{''} = e^{i\gamma_2\lambda_8} e^{i\beta_2\lambda_3} \nu_L^{'}\,. \tag{2.26}$$

For an arbitrary number of neutrino flavors n, the number of necessary mixing angles and phases in the leptonic mixing matrix is presented in table 2.1 for both fermion types. A special feature of Majorana neutrinos is that a potential CP violating phase already occurs for two neutrinos. Naively, one would expect that the increased number of phases trigger more CP violating interactions that could be observed in Nature, but unfortunately this effects due to Majorana phases appear together with neutrino masses, hence,suppressed by $\left(\frac{m_\nu}{E}\right)^2$ [65].

2.2.3. Neutrino oscillations & mass ordering

As generation mixing has been presented, we are now ready to discuss the phenomenological consequence of neutrino flavor oscillations. Their implications for neutrino mass ordering are covered and an overview of current experimental neutrino parameters is given. This subsection closes with a short description of direct neutrino mass measurements and current experimental limits, which will help to interpret the results and validity of the approaches in chapters 3 and 4 in context of future measurements.

Neutrino oscillations

The idea of neutrino oscillations is very old and was first mentioned by Pontecorvo in 1957 [6], who transferred the concept of flavor-oscillations in neutral mesons, discussed by Gell-Mann and Pais [68], to particle-antiparticle pairs and especially to the case of neutrinos. The main assumption for this process to occur in the neutrino sector is that there exists a mismatch between the mass basis, in which the individual particles propagate, and the flavor basis, in which neutrinos are usually produced and detected via weak interactions. As we have already discussed, this mismatch leads to the occurrence of a leptonic mixing matrix U_{PMMS} in the charged current Lagrangian for both Dirac and Majorana neutrinos, (2.16) and (2.19) respectively. Hence, it connects mass with flavor eigenstates and will be of importance for neutrino oscillations. Moreover, the conversion between different particle flavors leads to violation of the individual lepton numbers (L_e, L_μ, L_τ) while the total $L = L_e + L_\mu + L_\tau$ remains conserved.

Already from a quantum mechanical point of view, this phenomenon can easily be understood by looking at two-level system[8]. If a state is prepared as an eigenstate of the underlying Hamiltonian, the time-evolution operator will just contribute a phase factor and it will remain an eigenstate of the Hamiltonian. The situation is different, if a state appears as an admixture of several eigenstates. Here, time-evolution leads to an oscillations between the two different eigenstates such that the probability for measuring a certain eigenstate varies over time.

Neutrino states in the different bases are connected via the leptonic mixing matrix U_{PMNS} by the following transformation,

$$|\nu_\alpha\rangle = U^*_{\alpha i} \, |\nu'_i\rangle \, , \tag{2.27}$$

where the flavor states are indicated by Greek indices and the mass states with Latin ones. Since the dynamics are described much easier in the mass basis, we switch frames, although neutrinos are detected as flavor states. Thus, for a state at a certain time t we have to include the time translation factor, yielding a state $|\nu(t)\rangle = U^*_{\alpha j} e^{-iE_j t} \, |\nu_j\rangle$. The transition amplitude for a oscillation from flavor α to flavor β then follows as

$$\mathcal{A}(\nu_\alpha \to \nu_\beta; t) = \langle \nu_\beta | \nu(t) \rangle = U_{\beta i} U^*_{\alpha j} e^{-iE_j t} \, \langle \nu_i | \nu_j \rangle = U_{\beta j} e^{-iE_j t} U^*_{\alpha j} \tag{2.28}$$

and the corresponding transition probability is given by the amplitude's absolute square

$$P(\nu_\alpha \to \nu_\beta; t) = |\mathcal{A}(\nu_\alpha \to \nu_\beta; t)|^2 = |U_{\beta j} e^{-iE_j t} U^*_{\alpha j}|^2 \, . \tag{2.29}$$

This probability does not change when one switches the neutrino's fermionic nature, since additional Majorana phases cancel in the final expression. A more intuitive statement is that neutrino oscillations do not violate total lepton number L, which would be a smoking gun for Majorana masses, and hence cannot

[8] The situation is actually more complicated such that a treatment of neutrinos in wave-packages is needed, but fortunately both approaches yield the same results in the coherent limit [64].

distinguish between both Dirac and Majorana particles. The situation differs if one includes both mass terms later done in the most general seesaw approach. In this situation, total lepton number can be broken due to oscillations into sterile states according to $\nu_a \to \nu_b^c$. An introduction into the formalism of this general oscillation framework can be found in [69].

Example: Two-flavor oscillations To get more intuition of the phenomenon of neutrino oscillations, the simplest realization of two flavors called ν_e and ν_μ, is discussed in the following. In this case, the leptonic mixing matrix reduces to a (2×2) matrix U_2 incorporating only one mixing angle θ, such that the flavor states are given by

$$\begin{pmatrix} |\nu_e\rangle \\ |\nu_\mu\rangle \end{pmatrix} = \begin{pmatrix} c & s \\ -s & c \end{pmatrix} \begin{pmatrix} |\nu_1\rangle \\ |\nu_2\rangle \end{pmatrix} \tag{2.30}$$

Since neutrinos are very light, they can always be approximated as ultra-relativistic, $p_\nu \gg m_\nu$, and their energy-momentum relation is commonly rephrased in terms of energy $E_\nu = \sqrt{p_\nu + m_\nu^2} \simeq p_\nu + \frac{m_\nu^2}{2p_\nu} \simeq E_\nu + \frac{m_\nu^2}{2E_\nu}$. With this, expressions for the transition and survival probabilities can be simplified as

$$\begin{aligned} P(\nu_e \to \nu_\mu; t) &= P(\nu_\mu \to \nu_e; t) = \sin^2 2\theta \sin^2\left(\frac{\Delta m^2}{4E} t\right) \\ P(\nu_e \to \nu_e; t) &= P(\nu_\mu \to \nu_\mu; t) = 1 - P(\nu_e \to \nu_e; t), \end{aligned} \tag{2.31}$$

where the mass squared difference is defined as $\Delta m^2 \equiv m_2^2 - m_1^2$. A more convenient way is to re-express it in terms of the traveled distance, $t \simeq L$ for relativistic particles, and the so-called oscillation length $L_{osc} = 2\pi E/\Delta m^2 \simeq 2.48\,(E\,[\mathrm{MeV}]\,/\Delta m^2\,[\mathrm{eV}^2])\mathrm{m}$, which describes the length between one probability minimum and the next maximum or vice versa,

$$P(\nu_e \to \nu_\mu; t) = \sin^2 2\theta \sin^2\left(\pi \frac{L}{L_{osc}}\right) = \sin^2 2\theta \sin^2\left(1.27 \Delta m^2 \frac{L\,[\mathrm{m}]}{E\,[\mathrm{MeV}]}\right). \tag{2.32}$$

The first term including the mixing angle θ affects the oscillation probability amplitude and is maximal for an angle $\theta \sim 45°$, obviously referred to as *maximal mixing*, and minimal for $\theta \sim 0°$, $90°$ indicating the almost equivalence between mass and flavor basis. The second term describes the spatial oscillation behavior. For successful detection, the argument must not be too small or too large, as otherwise the oscillation pattern would vary too slow or too much, respectively. Averaging over small energy intervals regarding a detector's finite resolution or small variation in the traveled distance leads to cancellation of the oscillation pattern such that the observed quantity just depends on the mixing angle,

$$\overline{P(\nu_e \to \nu_\mu; t)} = \overline{P(\nu_\mu \to \nu_e; t)} = \frac{1}{2} \sin^2 2\theta\,. \tag{2.33}$$

The case of three oscillating flavors is governed by the full PMNS matrix (2.23) and leads to more complex expressions; for details see e.g. [62] or [64]. Hence, the

Approx.	phase	eff. description	survival probability
long baseline	$\frac{\Delta m^2_{31}}{2E} L \simeq \frac{\Delta m^2_{32}}{2E} L \gg 1$	$\Delta m^2 = \Delta m^2_{21}$ $\theta = \theta_{12}$	$P_{e\to e} \simeq c^2_{13} P + s^2_{13}$ $P = 1 - s^2_{2\theta} \sin^2\left(\frac{\Delta m^2}{4E} L\right)$
short baseline	$\frac{\Delta m^2_{21}}{2E} L \ll 1$	$\Delta m^2 = \Delta m^2_{31}$ $\theta = \theta_{13}$	$P_{e\to e} = 1 - s^2_{2\theta} \sin^2\left(\frac{\Delta m^2}{4E} L\right)$

Table 2.2.: Overview of different effective two-flavor approximations. The long baseline approximation can safely be used for solar neutrinos. Short baselines refer to accelerator and reactor experiments, but also for atmospheric neutrinos. With the presented formulas one should be able to understand the qualitative behavior of neutrino oscillations in the different regimes [67]. The common abbreviations for sine and cosine are used: $c_{ij} \equiv \cos\theta_{ij}$, $s^2_{2\theta} \equiv \sin^2 2\theta$.

three-flavor case follows

$$\begin{aligned} P_{\alpha\to\beta} &= \left|\langle \nu^\beta | \nu^\alpha \rangle\right|^2 = \sum_{i,j} U_{\alpha i} U^*_{\beta i} U^*_{\alpha j} U_{\beta j} e^{i\frac{m_i^2 - m_j^2}{2E} t} \\ &= \delta_{\alpha\beta} + \sum_{i,j} \left|U_{\alpha i} U_{\beta i} U_{\alpha j} U_{\beta j}\right| e^{i\phi_{\alpha\beta ij}} \left(e^{i\Delta_{ij} t} - 1\right) \end{aligned} \tag{2.34}$$

with $\phi_{\alpha\beta ij} = \arg\left(U_{\alpha i} U^*_{\beta i} U^*_{\alpha j} U_{\beta j}\right)$ and $\Delta_{ij} \frac{m_i^2 - m_j^2}{2E}$ [37]. Furthermore, ϕ is anti-symmetric in the last two indices and, due to cancellations, free of any Majorana phases $\phi_{\alpha\beta ij} \equiv \arg\left(\tilde{U}_{\alpha i} \tilde{U}^*_{\beta i} \tilde{U}^*_{\alpha j} \tilde{U}_{\beta j}\right)$, which underlines again that oscillations do not distinguish between Dirac and Majorana fermions.

Fortunately, there exist two common approximations related to certain values of $\frac{\Delta m^2}{2E} L$ which help to reduce the general three flavor scenario to an effective two flavor problem, that rely on the above expressions; see table 2.2.

Matter effects Finally, the topic of neutrino oscillations shall be closed with a short comment on matter effects as they play an important role in investigations of leptonic $\not{CP}$. The oscillation of neutrino flavors during their propagation in matter is generally modified since all flavors scatter of electrons as well as up- and down-quarks of the underlying matter distribution via neutral-current interactions. Under assumption of equal proton and electron number densities, their contributions cancel each other and just the component corresponding to neutron scattering contributes. Further, electron neutrinos undergo charged current interactions with electrons contained in the medium, giving rise to an additional effective potential only for the electron flavor. Then, coherent, elastic forward scattering leads to an amplification of the underlying transition probability. This could create a resonant enhancement of the oscillation amplitude, if the Mikheyev–Smirnov–Wolfenstein condition, that relates the electron number density with the neutrino mixing angle, energy and mass squared difference, is fulfilled [70, 71]. The important fact is, that

Observable	Units	Hierarchy	Best-fit value	$3\,\sigma$ confidence interval
Δm^2_{21}	$\left[10^{-5}\,\mathrm{eV}^2\right]$	both	$+7.50$	$[+7.03, +8.09]$
$\Delta m^2_{3\ell}$	$\left[10^{-3}\,\mathrm{eV}^2\right]$	NH	$+2.52$	$[+2.41, +2.64]$
		IH	-2.51	$[-2.64, -2.40]$
$\sin^2\theta_{12}$	$[10^{-1}]$	both	$+3.06$	$[+2.71, +3.45]$
$\sin^2\theta_{13}$	$[10^{-2}]$	NH	$+2.17$	$[+1.93, +2.39]$
		IH	$+2.18$	$[+1.95, +2.41]$
$\sin^2\theta_{23}$	$[10^{-1}]$	NH	$+4.41$	$[+3.85, +6.35]$
		IH	$+5.87$	$[+3.93, +6.40]$
δ	[deg]	NH	261	$[0, 360]$
		IH	277	$[0, 31] \oplus [145, 360]$

Table 2.3.: Best-fit values and $3\,\sigma$ confidence intervals for the five low-energy observables that are currently accessible in experiments and for the CP violating phase δ [8]. Further, we define $\Delta m^2_{ij} \equiv m^2_i - m^2_j$ in general and $\Delta m^2_{3\ell} \equiv \Delta m^2_{31} > 0$ for NH and $\Delta m^2_{3\ell} \equiv \Delta m^2_{32} < 0$ for IH in particular.

this matter effects treat neutrinos and anti-neutrinos differently. Investigations of leptonic $\not{CP}$ have to take this into account, since it can easily be mimicked by CP violating matter effects [72]. For detailed overview of high- and low-energy $\not{CP}$, see [73].

Neutrino mass measurements

To close the subject of neutrino oscillations, short overview of experimental attempts measuring their low-energy parameters is given[9]. We have learned in the last section, the amplitude of neutrino oscillations in the two-flavor approximation depends on corresponding mixing angle and the oscillation phase is proportional to the mass-squared difference. This allows us to determine all mixing angles and mass-squared differences while the absolute neutrino mass scale remains unknown. A common method is to combine all available datasets from solar, atmospheric and reactor neutrino experiments to obtain values for all parameters in so-called global fits [75, 76]. The detailed method is explained in [8, 77] and the corresponding values are displayed in table 2.3.

Although this sounds simple, the sign of the atmospheric mass-squared difference Δm^2 is not determined yet and gives rise to two possible mass orderings, referred

[9] We focus only on the neutrino parameters accessible in oscillation experiments and their absolute mass scale, as they are relevant for our work. Other parameters measurable at low-energy, e.g. electromagnetic properties [74], are also interesting, but will not affect our work

to the cases $m_1 \gg m_2 \gg m_3$ (normal mass hierarchy - NH) and $m_3 \gg m_1 \gg m_2$ (inverted mass hierarchy - IH); see figure C.1 for an illustration. The mass-squared differences defined in [77] are related to the actual neutrino masses via the following relations,

$$\delta m^2 = m_2^2 - m_1^2\,, \qquad \Delta m^2 = m_3^2 - \frac{1}{2}\left(m_2^2 + m_1^2\right)\,. \tag{2.35}$$

The precision of today's neutrino experiments in measuring yet unknown quantities, like the phase in the leptonic mixing matrix, is limited by this uncertainty and further progress is needed to solve this puzzle. In addition, other branches of neutrino physics rely on this knowledge too, especially experiments measuring $0\nu\beta\beta$, neutrino cosmology and theories trying to explain neutrino mass generation. A good overview of current state-of-the-art attempts of measuring the neutrino mass hierarchy are given in [10], from where we summarize the main points now.

The neutrino mass hierarchy can be further investigated by very precise measurements of transition probabilities for different baseline configurations in a similar way like it is done in former or currently running oscillation experiments. Different detection techniques and neutrino sources are used to improve the experiment's sensitivity. Experiments aiming for the detection of $0\nu\beta\beta$ need the mass hierarchy as input to interpret the measured decay rate; an unexpected detection could give hints as to which hierarchy to expect. Cosmology only gives information about the total sum of all neutrino masses mainly from anisotropies and B-mode polarization of the cosmic microwave background or large-scale structure formation. Here, the two different hierarchies change the the sum of neutrino masses only marginally, but the neutrino mass spectrum has to be known to guarantee determination power.

Conclusively, the final neutrino mass hierarchy is expected to be determined within the next two decades with new upcoming experiments, as the prospects of selected attempts already indicate, see table C.3.

So far, we know the values of all neutrino mixing angles and mass-squared differences quite precisely, but besides upper bounds on the sum of all neutrino masses from cosmology, $\sum m_i < 0.5$ eV [7], the absolute mass scale remains unclear. Measurements of $0\nu\beta\beta$ are capable of determining the so-called effective neutrino mass $\langle m_{ee} \rangle$, but rely on the mass hierarchy and experience large uncertainties from the corresponding nuclear matrix elements. In addition, the yet unknown CP phases may contribute. The key ingredient to observe such processes is the Majorana nature of neutrinos, hence being a smoking gun signature for LNV. Alternative processes like double electron capture or double positron emission are constrained due to a small number of suitable elements and phase-space arguments, respectively [60]. The only real direct mass measurements are based on kinematics and energy-momentum conservation, such as time-of-flight or precision weak decay measurements. Time-of-flight measurements are less favored since they require long baselines and strong sources like it is provided by a supernova. However, these events are very rare and the processes in such harsh environments are far from well-understood. Deduced mass limits are, therefore, strongly dependent on the supernova modeling, e.g. $m < 5.8$ eV (95% CL) from the supernova

SN1987a [78]. On the other hand, the precise measurements of weak decay products allow the extraction of the so-called averaged electron neutrino mass-squared without any assumption on the underlying mass model The quantity of interest is defined according to

$$m^2_{\nu_e} \equiv \sum_i |U^2_{ei}| m^2_i \,, \tag{2.36}$$

where the incoherent sum guarantees the independence of any phase in the leptonic mixing matrix. Different experimental attempts try to tackle the neutrino mass scale with beta decays, e.g. the KATRIN experiment [12] uses tritium decay in a source≠detector-setup. Additionally, experiments like MARE-1 (^{187}Re-decay) and ECHO (^{163}Ho-electron capture) try to assess it with different detector configurations, see [9] and references therein.

With these experiments a sensitivity to the neutrino mass scale of $\mathcal{O}(100\,\text{meV})$ will be obtained in the upcoming years [9].

2.2.4. Leptonic CP violation

To close the phenomenology of neutrino mixing and continue with mechanisms for mass generation, we want to address a topic that is also very important in the context of generating the BAU, leptonic $\not{CP}$.

The CP transformation on a neutrino is defined in such way that charge-conjugation converts a particle into its anti-particle and the corresponding parity-transformation switches the particle's chirality. To investigate leptonic $\not{CP}$, we first have to know, what the CP-conservation implies for the neutrino sector. The neutrino's transformation properties under CP directly affect the transition probabilities in oscillations. If the neutrino interactions would conserve CP, which they definitely do not, we would observe equal oscillation probabilities for neutrinos and anti-neutrinos,

$$CP : \nu_L \xrightarrow{CP} \bar{\nu}_R \Longrightarrow P(\nu_\alpha \to \nu_\beta; t) \overset{!}{=} P(\bar{\nu}_\alpha \to \bar{\nu}_\beta; t) \,, \tag{2.37}$$

A deeper look on the charged current Lagrangians of Dirac and Majorana neutrinos, (2.16) and (2.19), reveals that the action of charge conjugation implies a complex conjugation of the leptonic mixing matrix $U \xrightarrow{C} U^*$. Hence, these interactions are only CP-invariant, if U is real or its phases can be re-phased. As we already discussed the re-phasing possibilities of U, the complex phases in the leptonic mixing matrix can trigger $\not{CP}$. Moreover, CPT invariance demands $P(\nu_\alpha \to \nu_\beta; t) \overset{!}{=} P(\bar{\nu}_\beta \to \bar{\nu}_\alpha; t)$, implying that the survival probabilities of neutrinos and anti-neutrinos have to be equal. T-transformation simply interchanges initial and final states $P(\nu_\alpha \to \nu_\beta; t) \xrightarrow{T} P(\nu_\beta \to \nu_\alpha; t)$, ensuring that, under assumptions of CPT invariance, CP and T transformations are equivalent. For a more detailed discussion of $\not{CP}$ within the leptonic sector, see [73].

CP violation in neutrino oscillations

From the aforementioned transformations it should be obvious that leptonic $\not{CP}$ exists if oscillation probabilities of a neutrino and its corresponding anti-particle differ. Equivalently, one has a complex mixing matrix U with un-removable phases. As we see $\not{CP}$ in Nature [79], we expect the leptonic mixing matrix U_{PMNS} to be complex and incorporating a Dirac phase δ. Hence, the quantity describing $\not{CP}$ in oscillation experiments is the difference between a neutrino flavor transition and its CP-conjugate, $\Delta P_{\alpha\beta} \equiv P(\nu_\alpha \to \nu_\beta; t) - P(\bar{\nu}_\alpha \to \bar{\nu}_\beta; t)$.[10] In case of leptonic CP invariance, it clearly will be zero. It can be re-phrased in a more familiar way,

$$\Delta P_{\alpha\beta} = -16\, J \,\sin\frac{\Delta_{21}L}{2}\sin\frac{\Delta_{32}L}{2}\sin\frac{\Delta_{13}L}{2}\,, \tag{2.38}$$

with the Jarlskog invariant $J = -\Im U_{\beta 1}U^*_{\beta 2}U^*_{\alpha 1}U_{\alpha 2}$ as a measure for $\not{CP}$ [80], the re-scaled mass-squared differences $\Delta_{ij} \equiv \frac{(m_i^2 - m_j^2)}{2E}$ and L the travel distance. Hence, CP-conservation is achieved for

$$\theta_i = 0 \quad \text{or} \quad \theta_i = \frac{\pi}{2} \quad \text{and} \quad \delta = 0 \quad \text{or} \quad \delta = \pi. \tag{2.39}$$

As already mentioned, one subtlety of $\not{CP}$ investigations is that one always has to take matter effects into account as they are capable of inducing additional $\not{CP}$. To separate macroscopic from intrinsic $\not{CP}$, one has to use large baselines, since matter effects are proportional to the corresponding neutrino energy, making them constant for fixed L/E. For larger baselines, the oscillation's envelope increases and the following relation can be used as a rule of thumb to measure strong intrinsic $\not{CP}$ [37, 73],

$$\frac{L}{E} > 1000\frac{\text{km}}{\text{GeV}}. \tag{2.40}$$

CP violation from Majorana phases

Finally, we comment on the occurrence of Majorana phases in physical processes. Since the phases β' and γ' are present, if we have Majorana neutrinos, we expect them to be present in processes involving Majorana neutrinos. The most famous example is $0\nu\beta\beta$ which allows the investigation of Majorana phases at low-energy. Another example presented in [37] is a particular muon decay. Due to the neutrino's Majorana nature, besides the usual SM decay, also the process $\mu \to e\nu\nu$ can occur via a neutrino mass insertion. The interference of both reaction channels gives rise to $\not{CP}$ by means of the Majorana phases, but unfortunately, such effects are suppressed by the muon mass. Another possibility is the emergence of $\not{CP}$ at high energy scales in leptogenesis, where heavy RH neutrinos decay and leads to $\not{CP}$ in the early universe. By non-perturbative processes, sphalerons, this generated CP asymmetry can be transferred to the baryon sector, hence, generating the observed baryon asymmetry of our universe [38, 39].

[10] CPT invariance demands that $\Delta P_{\alpha\beta} = -\Delta P_{\beta\alpha}$.

2.3. Type-I seesaw mechanism

This section deals with the simplest scenario of neutrino mass generation, the type-I seesaw mechanism [19–22]. Before introducing this SM extension, some issues with neutrino masses in the conventional framework are discussed. The diagonalization procedure of the seesaw matrix and the model's parameter space with a commonly used parametrization is presented. This generic scenario is the basis that allows deeper understanding of investigations within this work.

2.3.1. Neutrino masses in the standard model

In the SM framework, neutrinos are only implemented as LH Weyl fermions as a result of the experiments performed by Wu [81] and Goldhaber [82]. They do not participate in Yukawa interactions with the Higgs and receive no mass through the Higgs vacuum expectation value (VEV) v_{EW} since the necessary RH component is missing. This is in clear contradiction to the observed neutrino oscillations and the corresponding measured mass-squared differences, see figure C.2. This gives rise to the yet unresolved puzzle of neutrino masses.

The naive approach of introducing a RH neutrino component, such that they are usual Dirac fermions, similar to all other matter particles in SM, seems not convincing and gives rise to further question, as we will see now. The implementation of a RH component gives rise to usual Yukawa interactions with its LH counterpart and the Higgs doublet. As the Higgs acquires its VEV $v_{EW} = 174\,\text{GeV}$, neutrino masses are generated similar to any other fermion mass in the SM,

$$-\mathcal{L}^{\nu}_{Yuk} \subset y_\nu \bar{\nu}_L \phi \nu_R + \text{h.c.} \xrightarrow{\langle\phi_0\rangle = v_{EW}} m_\nu \bar{\nu}_L \nu_R + \text{h.c.}\,, \tag{2.41}$$

with the neutrino mass $m_\nu \equiv v_{EW} y_\nu$. In principle, this account for neutrino mass, but if we compare the corresponding Yukawa couplings to the one of quarks and leptons, we realize that the required coupling is orders of magnitude, $\sim 10^{-12}$, smaller than the usual SM ones [54, 64]. Of course, this could be considered as a problem of theoretical aesthetics, but a deeper understanding why neutrino masses are much smaller than any other mass in the SM is not given. Within the SM, there is no other possibility to generate naturally small neutrino masses from non-renormalizable interactions. Already from this point of view, it should be clear that neutrino mass generation is clearly a subject of BSM. In the end, a short remark on RH neutrinos: As this particles are SM singlets, $\{1, 1, 0\}$ under the SM gauge group, and hence participate in no interaction, they are also known under the term *sterile* neutrinos. The only way, in which they reveal themselves, would be through missing or occurring neutrino due to oscillation into and from the sterile state respectively.

The above statements only apply, if neutrinos are Dirac particles ($\nu \neq \nu^C$). They are the only particles in the SM that could also be of Majorana nature, allowing for an additional Majorana mass term according to (2.18). Since LH Majorana mass terms are violating the SM gauge symmetry and can only arise, if $SU(2)_L \times U(1)_Y$ is already broken. Hence, they can only originate from a mechanism beyond our

current knowledge. In contrast, RH SM singlets, yield mass terms consistent with the SM gauge group already above the electroweak scale. Although this seems to be a nice feature, we are only shifting the problem to higher energies, since the RH mass term would violate lepton number, or more precisely $(B-L)$. As it is a favored quantum number of GUTs, RH neutrino masses are usually generated during $(B-L)$-breaking, for other symmetries related to Majorana mass generation see appendix C. Already by allowing neutrinos to be of Majorana nature, we transient to foundations of the type-I seesaw mechanism, which is subject of our discussion now.

2.3.2. (Type-I) seesaw framework

By extending the SM with three additional RH heavy neutrinos, N_i $i = 1, 2, 3$, and allowing neutrinos, in general, to be Majorana fermions, the basic principles of this simple model are already settled. Before we discuss the actual meaning of the word "seesaw", the implication of the introduced neutrinos are clarified at first.

As already explained in section 2.1, a Majorana particle's LH and RH components are linked, as we demand them to be real, see (2.6) and (2.10).

For SM neutrinos ν_L, the LH component is chosen, since it has to participate in weak interaction as usual, $\nu = \nu_L + (\nu_L)^C$. The newly introduced neutrinos must not interact, such that we chose the RH component to define them, $N = \nu_R + (\nu_R)^C$. As usual, we work with chiral components according to (2.12). The RH neutrinos ν_R can have the usual Yukawa coupling to leptons and the Higgs doublets without spoiling the SM's anomaly cancellation,[11] since $SU(2)_L$ singlets and neutral particles they do not contribute to any triangle diagrams. After spontaneous symmetry breaking (SSB), this interaction leads to the usual Dirac mass terms as for any other fermion in the SM. Their sterile character has, in addition, the consequence that the number of RH fields is unbounded, although at least two heavy neutrinos are needed to for consistency with experiment. The choice of three neutrinos simply corresponds to the number of SM generations and may be motivated by gauge-unifying theories.

Due to the their Majorana nature, the RH neutrino contribute additional mass terms, which already fixes the Lagrangian responsible for the type-I seesaw scenario. It is also possible to generate mass terms for the LH fields from higher-dimensional operators, which are non-renormalizable; this possibility is used in type-II seesaw models. If viewed as an effective description of a high-energy theory, such that non-propagating DOFs can be integrated out, they earn their justification.

One comment for completeness: Actually all seesaw variants are based on the same effective dimension-5 operator, the Weinberg operator [83], which generates tree-level mass for neutrinos,

$$\mathcal{L}_5 = \frac{1}{2}\frac{g}{\Lambda}\left(\bar{L}_L\tilde{\phi}\right)\left(\phi^* L_L^C\right). \tag{2.42}$$

[11] For details see chapter 30 of [54].

The type-I seesaw framework reduces to an effective theory described through (2.42), if we assume the heavy neutrinos to be very heavy in contrast to typical energy scales of the theory, hence non-propagating, and integrate them out. This complementary approach, where no assumptions about the UV region is made is usually referred to a bottom-up approach

Now, we come back to our top-down perspective, where we know details about the valid DOFs. We will assume for now, that a LH Majorana mass term exists in addition, allowing us to treat the most general seesaw mass matrix. The Lagrangian relevant to the seesaw mechanism is given by

$$\mathcal{L}_{seesaw} = \mathcal{L}_D + \mathcal{L}_M = -\overline{\nu}_L m_D \nu_R - \frac{1}{2}\overline{\nu}_L m_L \left(\nu_L\right)^C - \frac{1}{2}\overline{\left(\nu_R\right)^C} m_R \nu_R + \text{h.c.}\,. \quad (2.43)$$

The first term is the familiar Dirac mass coming SSB of $SU(2)_L \times U(1)_Y$ with mass proportional to the individual Yukawa coupling y_{ij} and the Higgs VEV. The last two terms are the Majorana mass terms of LH and RH neutrinos. One can now split the Dirac mass term according to

$$\bar{\nu}_L m_D \nu_R = \frac{1}{2}\left(\overline{\nu}_L m_D \nu_R + \left(\overline{\nu}_L m_D \nu_R\right)^T\right) = \frac{1}{2}\left(\overline{\nu}_L m_D \nu_R + \overline{\left(\nu_R\right)^C} m_D^T \left(\nu_L\right)^C\right), \quad (2.44)$$

which allows us to write the seesaw Lagrangian in a more elegant way

$$\begin{aligned} \mathcal{L}_{seesaw} &= -\frac{1}{2}\left(\bar{\nu}_L, \overline{\left(\nu_R\right)^C}\right)\begin{pmatrix} m_L & m_D \\ m_D^T & m_R \end{pmatrix}\begin{pmatrix} \left(\nu_L\right)^C \\ \nu_R \end{pmatrix} + \text{h.c.} \\ &= -\frac{1}{2} n_R^T C^{-1} m_{D+M} n_R + \text{h.c.}\,, \end{aligned} \quad (2.45)$$

with the vector $n_R \equiv \left(\left(\nu_L\right)^C, \nu_R\right)^T$ containing the three LH SM neutrinos, the three RH ones and the (6×6) neutrino mass matrix, m_{D+M}, incorporating the three original mass matrices as blocks.[12] The choice of n_R is usually a matter of convenience, since one can also interchange chiral components by taking elements of the Lagrangian's h.c.-part; e.g. in [64], n is defined in terms of LH chiral spinors, which just interchanges the position of m_D and m_D^T in the full seesaw matrix. In either case, the combined mass term has the form of a Majorana mass, compare with (2.11), given in terms of RH Dirac spinors. Therefore it is symmetric and diagonalizable by an unitary transformation according to (2.20). Details of this diagonalization process and the corresponding consequences are given in the subsequent part.

2.3.3. Seesaw diagonalization procedure

In the following, the diagonalization process of the seesaw mass matrix (2.45) is shown in detail, following the conventions of [84]. One might think that this is

[12] If more than three sterile neutrinos are introduced, $n_s > 3$, m_{D+M} is given by a $(3+n_s) \times (3+n_s)$ matrix. This would have also important consequences on the previously defined leptonic mixing matrix U_{PMNS}, i.e. deviation from unitarity as it is now just a block matrix, contained in a bigger mixing matrix. For this see [37, 64].

just some mathematical technicality, but the generation of small neutrino masses originates exactly from this steps. By assuming certain hierarchies between the different neutrino masses, the whole seesaw mass matrix can be brought into a form, where it is evident that an increase of the heavy state's mass naturally decreases the light-state's mass. Since the seesaw matrix is symmetric, it can be diagonalized unitary transformation as usual. The diagonalization procedure is performed in two steps: first a block-diagonalization in which the off-diagonal block are removed, and second an individual diagonalization of the diagonal blocks. Hence, a transformation matrix composed of two individual parts is obtained,

$$D_\nu = U_{seesaw}^T m_{D+M} U_{seesaw} = \begin{pmatrix} D_{light} & 0 \\ 0 & D_{heavy} \end{pmatrix} \quad \text{with } U_{seesaw} = U_B\, U_I\,. \tag{2.46}$$

U_B describes the transformation matrix needed for block-diagonalization and U_I the transformation necessary to diagonalize the individual block-diagonal entries. For the seesaw mechanism to work out, we assume the following existing hierarchy among the different block mass matrices: $m_L \ll m_D \ll m_R$. The contribution of the LH mass matrix should be the smallest as this term is forbidden in the SM and can only occur through an effective interaction, being suppressed by its characteristic energy scale Λ. The usual Dirac mass matrices, being induced by the Higgs VEV v_{EW}, should be of the order of common SM lepton masses. As mentioned, the masses of RH neutrinos usually emerge from high-energy $(B-L)$ breaking, thus, must be the heaviest for this mechanism to work out.

Block-diagonalization of the seesaw matrix m_{D+M}

The first diagonalization step assumes that the seesaw mass matrix can be brought into block diagonal form up to corrections of a small parameter c, which is determined by demanding exact block-diagonal form. Due to certain hierarchies among the block diagonal matrices, we can approximate $c \sim \mathcal{O}(m_D m_R^{-1})$. The nearly-diagonalization of the mass matrix is obtained by taking a nearly-unitary matrix according to

$$U_B = \begin{pmatrix} \mathbb{1} - \frac{1}{2} cc^\dagger & c \\ -c^\dagger & \mathbb{1} - \frac{1}{2} c^\dagger c \end{pmatrix}\,. \tag{2.47}$$

A check of its nearly-unitarity, confirms our ansatz,

$$\begin{aligned} UU^\dagger &= \begin{pmatrix} \mathbb{1} - \frac{1}{2} cc^\dagger & c \\ -c^\dagger & \mathbb{1} - \frac{1}{2} c^\dagger c \end{pmatrix} \begin{pmatrix} \mathbb{1} - \frac{1}{2} cc^\dagger & -c \\ b^\dagger & \mathbb{1} - \frac{1}{2} c^\dagger c \end{pmatrix} \\ &= \begin{pmatrix} \mathbb{1} + \frac{1}{4} cc^\dagger cc^\dagger & 0 \\ 0 & \mathbb{1} + \frac{1}{4} c^\dagger cc^\dagger c \end{pmatrix} = \mathbb{1} + \mathcal{O}(c^4) \simeq \mathbb{1}\,. \end{aligned} \tag{2.48}$$

Next, we obtain block-diagonal structure through $D_B \stackrel{!}{=} U_B^T m_{D+M} U_B$ and construct U_B in a way, where we keep terms of m_L with coefficients up to $\mathcal{O}(1)$,

m_D-terms up to $\mathcal{O}(c)$ and m_R-ones up to $\mathcal{O}(c^2)$,

$$\begin{aligned} D_B &= U_B^T m_{D+M} U_B \\ &= \begin{pmatrix} \mathbb{1} - \frac{1}{2}cc^\dagger & -c \\ b^\dagger & \mathbb{1} - \frac{1}{2}c^\dagger c \end{pmatrix} \begin{pmatrix} m_L & m_D \\ m_D^T & m_R \end{pmatrix} \begin{pmatrix} \mathbb{1} - \frac{1}{2}cc^\dagger & c \\ -c^\dagger & \mathbb{1} - \frac{1}{2}c^\dagger c \end{pmatrix} \\ &\simeq \begin{pmatrix} m_L - c^* m_D^T - m_D c^\dagger + c^* m_R c^\dagger & m_D - c^* m_R \\ m_D^T - m_R c^\dagger & m_D^T c + c^T m_D + m_R - \frac{1}{2}c^T c^* m_R - \frac{1}{2}m_R c^\dagger c \end{pmatrix} \\ &\stackrel{!}{=} \begin{pmatrix} m_\nu & 0 \\ 0 & m_R \end{pmatrix} . \end{aligned} \tag{2.49}$$

By this requirement, we obtain an expression for the small parameter c that eliminates the off-diagonal terms:

$$m_D - c^* m_R \stackrel{!}{=} 0 \qquad \longrightarrow \qquad c = \left(m_D m_R^{-1}\right)^* . \tag{2.50}$$

In the end, the block diagonal form of the seesaw matrix is given by

$$D_B = U_B^T m_{D+M} U_B = \begin{pmatrix} m_{light} & 0 \\ 0 & m_{heavy} \end{pmatrix} \simeq \begin{pmatrix} m_L - m_D m_R^{-1} m_D^T & 0 \\ 0 & m_R \end{pmatrix} . \tag{2.51}$$

It already allows us to infer how light-neutrino masses can be achieved. The light matrix m_{light} can be viewed as the squared Dirac mass, suppressed by the inverse of the heavy RH mass matrix. Hence, the name seesaw mechanism deserves its justification through the fact, that we can tune the usual SM neutrino masses arbitrary small by increasing the RH neutrino mass appropriately. Hence, the lightness of LH neutrinos is now linked to the heaviness of their RH partners. In the type-I seesaw scenario, m_L is not present, such that the light neutrino masses are given by the simple relation,

$$m_{light} = -m_D m_R^{-1} m_D^T , \tag{2.52}$$

which is commonly known as the type-I seesaw formula.

Moreover, a closer look to the eigenstates reveals that the heavy RH neutrino mass not only affects the mass eigenvalues, but also eigenstates. Thus, we obtain the following eigenstates due to RH neutrino suppression,

$$\nu_{light} \approx \nu_L \qquad \nu_{heavy} \approx \nu_R , \tag{2.53}$$

which confirms that the usual SM neutrino are equivalent to the light neutrino states.

Diagonalization of block matrices m_{light} and m_{heavy}

For the next step, we can already rely on knowledge gained in the previous section. If we view the light-neutrino mass matrix m_{light} as the one present in the context of generation mixing, see section 2.2, we can perform the usual steps, which result in appearance of the familiar leptonic mixing matrix $U_{PMNS} \equiv U_L^{e\dagger} U_L^\nu$. Working in the charged lepton basis, i.e. $U_e = \mathbb{1}$, sets the transformation between

mass and weak eigenstates to be directly to the PMNS matrix, $U^{\nu} = U_{PMNS}$. Hence, the light-neutrino mass matrix is diagonalized by the PMNS matrix $D_{light} = U_{PMNS}^{T}\, m_{light}\, U_{PMNS}$.

Equivalently, the heavy neutrino matrix is diagonalized by an unitary transformation, $D_{heavy} = V_R^{T}\, m_{heavy}\, V_R$. As V_R is related to the high-energy region, unfortunately we cannot infer heavy neutrino mixing at low energy. But they might be of importance for processes occurring at high-energy or in the early Universe. The remaining block matrices are diagonalized by a combined transformation U_I that incorporates the mentioned transformations, $U_I = \mathrm{diag}\,(U_{PMNS}, V_R)$.

To summarize this section, the full transformation, capable of diagonalizing the seesaw matrix m_{D+M}, is presented and a numerical example is given to illustrate the generation of light-neutrino masses. The full diagonal mass matrix (2.46) is obtained by application of the combined transformation

$$U_{seesaw} = \begin{pmatrix} \mathbb{1} - m_D^{*} m_R^{-1*} m_R^{-1} m_D^{T} & m_D^{*} m_R^{-1*} \\ -m_R^{-1} m_D^{T} & \mathbb{1} - \frac{1}{2} m_R^{-1} m_D^{T} m_D^{*} m_R^{-1*} \end{pmatrix} \begin{pmatrix} U_{PMNS} & 0 \\ 0 & V_R \end{pmatrix} . \tag{2.54}$$

To illustrate the type-I seesaw mechanism, we simplify the whole set-up to the case of one light and one heavy neutrino. By doing so, we avoid matrices in (2.45) and can directly infer the corresponding mass eigenvalues. The type-I seesaw mass matrix shrinks to a (2×2) matrix of the form

$$m_{D+M} = \begin{pmatrix} 0 & m_D \\ m_D & m_R \end{pmatrix} , \tag{2.55}$$

with the mass eigenvalues $m_{heavy/light} = \frac{m_R}{2} \pm \sqrt{\frac{m_R^4}{4} + m_D^2}$. Assuming the RH neutrino mass to be much heavier than the LH mass, $m_R \ll m_D$, yields the following mass eigenvalues,

$$m_{light} \approx \frac{m_D^2}{m_R} = \frac{y^2 v_{EW}^2}{m_R} , \qquad m_{heavy} \approx m_R . \tag{2.56}$$

From this expressions, it is evident how the light-neutrino masses are suppressed by heavy RH ones. Assuming a natural Dirac mass of the order of the electroweak scale $m_D \approx 100\,\mathrm{GeV}$ and large Majorana mass associated with the GUT scale $m_R \approx 10^{16}\,\mathrm{GeV}$ gives rise to light-neutrino masses $m_{light} \sim \mathcal{O}(10^{-6})\,\mathrm{eV}$. This explain the generation of very small neutrino masses in a very natural way. Of course, a huge parameter space is spanned by appropriately chosen Dirac and Majorana masses, but the origin of light-neutrino masses for generic assumptions is the strength of this model.

2.3.4. Parameter space and parametrization

Now that the basic principle of the seesaw mechanism has been shown, the model's parameter space is presented and a very useful parametrization is discussed.

The generic seesaw-Lagrangian (2.45) has in total 18 free real parameters originating from the following quantities: The diagonal heavy neutrino mass matrix contributes three real and positive masses, M_i $i = 1, 2, 3$. The remaining DOFs are given in terms of nine moduli and six phases incorporated in the neutrino Yukawa matrix y.[13]

These can be further classified according to the energy regions, where they become important. The low-energy parameters are mainly those of the SM extended with massive neutrinos: three neutrino masses (m_1, m_2, m_3) and the three mixing angles and phases from the leptonic mixing matrix U_{PMNS} (2.23) (θ_{12}, θ_{13}, θ_{23}, Dirac phase δ, Majorana phases σ and τ). Five parameters have already been measured in terms of three mixing angles ($\sin^2\theta_{12}$, $\sin^2\theta_{13}$, $\sin^2\theta_{23}$) and two mass-squared differences (Δm^2, δm^2). In addition, there exist bounds on the absolute neutrino mass scale (e.g. m_1) as well as on the Dirac phase δ, see e.g. table C.2 for current bounds. The two Majorana phases, σ and τ, are difficult to measure and can only be inferred indirectly through processes like $0\nu\beta\beta$. The remaining six parameters are related to high-energy scales and could be relevant for processes like leptogenesis [38]. The three heavy neutrino masses (M_1, M_2, M_3) and their corresponding mixing parameters in V_R (three additional angles and phases), constitute to the high-scale part of the type-I seesaw mechanism.

The 18 parameters listed with their separation into low- and high-energy regimes is just a generic choice of parametrization. The entire lepton sector of the "seesaw-augmented" SM can generally be described by the diagonalized charged lepton Yukawa matrix y^l, two diagonal matrices or equivalently their real eigenvalues, and the corresponding transformations yielding their diagonal form. In the literature, three typical parametrization are used in dependence of the particular framework, see [39] for a detailed overview.

Casas-Ibarra parametrization

The Casas-Ibarra parametrization (CIP) [85] is a very useful tool for calculations in type-I seesaw models since it uses the diagonal light and heavy neutrino mass matrices, D_m and D_M, together with the transformation that diagonalizes the light-neutrino mass matrix, U, and an additional rotation matrix R. By its application, the maximal number of, in principle, observable parameters is used, while the inaccessible ones are casted into the complex and orthogonal transformation matrix R. In the following, we will construct it from scratch, while we refer to [84] for details.

Our starting point is the type-I seesaw formula (2.52) with diagonal heavy neutrino and charged lepton mass matrices, D_N and D_l respectively. In the charged lepton basis, the diagonal light-neutrino mass matrix is then given by $D_\nu = U^T m_\nu U$ with $U \equiv U_{PMNS}$, hence making this transformation parameter accessible at low-energy. Further, we define the RH neutrino mass matrix to be

[13] The neutrino Yukawa matrix y is in general complex, yielding 18 independent DOFs. By re-phasing of the lepton fields l_α, $\alpha = e, \mu, \tau$, three phases can be absorbed such that only 15 physical DOFs remain.

diagonal, such that can safely set $m_R \to D_N$. By defining the following quantities,

$$D_{\sqrt{\nu}} \equiv \text{diag}(\sqrt{m_1}, \sqrt{m_2}, \sqrt{m_3}) \qquad D_{\sqrt{N}} \equiv \text{diag}(\sqrt{N_1}, \sqrt{N_2}, \sqrt{N_3}), \quad (2.57)$$

and using (2.52), the diagonal light-neutrino mass matrix can be re-expressed as

$$\begin{aligned} D_\nu &= U^T m_\nu U = -U^T m_D M_R^{-1} m_D^T U \\ D_{\sqrt{\nu}} D_{\sqrt{\nu}} &= U^T i m_D D_{\sqrt{N}}^{-1}\ D_{\sqrt{N}}^{-1} i m_D^T U\,. \end{aligned} \quad (2.58)$$

By multiplication of both sides with $D_{\sqrt{\nu}}^{-1}$ from left and right, a complex orthogonal matrix R is obtained:

$$\begin{aligned} \mathbb{1} &= D_{\sqrt{\nu}}^{-1} U^T i m_D D_{\sqrt{N}}^{-1}\ D_{\sqrt{N}}^{-1} i m_D^T U D_{\sqrt{\nu}}^{-1} \\ &= \left[D_{\sqrt{N}}^{-1} i m_D^T U D_{\sqrt{\nu}}^{-1}\right]^T \left[D_{\sqrt{N}}^{-1} i m_D^T U D_{\sqrt{\nu}}^{-1}\right] \\ &= R^T R\,. \end{aligned} \quad (2.59)$$

Thus, the orthogonal transformation R is given by

$$R = i D_{\sqrt{N}}^{-1} m_D^T U D_{\sqrt{\nu}}^{-1}\,. \quad (2.60)$$

On the other hand, R can generally be parametrized by three rotation matrices $R = R_{12} R_{13} R_{23}$ with R_{ij} describing the rotation in the (i,j)-plane by an complex angle $z_{ij} = z_{R,ij} + i\, z_{I,ij}$. This will proof a very useful tool in later investigation, as it allows a nice separation of high- and low-energy parameters. By this procedure the type-I seesaw parameter space is now characterized as follows; three heavy and light neutrino masses, D_m and D_N, six parameters related to the light neutrino transformation U_{PMNS}, and three complex rotation angles z_{ij}.

It should be noted that this parametrization can be extended to other seesaw mechanism at the cost of loosing the direct relation between R and U_{PMNS} given by (2.60) If the number of heavy neutrinos deviate from the generic three flavor case, the structure of this parametrization has to be modified appropriately. We encounter such a situation in the investigations of chapter 3, where we state the necessary changes.

2.4. Alternative neutrino mass generation

Of course, the type-I seesaw mechanism is not the only way of generating neutrino masses. Such mechanisms can mainly be divided into two classes: tree-level mass generation, which also includes the seesaw mechanisms, and loop-level mass generation. As both are realizable in bigger frameworks, like GUTs or left-right symmetric models, their variations are extensive. This chapter gives an overview of the different attempts to generate light neutrino masses.

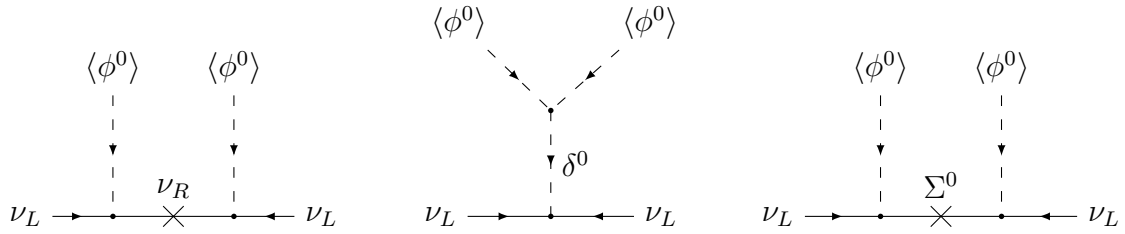

(a) seesaw type-I **(b)** seesaw type-II **(c)** seesaw type-III

Figure 2.1.: Tree-level realizations of the Weinberg operator [83].

Type-II/-III seesaw mechanism

All seesaw models have in common that the light-neutrino mass emerges from an effective dimension-5 operator, usually called Weinberg operator (2.42) and differ only in its realization through different intermediate states. These particles have to be generally very heavy such that they will only be relevant in the high-energy regime. At low-energy they are considered as non-propagating DOFs and can be integrated out, hence giving rise to a dimension-5 operator. Besides the "vanilla" type-I scenario, where fermionic RH SM singlets, are introduced, two more seesaw-like models can be found.

Type-II seesaw model Type-II seesaw mechanisms do not introduce any further fermions but instead modify the SM's scalar sector by adding a complex scalar Δ_L, transforming as a $SU(2)_L$-triplet [23–27]. Furthermore, this scalar has to be a color-singlet, carry hypercharge $Y = 1$ and is usually written as a complex (2×2) matrix of the form

$$\Delta_L = \begin{pmatrix} \frac{\delta^+}{\sqrt{2}} & \delta^{++} \\ \delta^0 & \frac{\delta^+}{\sqrt{2}} \end{pmatrix} . \tag{2.61}$$

It gives rise to the following Lagrangian,

$$\begin{aligned} \mathcal{L}_{II} = & Tr\left[(D_\mu \Delta_L)^\dagger (D^\mu \Delta_L)\right] - m_\Delta^2 Tr\left[\Delta_L^\dagger \Delta_L\right] \\ & + \frac{1}{2}\left(-\lambda^\Delta_{\alpha\beta} L_\alpha^T C i\sigma_2 \Delta_L L_\beta + \lambda^\phi \phi^T i\sigma_2 \Delta_L \phi + \text{h.c.}\right) , \end{aligned} \tag{2.62}$$

with λ^Δ the (3×3) complex matrix of dimensionless Yukawa couplings between the triplet and fermionic doublets and λ^ϕ as dimensionless coupling between the two scalars. As the scalar triplet is assumed to be very heavy, integrating it out gives rise to the Weinberg operator, thus, after SSB a neutrino mass term of the form

$$m_\nu^{II} = \frac{\lambda^\Delta \lambda^\phi v_{EW}^2}{m_\Delta^2}. \tag{2.63}$$

Increasing the triplet mass generically reduces the light-neutrino mass and hence leads to a seesaw mechanism. This model has in general eleven real DOFs; nine

coming from the new complex, symmetric Yukawa matrix, that are accessible at low-energy, as well as the heavy triplet mass m_Δ and the coupling the SM Higgs ϕ, which are relevant at high-energy. In addition, no appropriate assignment of lepton number to Δ_L is possible, indicating the appearance of lepton number violating processes. CP-violation might originate from phases of the new Yukawa coupling λ^Δ and λ^ϕ. The new scalar also interact with the SM $SU(2)_L$ gauge bosons and could spoils the well-tested ρ-parameter, $\rho \equiv \frac{m_W^2}{m_Z^2 \cos^2\theta_W} = (1 \text{ in the SM})$, if the neutral component δ^0 acquires a VEV. Special care has to be taken in suppressing such contributions. Electroweak precision measurements constrains the neutral component's VEV to be of $\mathcal{O}(1\,\text{GeV})$ [86].

Type-III seesaw - Triplet fermions The type-III model enhances the fermion sector, but instead of fermionic singlets, $SU(2)_L$-triplets are introduced [28–30]. In this framework, they carry hypercharge $Y = 0$, are color singlets and again arranged in a (2×2) matrix,

$$\Sigma = \begin{pmatrix} \frac{\Sigma^0}{\sqrt{2}} & \Sigma^+ \\ \Sigma^- & \frac{\Sigma^0}{\sqrt{2}} \end{pmatrix} . \tag{2.64}$$

The Lagrangian of this SM extension is written as

$$\mathcal{L}_{III} = tr\left[\bar{\Sigma} \not{D} \Sigma\right] - \frac{1}{2} tr\left[\bar{\Sigma} m_\Sigma \Sigma^c + \bar{\Sigma}^c m_\Sigma^* \Sigma\right] - \sqrt{2}\bar{L}\lambda_\Sigma^\dagger \Sigma i\sigma_2 \phi + \text{h.c.}\,, \tag{2.65}$$

with λ_Σ as (3×3) complex dimensionless Yukawa matrix and m_Σ being the triplet mass matrix. Integrating out the heavy DOFs, leads again to a dimension-5 operator and, thus, neutrino mass generation according to

$$m_\nu^{III} = v_{EW}^2 \lambda_\Sigma^T m_\sigma^{-1} \lambda_\sigma \,. \tag{2.66}$$

This implements a "seesaw" between the neutrino masses and the heavy triplet mass. This type-III ansatz has 15 free parameters, similar to the type-I case, and an effective description is also obtained by the general seesaw mass matrix of (2.45), setting $m_L = 0$. Equivalent to the previous case, consistent lepton number assignment is impossible for the lepton triplet Σ, hence implementing LNV. CP violating processes are introduced by the complex phases of the Yukawa coupling matrix λ_Σ.

The three types of seesaw model are merely indistinguishable at low-energy since elimination of heavier states yields the same operator. Only be taking into account further model-specific processes, like occurring double-charged particles in the type-II context, one might be able to separate their phenomenology. But all in all, only at high-energy all three models show their distinct properties when the heavy states become dynamical DOFs again.

Radiative neutrino mass generation

In contrast to seesaw mechanisms, where effective tree-level mass generation is the driving principle, the class of radiative neutrino mass generation aim for loop-level

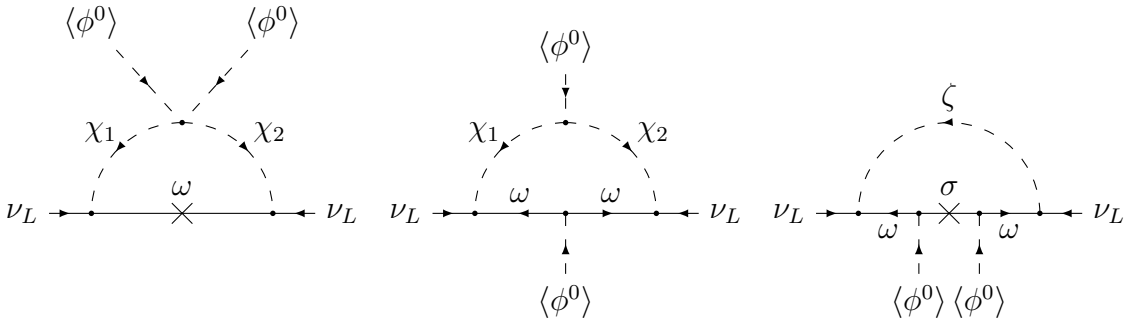

Figure 2.2.: One-loop realizations of the Weinberg operator as given in [29].

realizations of the Weinberg operator (2.42). The fundamental principle behind this ansatz is that, in quantum field theory, mass shifts can be introduced through radiative corrections. The occurring loop suppression factor $(4\pi)^{-2}$ allows the intermediate particles, propagating in the loop, to have lower masses down to TeV scales, that can in principle be probed at the LHC or future colliders. Three different loop-level realizations are shown in figure 2.2. The first diagrams is, i.e. used in the scotogenic model [35], where an additional scalar in the loop leads to the neutrino mass generation. Of course, more scalars or fermions can be used. Zee-Wolfenstein models [32,33] are based on the realization of the second diagram and the third one is used in the model of Babu and Ma [34]. A more general classification is done by grouping the models, in how the full mass spectra are obtained: either going to higher loop orders [31] or using effective operators of higher dimensions [36]. An overview of the mentioned mechanisms is given in [87].

Dirac seesaw and more exotic models

Of course, there exist also models that assume the neutrino's particle nature to be of Dirac type and just add yet undiscovered RH neutrino components. A specific example of the Dirac seesaw has been found by Mohapatra and Valle [88] in the context of a SUSY model,i.e. two Higgs doublets. The quintessence is the existence of a chiral $U(1)$ symmetry, which forbids the RH neutrino component to have a Dirac mass. On the contrary, heavy singlet fermions, $\bar{N}_R$ and N_L with opposite $U(1)$-charges receive a usual Dirac mass and couple to usual SM leptons. Another Higgs χ is introduced for $U(1)$-breaking and contributes further Yukawa coupling. The corresponding Lagrangian is given by

$$\begin{aligned}\mathcal{L}^D_{Seesaw} &= g\bar{N}_R l_L \phi_1 + h\bar{\nu}_R N_L \chi + M\bar{N}_R N_L \\ &= (\bar{\nu}_R, \bar{N}_R)\begin{pmatrix} 0 & g\langle\chi\rangle \\ g\langle\phi_1\rangle & M\end{pmatrix}\begin{pmatrix}\nu_L \\ N_L\end{pmatrix} \quad \Longrightarrow \quad m_\nu^D \simeq hg\frac{\langle\chi\rangle\langle\phi_1\rangle}{M}\,,\end{aligned} \tag{2.67}$$

where $\langle\chi\rangle$ and $\langle\phi_1\rangle$ reflect the Higgs VEVs and h, g the corresponding Yukawa couplings. As $\bar{\nu}_R$ and N_L do not couple to χ, lepton number remains conserved.

Dirac neutrino masses can also emerge from more exotic theories, e.g. higher-dimensional models discussed as a solution to the hierarchy problem [89]. The underlying assumption is that Nature may be realized in a $(4+1)$-dimensional

space, whereas our would with the SM is located on a (3+1)-dimensional boundary. By integrating out the extra-dimension, which is assumed to be finite, from the five-dimensional Einstein-Hilbert action, leads to a reduced Planck mass, such that the weakness of gravity is understood as a result from compactification of the fifth dimension. As the RH neutrino component does not couple to the SM (boundary), it can be located into the fifth dimension with a possible Yukawa interaction at the SM boundary [90,91]. Integrating over the extra-dimension generates a suppressed Yukawa interaction,

$$\mathcal{S}_4 = \int \sqrt{-g_4}\bar{\nu}_R \partial\!\!\!/ \nu_R \, d^4x + \int \sqrt{-g_4}\frac{M_*}{m_{Pl}} y_\nu \bar{\nu}_R L_L \phi \, d^4x + \text{h.c.}\,, \tag{2.68}$$

where $\sqrt{-g_4}$ is the determinant of the four-dimensional metric and M_* the reduced Planck mass. Assuming $y_\nu \sim 1$ and $M_* \sim 1\,\text{TeV}$, yields a small Dirac neutrino mass $m_\nu^D \simeq 10^{-5}\,\text{eV}$.

2.5. Leptogenesis

To close the chapter about massive neutrinos, we want to briefly discuss an important scenario called leptogenesis that may contribute to the generation of the Universe's baryon asymmetry [38]. According to the Sakharov conditions [92], three ingredients are needed in the early Universe to account for the observed BAU: baryon number-violation, C and CP violation as well as some interaction dropping out of thermal equilibrium. Key ingredient of the leptogenesis framework is that a CP-asymmetry is created the lepton sector through the decay of heavy singlet neutrinos, which are naturally present in the type-I seesaw framework. The created asymmetry is then transfered into the baryon sector through so-called sphaleron processes [93–95]. These are non-perturbative effects that arise from the SM's chiral anomaly [54] and violate $B+L$ quantum number, while preserving $B-L$.[14] At temperatures above the electroweak phase transition (EWPT), these effects occur frequently and lead to rapid $B+L$ violating particle reactions, which are used to transfer the created lepton asymmetry into the baryon sector.

The leptonic CP-asymmetry, ϵ, originates from heavy Majorana neutrino decays, that violate lepton number; more precisely from the interference between tree- and loop-level decays, see figure 2.3.

The net lepton asymmetry $\epsilon_{\alpha\alpha}$ in a certain flavor α from the decay of a heavy Majorana neutrino N_1 is given by

$$\epsilon_{\alpha\alpha} \equiv \frac{\Gamma\left(N_I \to H\, L_\alpha\right) - \Gamma\left(N_I \to \bar{H}\, \bar{L}_\alpha\right)}{\Gamma\left(N_I \to H\, L_\alpha\right) + \Gamma\left(N_I \to \bar{H}\, \bar{L}_\alpha\right)}\,. \tag{2.69}$$

The departure from thermal equilibrium is guaranteed by the Universe's expansion. Any interaction rate that is at the order, or slower, than the Hubble rate H is not fast enough to reach equilibrium anymore. Simultaneous to heavy neutrino decays,

[14] B and L refer to baryon and lepton number respectively.

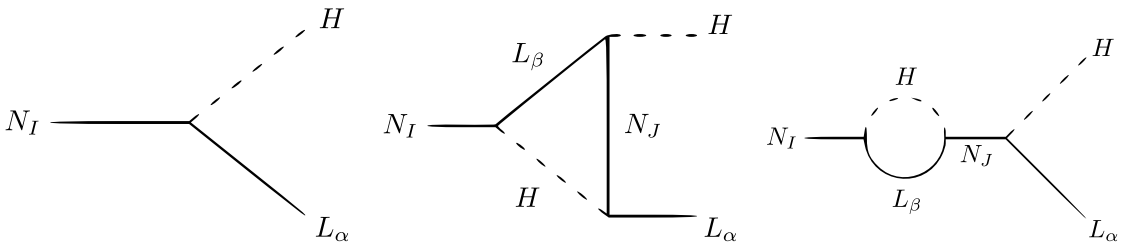

Figure 2.3.: Possible heavy neutrino decays in the leptogenesis scenario. Interference between the tree-level diagram, right diagrame and the loop-level diagrams, middle and left diagrame, gives rise to $\not{CP}$.

inverse-decay processes are taking place that redistribute any previously produced net asymmetry ϵ. Hence, a remaining lepton asymmetry is only created if the decay process exceeds its inverse reaction. These dynamics are usually described in terms of Boltzmann equations, although analytic approximations for certain regions of "time" evolution are possible [52]

One can imagine that the entire scenario can be arbitrarily complex, depending on how many heavy neutrinos contribute, or whether flavor and thermal effects are taken into account. A review, where all these aspects can be find in [39]. There, a simple toy model is presented, assuming only contributions of one heavy neutrino N_1 to the lepton asymmetry of a single flavor α. A hierarchical structure among the heavy neutrinos is assumed, whereas only the lightest, N_1, is considered as propagating and contributing to leptogenesis. The (thermal) leptogenesis mass scale is approximated by the mass of the decaying particle, $\Lambda \sim M_1 \sim 10^9$ GeV. The approximated BAU, in terms of the number-to-entropy density ratio, is described through the following expression, where each Sakharov condition contributes one suppression factor [39],

$$Y_{BAU} \simeq \frac{135\,\zeta(3)}{4\pi^4 g_*}\epsilon_{\alpha\alpha} \times \eta_\alpha \times \mathcal{C}\,, \tag{2.70}$$

where $\zeta(x)$ is the Riemann zeta function, η_α an efficiency factor due to inverse decays or other "washout" effects and $\mathcal{C}$ represents a reduction factor due to occurring Yukawa interaction and sphaleron processes. $g_* \simeq 106$ corresponds to the available SM DOFs. In the leptogenesis scenario, the baryon number violation is provides by the sphaleron processes. The heavy neutrino decays are responsible for $\not{CP}$, which also implies C violation, and the Universe's accelerated expansion leads to out-of-equilibrium dynamics if the interaction rate drops below the Hubbe rate H. In the end, we want to mention that the generic case of thermal leptogenesis suffers from problems due to the contributing heavy particles. Induced radiative corrections to the Higgs mass parameters μ^2, arising from a heavy neutrino mass of $\mathcal{O}(10^9)$ GeV, contradict with arguments of electroweak naturalness [96]. Furthermore their decay would lead to gravitino overproduction in the universe, which would have been already measured, see [97] and references therein. One can lower the relevant heavy neutrino mass by using nearly-degenerate neutrinos, such that their decay is enhanced due to resonance effects. Such scenarios are referred to as the term "resonant leptogenesis" [98–100] and will be of importance in chapter 4.

3. From CP phases to Yukawa textures

In the following a minimal realization of the type-I seesaw model with so-called two-zero texture in the neutrino Yukawa matrix is studied under the assumption of small perturbations instead of exact zeros. In a data-driven, bottom-up approach possible Yukawa structures for normal and inverted mass ordering are investigated concerning their consistency with recent low-energy neutrino observables. This chapter deals with the procedures and results of [50] and complements the gained knowledge, where it is necessary.

3.1. Motivation and general approach

After the first detection of neutrino oscillations, a lot of effort has been spent to measure underlying neutrino parameters, i.e. three mixing angles and two mass-squared differences, see section 2.2 and for details [101]. Up to now, all mentioned parameters have been measured with satisfying accuracy [77] and only the absolute neutrino mass scale [9] as well as leptonic CP violating effects [102] remain undetected. The later is strongly expected from theory-site since it is associated with a non-vanishing Dirac phase δ in present the leptonic mixing matrix U_{PMNS} [59, 63, 73]. Experiments attempting to measure both outstanding questions are going to be build, or already under commissioning, e.g. KATRIN [12] for the absolute neutrino mass scale and DUNE [103] to measure occurring phases in neutrino mixing. Current oscillation experiments like NOνa [13] and T2K [14] prove that experimental methods have reached a level of sensitivity that makes deeper investigations of $\not{CP}$ in the neutrino sector possible. While the experimental site is taking steps towards measuring the last missing quantities in the low-energy neutrino sector, the question arises, whether one is able to infer any properties related to the UV regime. For example, is it possible to make a statement about $\not{CP}$ at high-energy, which could have important consequences for the generation BAU in the early universe [38] or can we learn more about mechanisms generating neutrino masses at high scales?

In the following, the influence of experimental progress, i.e. a measured CP phase δ, is approached in the context of a minimal type-I seesaw scenario, picked because of its simplicity in generating neutrino masses, see section 2.3. Due to a large parameter space, prediction of distinct signatures or properties at low-energy is very difficult in the generic seesaw framework and a lot of work has been done to circumvent this issue. For example, the assumption of a certain flavor symmetry at high-energy could restrict interactions in the leptonic sector, hence reducing

the number of free parameters relevant for the seesaw mechanism [104, 105]. This comes with the cost of introducing additional scalars, which would increase the model's particle content and shift the problem just to higher energies. A more pragmatic way is to work only with two heavy neutrinos, reducing three complex Yukawa couplings [41–43, 45]. This could, for instance, be an effective description of a situation, in which two heavy neutrinos have masses of the same order of magnitude and a third one being much heavier. As a barely propagating DOF it is then said to decouples from the theory and, as a result, the main low-energy neutrino phenomenology would be dictated by the two lighter ones. This minimal type-I model with two RH neutrinos has only four parameters left; among them two CP phases. Being more predictive comes with the cost of one light neutrino being exactly massless. In the spirit of Ockham's razor this framework is enough to reproduce the current observed phenomena and yields an sufficient effective description for an appropriately low neutrino mass scale [106]. Further, the CP phase δ in the resulting leptonic mixing matrix enters the effective neutrino mass $\langle m_{ee} \rangle$, accessible in $0\nu\beta\beta$ experiments like GERDA [11], and direct mass measurements performed in KATRIN. Additionally, these models provide enough $\not{CP}$ for successful baryogenesis via leptogenesis [92, 107]. Together, this yields constraints, or at least some benchmarks, a successful high-energy theory for neutrino masses has to fulfill. Recently such kind of models have been studied in the context of resonant leptogenesis [99, 108] and further theoretical arguments like naturalness, vacuum (meta-)stability and detectable $0\nu\beta\beta$ [109]. Constraints in terms of so-called zero-texture, entries in the neutrino Yukawa matrix equaling exactly zero, originate from a flavor symmetry at much higher energies and reduce the number of free parameters even further [45, 110–112]. This ansatz has proven successful in the past for prediction of the Cabibbo angle [113], but all such approaches share common reliance on some kind of high-energy origin; justifying their name as so-called top-down approaches.

This chapter heads directly into the opposite direction and choses a bottom-up approach by only referring to experimental data and remaining as model-independent as possible within the given framework of a minimal type-I seesaw model. From theory-site it is expected that exact zeros within the Yukawa matrix experience some perturbation by radiative or gravitational corrections [114], such that we relax this assumption and allow instead for some small parameter. Of course, this enlarges the valid parameter space, but in principle a precise study of Yukawa structures and corresponding hierarchies among couplings, consistent with experimental data, should be possible without relying on some specific UV flavor model. In this way, our approach concerns all possible flavor models, which can be implemented in the seesaw framework, and further qualifies how large perturbations for certain Yukawa structures are allowed to be for consistency with experiments. The precise UV model, creating an exact zero-texture within the neutrino Yukawa matrix, will still give some prediction for the yet unmeasured CP phases at low-energy. By allowing for small perturbations at the position of the exact zero entry, we can assign a theoretical error bar to the definite prediction. From the top-down point of view, the following investigation can be seen

as a generalization of the usually performed texture ansatz. One could criticize this approach since the direct connection to a certain symmetry is lost, but as we expect the assumed flavor symmetry to be broken at some high-energy, we are not able to directly infer it from the low-energy anyway. From the bottom-up perspective, this approach is most agnostic about UV physics and effectively helps to distill even more knowledge out of experimental data.

3.2. Minimal type-I seesaw model with two heavy neutrinos

As already mentioned, the framework of this investigation is a minimization of the generic seesaw type-I mechanism, in the sense of only having two instead of three RH neutrinos. All steps presented in chapter 2 are equivalent, up to some small modifications in the corresponding states and matrices respectively. In this section, we will give a short overview of the modified formalism and comment on the zero-texture ansatz, commonly applied at high-energy.

Starting point is the seesaw Lagrangian with all possible mass terms (2.43), but with the difference of ν_R just being a two-component vector in flavor-space. This directly reduces the Majorana mass term to a (2×2) matrix. Now, the Dirac mass matrix, or the neutrino Yukawa matrix respectively, has to be of (3×2) structure. The procedures presented in section 2.3 can be adjusted in terms of ν_L being a usual three-component vector in flavor space, whereas ν_R has two components now. After diagonalization, one arrives at the expected light neutrino Lagrangian and the familiar type-I seesaw formula (2.52),

$$\mathcal{L}_{min} = -\bar{\nu}_L\, m_{light}\, \nu_L\,, \qquad\qquad m_{light} = -m_D\, m_R^{-1}\, m_D^T\,, \tag{3.1}$$

with the Dirac mass matrix being of (3×2) type and the Majorana mass matrix being (2×2) as assumed above. Hence, the light neutrino mass matrix m_{light} has rank two, which is the reason why one neutrino has to remain exactly massless. A simple illustration of this minimal seesaw framework is given by figure 3.1. As mentioned in section 2.3, the sign of the atmospheric neutrino mass squared-difference it yet unknown, thus allowing for different mass arrangements in the light neutrino sector. In our context, only the normal mass hierarchy $m_1 \ll m_2 \ll m_3$ and the inverted mass hierarchy $m_3 \ll m_1 \ll m_2$ are relevant and the definition of mass-squared difference (2.35) yields the following mass spectra,

$$\begin{aligned}
&\text{NH:}\quad m_1 = 0\,, && \text{IH:}\quad m_1 = \sqrt{-\Delta m^2 - \frac{1}{2}\delta m^2}\,,\\
&\qquad m_2 = \sqrt{\delta m^2}\,, && \qquad m_2 = \sqrt{-\Delta m^2 + \frac{1}{2}\delta m^2}\,,\\
&\qquad m_3 = \sqrt{\Delta m^2 + \frac{1}{2}\delta m^2}\,, && \qquad m_3 = 0\,.
\end{aligned} \tag{3.2}$$

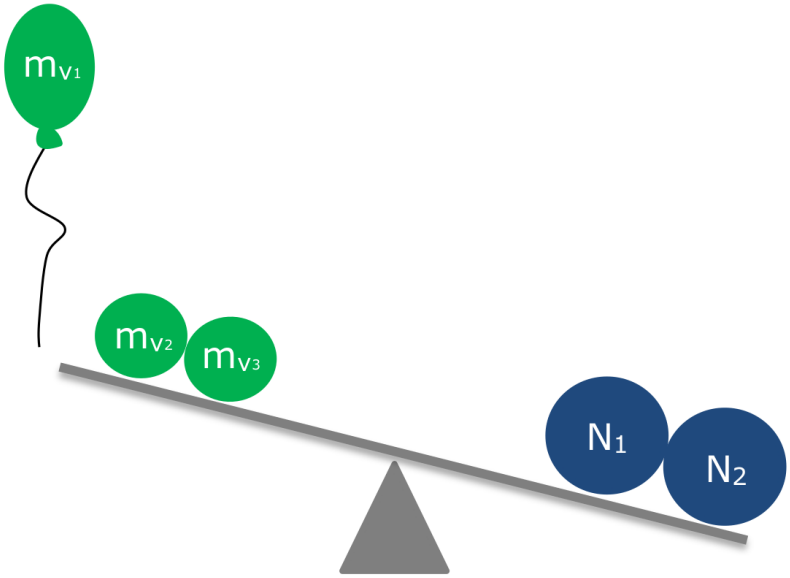

Figure 3.1.: Illustration of the minimal type-I seesaw model. Due to the reduced rank of the neutrino mass matrix, one particle remains massless, while the others obtain light masses through suppression by the two heavy neutrino masses. The corresponding values can be obtained through (3.2) according to the underlying mass ordering.

The diagonalization is performed, as usual, by going into the charged lepton basis and using an unitary transformation according to (2.20), leading to the identification of U with the leptonic mixing matrix U_{PMNS}. We have already discussed the feature of additional phases in the leptonic mixing matrix for the generic case of three Majorana neutrinos, see section 2.2. Since we are dealing with a reduced number of heavy Majorana neutrinos only *one* additional phase σ arises, besides the conventional Dirac phase δ in the PMNS matrix, which is given by (2.25),

$$U = \begin{pmatrix} c_{12}\, c_{13} & s_{12}\, c_{13} & s_{13}\, e^{-i\delta} \\ -s_{12}\, c_{23} - c_{12}\, s_{13}\, s_{23}\, e^{i\delta} & c_{12}\, c_{23} - s_{12}\, s_{13}\, s_{23}\, e^{i\delta} & s_{23}\, c_{13} \\ s_{12}\, s_{23} - c_{12}\, s_{13}\, c_{23}\, e^{i\delta} & -c_{12}\, s_{23} - s_{12}\, s_{13}\, c_{23}\, e^{i\delta} & c_{23}\, c_{13} \end{pmatrix} \begin{pmatrix} 1 & 0 & 0 \\ 0 & e^{i\sigma} & 0 \\ 0 & 0 & 1 \end{pmatrix} . \quad (3.3)$$

As we know from section 2.2, the phases in the leptonic mixing matrix lie in different domains, $\delta \in [0, 2\pi)$ and $\sigma \in [0, \pi)$, due to their different origins.

We chose this minimal approach of only two RH neutrinos due to its reduced of parameter space, which we will now justify by comparing its DOFs with the generic three-neutrino case. The neutrino Yukawa couplings are incorporated in a complex (3×2) matrix, having in total twelve real DOFs. Three of those can be absorbed into the charged lepton fields, which gives nine real parameters in contrast to the generic case exhibiting fifteen reals DOFs. Although the RH neutrino mass could also be counted, it can be absorbed into the Yukawa couplings without loss of generality since the following transformation allows to compensate

for any rescaling in the seesaw formula (2.52),

$$m_i \to m_i^{'} \qquad\qquad y_{\alpha i} \to \sqrt{\frac{m_i^{'}}{m_i}} y_{\alpha i}\,. \tag{3.4}$$

The nine DOFs at high-energy have to match all low-energy observables, which are given by three mixing angles θ_{12}, θ_{13} and θ_{23}, two CP phases δ and σ and two mass-squared differences, δm^2 and Δm^2. [1] A common way to relate these parameters of different energy regions is the CIP, see section (2.3), which will prove very convenient below. In the case of the seesaw formula (2.52), the individual CIP quantities have to be adjusted to the reduced number of heavy neutrinos. We have already discussed this parametrization in detail, such that we can rely on the formulas given in section 2.3. Taking the orthogonal transformation matrix R (2.60) and rearranging it, yields an expression for the neutrino Yukawa matrix,

$$y = \frac{i}{v_{EW}} U^* D_{\sqrt{\nu}}\, R\, D_{\sqrt{N}}\,, \tag{3.5}$$

where we have the matrices with square-root mass eigenvalues on the diagonal of light $D_{\sqrt{\nu}}$ and heavy neutrinos being $D_{\sqrt{N}}$ being a (3×3) and (2×2) matrix, respectively. Further, the complex conjugated leptonic mixing matrix U^* is present as well as a (3×2) "rotation" matrix R with complex angle z, where the latter is related to two remaining DOFs in the high-energy regime. It is to mention that R is not exactly an orthogonal matrix in case of only two heavy neutrinos, as it only satisfies $R^T R = \mathbb{1}_2$, but not $RR^T = \mathbb{1}_3$. In addition, R differs for normal and inverted mass ordering,

$$\begin{aligned} \text{NH:}\quad & m_1 = 0\,, \quad R = \begin{pmatrix} 0 & 0 \\ \cos z & -\sin z \\ \eta \sin z & \eta \cos z \end{pmatrix}\,, \\ \text{IH:}\quad & m_3 = 0\,, \quad R = \begin{pmatrix} \cos z & -\sin z \\ \eta \sin z & \eta \cos z \\ 0 & 0 \end{pmatrix}\,. \end{aligned} \tag{3.6}$$

The parameter $\eta = \pm 1$ is used to distinguish between two different branches of possible rotation matrices R, named according to the sign of η. It is possible to map both branches onto each other, but before doing this, we will define two dimensionless quantities to simplify notation. From now, we will switch to index-notation since it allows to write expressions in a more compact form. The two quantities of our interest are the rescaled version of the Yukawa coupling matrix κ and the dimensionless version of the leptonic mixing matrux V,

$$\kappa_{\alpha I} = -i\, y_{\alpha I} \sqrt{\frac{v_{\text{ew}}}{M_I}}\,, \qquad\qquad V_{\alpha i} = U^*_{\alpha i} \sqrt{\frac{m_i}{v_{\text{ew}}}}\,, \tag{3.7}$$

[1] In our context, the absolute neutrino mass scale is assumed to be vanishingly small as one neutrino must be massless. The other masses are then just simply constructed according to (3.2).

which allow us to remove any dimension from the CIP and rewrite our parameter set even more compactly,

$$\begin{pmatrix} \kappa_{\alpha 1} \\ \kappa_{\alpha 1} \end{pmatrix} = \begin{pmatrix} \cos z & \eta \sin z \\ -\sin z & \eta \cos z \end{pmatrix} \begin{pmatrix} V_{\alpha k} \\ V_{\alpha l} \end{pmatrix} , \tag{3.8}$$

with $(k, l) = (2, 3)$ for normal hierarchy (NH) and $(k, l) = (1, 2)$ for inverted hierarchy (IH). The couplings of both branches are related via the following relation [40],

$$\kappa^-_{\alpha 1}(z) = -\kappa^+_{\alpha 2}(\frac{\pi}{2} - z) , \qquad \kappa^-_{\alpha 2}(z) = -\kappa^+_{\alpha 1}(\frac{\pi}{2} - z) . \tag{3.9}$$

Hence, couplings from the negative branch follow from their positive counter-part by application of the following steps:

1. Sign-flip of all coupling constants: $\kappa_{\alpha i} \to -\kappa_{\alpha i}$
2. Exchange of both matrix columns: $\kappa_{\alpha 1} \leftrightarrow \kappa_{\alpha 2}$
3. Shift of the complex rotation angle z: $\Re(z) \to \frac{\pi}{2} - \Re(z)$

Due to this properties, it suffices to select just one branch since a mapping to the other one is always possible by the above instructions. Without loss of generality, we set $\eta = 1$ for the rest of our investigation, thus remaining in the CIP's positive branch.

By absorption of neutrino masses in the Yukawa couplings and the mixing matrix respectively, the right-hand sides of (3.8) do no longer depend on the heavy neutrino masses and we achieve a nice separation according to the parameter's energy scale. Now, only high-energy parameter appear on the right-hand site, while low-energy observables remain on the left-hand site with the complex rotation angle z linking them to the UV domain. In our pursuit of finding maximal realizable hierarchies between different Yukawa entries, this rotation angle can be viewed from the low-energy regime as an auxiliary parameter, that tunes a certain hierarchy according to the high-energy assumption. Hence, scanning it helps us to find the strongest realizable Yukawa structures. During our analysis a more general procedure was developed, which uses exactly one of these steps.

3.2.1. The zero-texture ansatz

Before diving into the details of our study, common approaches of zero-texture in the minimal type-I seesaw model are discussed. A usual procedure to reduce a model's DOFs or to explain the dominance of some interaction is to assume a certain symmetry at a higher energy scale that causes small or vanishing entries in the corresponding coupling matrix. Especially in flavor-related topics, such assumptions are of common use [115]. An exact zero-texture in the neutrino Yukawa matrix could, for example, rely on some high-energy flavor symmetry that is broken at lower scales. Naively, one would expect that such zero entries receive perturbations due to radiative corrections or gravitational effects [114]. Before we

cover a more general case with our analysis, we repeat the consequences of such leading order zero-texture approaches.

Regarding the minimal type-I seesaw scenario, a lot of work has been done [112, 116] in the last years that shall be summarized now. Note, that we already deal with a reduced parameter space as only two RH neutrinos are introduced. It is expected that further assumptions result in new connections among the remaining DOFs and as a consequence the model's consistency with experimental data is to be checked for each individual case. At this point, the issue with top-down approaches becomes evident, as one has to apply a symmetry, that may result in some specific Yukawa pattern in our minimal seesaw model. Then, the resulting phenomenology must be consistent with low-energy observables. While the Dirac CP phase is to be measured in the upcoming years, it is even unclear if a related exact high-energy model exists or can be identified. Moreover, multiple models could predict the same Dirac phase, making the situation even more complicated.

One-zero textures

In our minimal seesaw model, it is always possible to set one entry of the neutrino Yukawa matrix to an exact zero. Such one-zero texture approaches have been studied in the context of normal mass ordering [111] and successful leptogenesis [116]. Therein, the demand of having one exact zero leads to connections among two matrix entries such that a matching between experimental observables and theoretical DOFs can be achieved. Six Yukawa textures can be obtained that result in different phenomenological consequences that have to agree with experimental data, subsequently. The application of our dimensionless CIP (3.8) helps to find the complex rotation angle z that sets the desired entry to an exact zero,

$$\begin{aligned} \text{NH:}\quad & \kappa_{\alpha 1} = 0 \quad \Rightarrow \tan z = -\frac{V_{\alpha 2}}{V_{\alpha 3}}\,, \qquad \text{IH:}\quad \kappa_{\alpha 1} = 0 \quad \Rightarrow \tan z = -\frac{V_{\alpha 1}}{V_{\alpha 2}}\,, \\ & \kappa_{\alpha 2} = 0 \quad \Rightarrow \tan z = +\frac{V_{\alpha 3}}{V_{\alpha 2}}\,, \qquad\qquad\;\; \kappa_{\alpha 2} = 0 \quad \Rightarrow \tan z = +\frac{V_{\alpha 2}}{V_{\alpha 1}}\,. \end{aligned} \tag{3.10}$$

The above conditions determine the complex rotation angle z as the ratio of two Yukawa elements, which can easily be calculated by inserting the experimental observables of table C.2.

Two-zero textures

Two zeros within the neutrino Yukawa matrix are the most minimal assumption that is allowed by current data sets [45, 106]. The implementation of further zero entries would lead to vanishing mixing angles at low-energy, clearly in disagreement with the measured observables. In this sense the type-I seesaw model with two RH neutrino and a two exact-texture is the minimal realization possible at the moment. Setting two entries of the (3×2) neutrino Yukawa matrix to zero, yields in total fifteen possible patterns that can be grouped in different texture classes. In the notion of [112], the following two-zero textures for the Yukawa matrix κ are

realizable,

$$
\begin{aligned}
A_1 &: \begin{pmatrix} 0 & 0 \\ \times & \times \\ \times & \times \end{pmatrix}, \quad A_2 : \begin{pmatrix} \times & \times \\ 0 & 0 \\ \times & \times \end{pmatrix}, \quad A_3 : \begin{pmatrix} \times & \times \\ \times & \times \\ 0 & 0 \end{pmatrix}, \\
B_1 &: \begin{pmatrix} 0 & \times \\ \times & 0 \\ \times & \times \end{pmatrix}, \quad B_2 : \begin{pmatrix} 0 & \times \\ \times & \times \\ \times & 0 \end{pmatrix}, \quad B_3 : \begin{pmatrix} \times & \times \\ 0 & \times \\ \times & 0 \end{pmatrix}, \\
B_4 &: \begin{pmatrix} \times & 0 \\ 0 & \times \\ \times & \times \end{pmatrix}, \quad B_5 : \begin{pmatrix} \times & 0 \\ \times & \times \\ 0 & \times \end{pmatrix}, \quad B_6 : \begin{pmatrix} \times & \times \\ \times & 0 \\ 0 & \times \end{pmatrix}, \\
C_1 &: \begin{pmatrix} 0 & \times \\ 0 & \times \\ \times & \times \end{pmatrix}, \quad C_2 : \begin{pmatrix} 0 & \times \\ \times & \times \\ 0 & \times \end{pmatrix}, \quad C_3 : \begin{pmatrix} \times & \times \\ 0 & \times \\ 0 & \times \end{pmatrix}, \\
C_4 &: \begin{pmatrix} \times & 0 \\ \times & 0 \\ \times & \times \end{pmatrix}, \quad C_5 : \begin{pmatrix} \times & 0 \\ \times & \times \\ \times & 0 \end{pmatrix}, \quad C_6 : \begin{pmatrix} \times & \times \\ \times & 0 \\ \times & 0 \end{pmatrix}.
\end{aligned}
\tag{3.11}
$$

Moreover, the constraints of having two Yukawa entries being exactly zero, leads to new connections between the other matrix elements. Instead of two entries, now four Yukawa coupling are intertwined according to

$$
(\kappa_{\alpha I}, \kappa_{\beta J}) = (0,0)\,, \quad (\alpha, I) \neq (\beta, J) \quad \Rightarrow \quad \frac{V_1}{V_2} = \pm \frac{V_3}{V_4}\,. \tag{3.12}
$$

These connections give the two-zero texture ansatz a very strong prediction power and extensive studies showed that only four of the presented patterns are compatible with observations in the case of IH [112]. NH in context of the minimal type-I seesaw exhibiting exact two-zero textures is always inconsistent with experimental data! The still valid textures for IH, are B_1, B_4, B_2 and B_5, while the first and last two only differ by an exchange of matrix columns. The case of two-zero textures but three heavy neutrinos is covered in [106]. The model's strong predictive power manifests itself in precise forecasts for the Dirac and Majorana CP phases, δ and σ. To leading-order (LO) in the reactor mixing angle s_{13} [112], they are given by

$$
\cos\delta \simeq \begin{cases} +\frac{\sin 2\theta_{12}\left(1-m_1^2/m_2^2\right)}{4\tan\theta_{23}\sin\theta_{13}} - \frac{\tan\theta_{23}\sin\theta_{13}}{\tan 2\theta_{12}} \\ -\frac{\sin 2\theta_{12}\left(1-m_1^2/m_2^2\right)}{4\cot\theta_{23}\sin\theta_{13}} + \frac{\cot\theta_{23}\sin\theta_{13}}{\tan 2\theta_{12}} \end{cases}, \quad \cos 2\sigma \simeq \begin{cases} 1 - \frac{\tan^2\theta_{23}\sin^2\theta_{13}}{2\sin^2\theta_{12}\cos^2\theta_{12}} & (B_{1,4}) \\ 1 - \frac{\cot^2\theta_{23}\sin^2\theta_{13}}{2\sin^2\theta_{12}\cos^2\theta_{12}} & (B_{2,5}) \end{cases}. \tag{3.13}
$$

With the measured mass-squared differences and mixing angles of table C.2 one can determine the points of exact two-zero textures as

$$
\frac{(\delta,\sigma)}{\pi} \simeq \begin{cases} (0.51, 0.94) \quad \text{or} \quad (1.49, 0.06) & (B_{1,4}) \\ (0.50, 0.04) \quad \text{or} \quad (1.50, 0.96) & (B_{2,5}) \end{cases}. \tag{3.14}
$$

Therefore, by a future measuring of the Dirac phase δ one can roughly discriminate between the valid textures and give some expectation for the Majorana phase σ.

Or rephrased, by measuring both CP phases, δ and σ, one is capable of pinning down the structure of the neutrino Yukawa matrix. These kind of statements are just true, if our framework is a valid, at least effective, description of nature. One interesting fact about the valid Yukawa structures is to be mentioned:
All patterns with two-zero texture, that are in agreement with current observations, exhibit a Dirac phase δ that is close-to-maximal CP violating with a value of $\delta \simeq \pm\frac{\pi}{2} \mod 2\pi$, according to (2.38).

3.3. Agnostic approach and identification of Yukawa hierarchies

Our framework's clear prediction (3.14) results in a maximal reduction of valid parameter space and represents the minimal possible realization that is consistent with current experimental data. If the CP phases are measured as predicted, it confirms the assumed model at least as an effective description of nature. As former experiments taught us, nature does not always reveals itself the way we want it to be. So what about a situation where experiments measure slight deviations from the model's prediction? Immediate abandoning the whole framework, which is based on some good theoretical arguments, would be a bit to premature. One argument that justifies slight deviations is that we just used best-fit values of the entering neutrino observables, see table C.2, while experimental uncertainties have to be considered as well. We are going to analyze the influence of experimental uncertainties in section 3.5, allowing us to judge the stability of the obtained results. Furthermore, one could analyze the theory to find its uncertainties on the predicted values. Earlier, we mentioned that exact-zero textures could just be a leading order approximation and, in reality, simply some hierarchy between certain Yukawa coupling could be introduced by some flavor symmetry breaking, i.e. two entries in the neutrino Yukawa matrix are much smaller than the remaining ones. Alternatively, the theory could exhibit exact zero Yukawa couplings at tree-level but receive radiative corrections at higher order which would induce some small perturbations. All these things would contribute to an systematic uncertainty that should be considered as a theoretical error bar complementing the experimental uncertainty. Such an approach would need to know about all possible UV seesaw models capable of achieving such effects in the context of the minimal seesaw model, which is obviously far from possible. For this reason, we re-phrase our previous question in a more agnostic way: What are the maximal hierarchies achievable for a measured set of CP phases (δ, σ)? In this way, we can check what perturbations are still allowed to contribute to an exact-zero texture and, even better, are capable of also tracking some approximate zero-textures. As a results, we are now taking a more data-driven path and look how large the former texture zeros have to be, to allow for certain approximate Yukawa structures (3.11), which are still consistent with experiments. We are staying as model-independent as possible since no assumption on the UV flavor theory, which might be relevant in our context, is needed. Hence, the strongest hierarchies consistent with neutrino

data are subject of our investigation.

In doing so, the CIP proves very useful for given set of (δ, σ), as variation of the complex rotation angle z yields a whole set of Yukawa matrices that can be associated with a particular known or unknown UV completion of the seesaw mechanism, reconciling the experimental data. The two DOFs of z can then be interpreted as some index or label of such a UV seesaw flavor model. By scanning the complex z plane, we can check all possible UV flavor models compatible with the seesaw framework and investigate which one produces the strongest hierarchy among all Yukawa coupling. Of course, we are not able to give stronger insights about the high-energy theory that is exactly responsible for a certain Yukawa structure. From our data-driven point of view, we are just interested which z values exhibits the strongest hierarchy. In principle, this z *can* be related to one or several UV flavor model in our minimal seesaw framework, if known. In this sense, we address all high-energy models, again in the context of our minimal seesaw model, and guarantee independence of any particular assumption. The obtained results can then be interpreted as *upper bounds* on the corresponding Yukawa structure for a given set of (δ, σ).

3.3.1. Investigation of Yukawa hierarchies

Before the actual results are presented, the systematics of the applied method are discussed. The hierarchy of a Yukawa matrix is assessed via a self-defined parameter R_{23} which has very useful properties for our discussions. From the previous section we know that the minimal type-I seesaw model with exact two-zero texture is capable of giving precise predictions on the CP phases δ and σ[2]. As we now allow these zeros to be small parameters, our model should exhibit two additional DOFs as the strong linkage between elements according to (3.12) is lost. Hence, one particular Yukawa matrix, whose hierarchy is to be determined, is characterized by a given set of (δ, σ, z). In the following section, a method capable of assessing the hierarchies among certain matrix indices is presented.

As a first step, all individual Yukawa couplings are sorted according to their absolute value, such that we have

$$\hat{\kappa} = (\hat{\kappa}_1, \hat{\kappa}_2, \hat{\kappa}_3, \hat{\kappa}_4, \hat{\kappa}_5, \hat{\kappa}_6,), \quad |\hat{\kappa}_i| \leq |\hat{\kappa}_{i+1}|, \quad i = 1, 2, ..., 5\,. \tag{3.15}$$

Now, the manifestation of an exact zero textures can easily be checked by counting the number of zeros in this sorted list as we have

$$\begin{aligned} \text{One texture zero:} \quad & \hat{\kappa}_1 = 0, \quad \hat{\kappa}_2 > 0\,, \\ \text{Two texture zeros:} \quad & \hat{\kappa}_1 = 0, \quad \hat{\kappa}_2 = 0, \quad \hat{\kappa}_3 > 0\,, \\ & \text{etc.} \end{aligned} \tag{3.16}$$

The information about their exact positions is lost, but will not be of importance at the moment. Since we are also interested in scenarios of approximate zero texture,

[2]The number of DOFs is now precisely matching the number of experimental observables. Eight real DOFs are provided by the two-zero Yukawa texture, from which three can be absorbed in the charged lepton fields, giving in total five DOFs.

the two smallest entries $\hat{\kappa}_{1,2}$ and their corresponding difference to the remaining one $\hat{\kappa}_{3,4,5,6}$ are subject of our concerns. A good quantifier of this hierarchy is the simple ratio of absolute values between the second and third list element, which we will call *hierarchy parameter* from now on,

$$R_{23}(\delta, \sigma; z) \equiv \frac{|\hat{\kappa_2}|}{|\hat{\kappa_3}|} \,. \tag{3.17}$$

Taking (3.7) and assuming that both heavy neutrinos are almost degenerate in mass, or at least have masses in the same order of magnitude $M_1/M_2 \sim \mathcal{O}(1)$, we can simplify it even further,

$$R_{23} = \frac{|\hat{\kappa}_2|}{|\hat{\kappa}_3|} = \sqrt{\frac{\hat{M}_3}{\hat{M}_2}} \frac{|\hat{y}_2|}{|\hat{y}_3|} \simeq \frac{|\hat{y}_2|}{|\hat{y}_3|} \,. \tag{3.18}$$

Thus, our hierarchy parameter is able to reflect the ratio of the actual second and third smallest Yukawa couplings in the case of both heavy neutrinos sharing almost the same mass scale. R_{23} varies in the range from zero to one and quantifies the hierarchy among the corresponding Yukawa couplings. A vanishing R_{23} indicates a real zero-texture and a maximal value of unity no hierarchy at all. By this definition, our analysis is independent of any heavy neutrino mass if those are of the same order of magnitude. If this is not the case and both neutrino masses are separated over large ranges, our results have to be multiplied by the ratio of both masses, according to (3.18). Moreover, the general conclusions, we draw below, are not affected by this rescaling. Exact zero-textures with a vanishing hierarchy parameter still exhibit a zero value, whereas maximal hierarchy parameter will remain maximal. Hence, we collect all the model's important features by assuming degenerate heavy neutrino masses.

Now, the properties of R_{23} and some special regions of the parameter space are commented on.

Properties of the hierarchy parameter R_{23}

In figure 3.2, we plotted the introduced *hierarchy parameter* R_{23} in the complex z-plane. As already explained, varying heavy neutrino masses only affect the absolute value of R_{23}, whereby characteristic points remain unchanged. Accordingly, zeros of our hierarchy parameter stay still zero and indicate exact zero Yukawa textures.

As we can infer from figure 3.2, R_{23} is periodic in the real z-component with a period of $\frac{\pi}{2}$,

$$R_{23}(\delta, \sigma; z) = R_{23}(\delta, \sigma; z + n\frac{\pi}{2}), \qquad \text{with } n \in \mathbb{Z} \,. \tag{3.19}$$

This periodicity originates from general properties of the applied CIP (3.9), see appendix B of [40] for details, and is in our context nothing but an interchange of Yukawa columns according to

$$z \to z + \frac{\pi}{2} \quad \Longrightarrow \quad \kappa_{\alpha 1} \to \kappa_{\alpha 2}, \quad \kappa_{\alpha 2} \to -\kappa_{\alpha 1} \,. \tag{3.20}$$

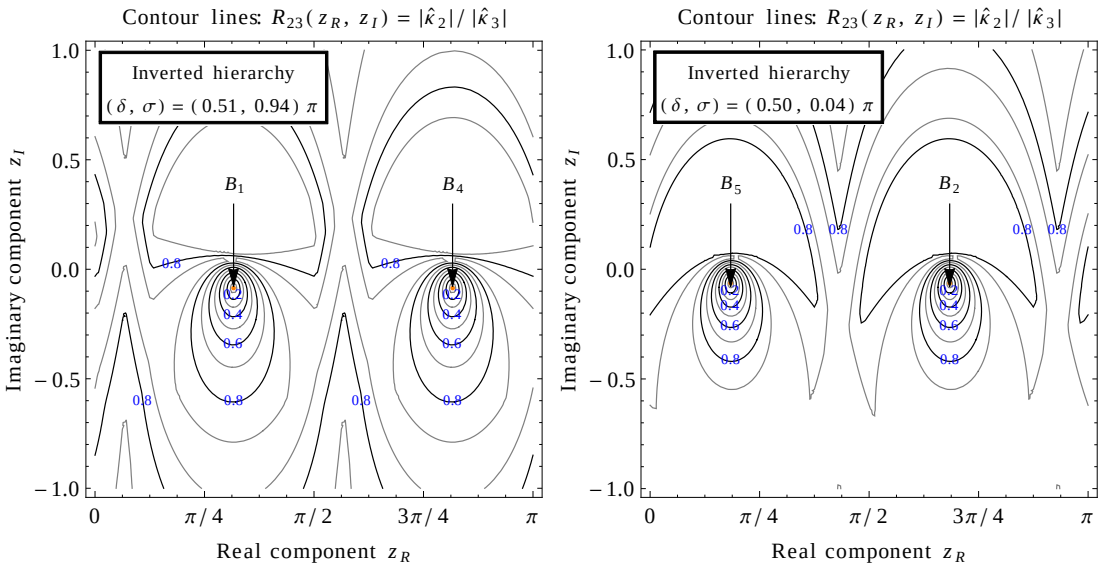

Figure 3.2.: The defined hierarchy parameter R_{23}, see (3.17), as a function of the complex rotation angle z for particular choices of the phases δ and σ. The **left panel** shows R_{23} for the Yukawa texture $B_{1,4}$ and the **right panel** corresponds to the case of a $B_{2,5}$ Yukawa pattern. These are the only two-zero texture exhibiting a vanishing hierarchy parameter.

The sign change in the second Yukawa coupling does not affect our procedure since we sort them according to their absolute values and also R_{23}, defined as a ratio of two absolute values, is invariant under this transformation. Additionally, it remains unchanged under complex conjugation of z and simultaneous sign changes of the CP phases,

$$z \to z^*, \qquad \delta \to -\delta\,, \qquad \sigma \to -\sigma\,, \tag{3.21}$$

having the same effect as complex conjugation of each Yukawa entry. As a result, this property gives rise to some "reflection symmetry" which simplifies our further investigation by halving the domain of potential δ phases,

$$R_{23}\,(2\pi - \delta, \sigma; z) = R_{23}\,(\delta, \pi - \sigma, z^*)\ . \tag{3.22}$$

This proves to be very useful in numerical scans that have to be performed over the whole parameter space. Each solution we find in the restricted range $\delta \in [0, \pi)$, yields another solution according to (3.22), hence, giving two phase sets (δ, σ) for each upper hierarchy bound.

Flavor-aligned parameter space

In contrast to the real axis z_R, its imaginary one z_I is not restricted and the parameter space of our model is unbounded. By using large test values, one recognized a special feature of the corresponding Yukawa entries: The larger z_I gets, the more both Yukawa columns approach each other, up to some relative phase.

Such behavior indicates some kind of alignment in flavor space, which couples the two heavy neutrino equally to the same lepton flavor. In our approach, no further assumption on flavor symmetries is made, such that this configuration seems to be unnatural or fine-tuned. For nearly-aligned Yukawa coupling, large cancellations among certain entries have to appear to still accommodate for the measured low-energy neutrino observables. Again, this requirement can be considered as fine-tuning of the underlying theory and is, hence, disfavored. Beyond that, exact flavor alignment would drastically reduce the number of DOFs, in such a way that consistence with neutrino observables is impossible.

To understand this region of our model's parameter space better, we dive more into details. If we decompose the complex rotation angle z into its parameter form, $z = z_R + z_I$, the CIP (3.8) takes the form

$$\begin{aligned} \kappa_{\alpha 1} &= \frac{1}{2}\left[(V_{\alpha k} + i\,V_{\alpha l})\,e^{z_I - i\,z_R} + (V_{\alpha k} - i\,V_{\alpha l})\,e^{-z_I + i\,z_R}\right] , \\ \kappa_{\alpha 2} &= \frac{1}{2}\left[(V_{\alpha l} - i\,V_{\alpha k})\,e^{z_I - i\,z_R} + (V_{\alpha l} + i\,V_{\alpha k})\,e^{-z_I + i\,z_R}\right] , \end{aligned} \tag{3.23}$$

with the usual convention $(k,l) = (2,3)$ in the case of NH and $(k,l) = (1,2)$ for the IH case. By going into the large-$|z_I|$ limit, the exponentials containing $\pm z_I$ yield strong suppressions, such that the above terms can be simplified,

$$\begin{aligned} z_I \gg 1 \quad &\Longrightarrow \quad \kappa_{\alpha 1} \simeq i\,\kappa_{\alpha 2} \simeq \frac{1}{2}\,(V_{\alpha k} + i\,V_{\alpha l})\,e^{z_I - i\,z_R} , \\ z_I \ll -1 \quad &\Longrightarrow \quad \kappa_{\alpha 2} \simeq i\,\kappa_{\alpha 1} \simeq \frac{1}{2}\,(V_{\alpha l} + i\,V_{\alpha k})\,e^{-z_I + i\,z_R} . \end{aligned} \tag{3.24}$$

Here, we directly see the relative phase between both columns emerging due to the simplification made. Because of flavor alignment, the sorted list of Yukawa couplings, $\hat{\kappa}$, now only contains three different entries with a certain ordering among themselves, $\kappa_{\alpha_1 I} \leq \kappa_{\alpha_2 I} \leq \kappa_{\alpha_3 I}$, irrespectively of $I = 1$ and $I = 2$. Exact flavor alignment obviously corresponds to the case $\kappa_{\alpha_1} \equiv \kappa_{\alpha_2}$. An interesting feature of the performed simplifications (3.24) is that in the limit of flavor alignment, $z_I \pm \infty$, our hierarchy parameter (3.17) becomes independent of the complex angle z and asymptotically approaches a constant value, following

$$z_I \to \pm\infty \quad \Longrightarrow \quad R_{23} \to R_{23}^{\pm} = \left| \frac{V_{\alpha_1 k} \pm i\,V_{\alpha_1 l}}{V_{\alpha_2 k} \pm i\,V_{\alpha_2 l}} \right| . \tag{3.25}$$

For the exact-zero texture case we presented in figure 3.2, the asymptotic hierarchies for flavor-aligned textures are given by

$$\left(R_{23}^{+}, R_{23}^{-}\right) = \begin{cases} (0.81, 0.68) & ; \quad (\delta, \sigma) = (0.51, 0.94)\,\pi \\ (0.61, 0.89) & ; \quad (\delta, \sigma) = (0.50, 0.04)\,\pi \end{cases} , \tag{3.26}$$

showing that we could potentially track the maximal asymptotic hierarchies by plotting a region with $|z_I| \ll 10$[3].

[3] This is consistent with a more advanced study of the transition towards flavor-aligned parameter space regions of chapter 4, see figure 4.2. Although viewed in a slightly different context, we found that the condition $|z_I| \simeq 2$ is sufficient.

We noted that flavor aligned regions reflect a special case of the model's parameter space that could be considered as "tuned", therefore, regions with $|z_I| \sim \mathcal{O}(1)$ are theoretically more favored. However, nature could reveal itself in such manner, so exclusion would reduce the generality of our ansatz. In the upcoming part, we will study flavor-aligned regions to draw the most general picture, which experimental data and our framework allow.

3.4. Maximal Yukawa hierarchies

Now, that the main principles of the method are clarified, we can continue with details of the performed analysis and its corresponding results.

3.4.1. Detailed methodology

As already mentioned above, the framework of a minimal type-I seesaw model in combination with the CIP [85], equips us with special possibilities for our general approach. We only have one complex parameter, z, that connects the low-energy observables in V with the Yukawa coupling relevant for the high-energy region. Hence, by scanning the complex z-plane, one can address all possible UV flavor theories within the framework of our minimal seesaw model, which prove very effective in our investigation of maximal hierarchies. Our self-defined hierarchy parameter R_{23} exhibits some elegant features, which have been explained in the previous section, and allows the evaluation of the model's parameter space, not only in context of exact zero-textures, but also for approximate realizations that seem mandatory from a theoretical point of view. Approximate zero-textures reveal themselves by a particular small value of R_{23}, hence we "only" have to minimize it over the inaccessible parameter z to find maximal hierarchies that are close to zero-textures. Therefore, we define a *minimized hierarchy parameter* $H_{23}(\delta, \sigma)$ that depends only on the model's two CP phases, δ and σ,

$$H_{23}(\delta, \sigma) \equiv \min_{z_R, z_I} R_{23}(\delta, \sigma; z)\,. \tag{3.27}$$

It exhibits all features of the former hierarchy parameter without depending on the complex rotation angle z. At this point, it shall again be noted that we just obtain maximal hierarchies for a given set of (δ, σ) and that there is no guarantee for nature following exactly this behavior. Our results have to be interpreted as *upper bounds* being consistent with current experimental measurements. They rely on no further assumption about the seesaw's UV sector, which is a clear advantage in contrast to common top-down approaches. With our method we are able to give generic statements about hierarchies among entries in the neutrino Yukawa matrix that coincide with experiments and have to be fulfilled by any UV flavor theory in the context of minimal seesaw models. Hence, we are capable of distilling more information from experimental measurements than is usually done, which results in further meaningful constraints. The minimization over the complex z-plane ensures that any UV flavor seesaw model is covered since z can be considered as

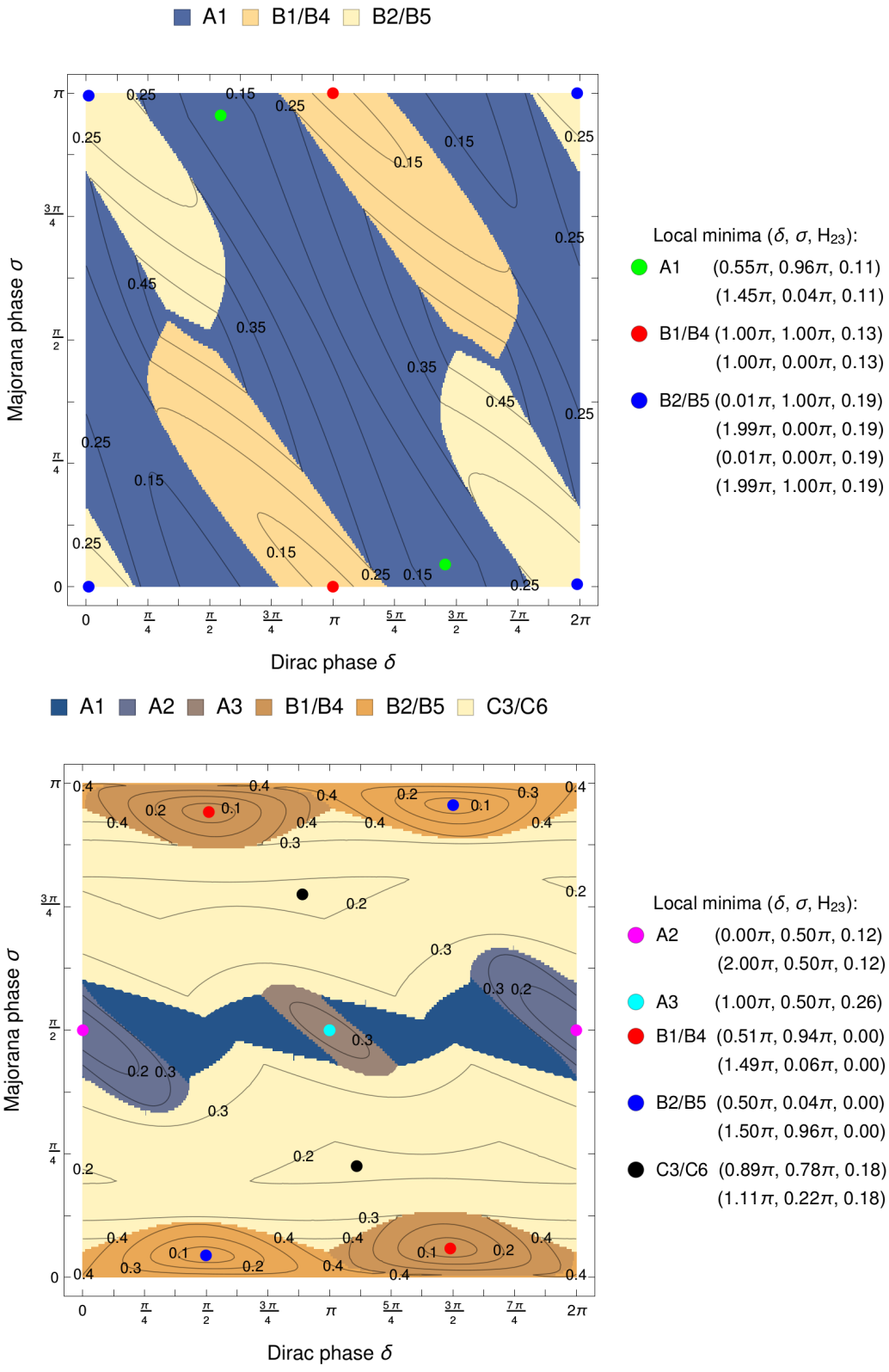

Figure 3.3.: Minimized hierarchy parameter H_{23} as a function of the CP phases δ and σ without any assumption on z_I. The case of normal, **upper panel**, and inverted neutrino mass ordering, **lower panel**, are investigated separately. Contours represent the found H_{23}-values and colors correspond to the underlying Yukawa texture class, listed in (3.11). Local texture minima are denoted by the colored points.

a corresponding label. This approach can easily be generalized for more involved models and arbitrary Yukawa patterns, by doing the following three steps:

1. Parametrize the model's Yukawa couplings in terms of two parameter sets: low-energy observables and unphysical quantities irrelevant at low-energy, e.g. CIP (3.8).

2. Construct parameter sensitive to the matrix pattern of interest, e.g. a ratio of (sorted) Yukawa couplings.

3. Marginalize this parameter over all inaccessible parameters.

By this, one always obtains general phenomenological constraints on the Yukawa structure of interest, which is consistent with available low-energy observables. Due to obvious reasons, the complexity of our approach grows with the number of unobservable DOFs.

For our framework, H_{23} is well-applicable as we are only dealing with two auxiliary parameters, z_R and z_I. Moreover, the model allows a direct connection of both CP phases by the assumption of maximal hierarchies. Hence, our analysis can be understood as a first proof of principle of our more general method. An issue of application in our context is that R_{23} is not a smooth function of the auxiliary parameters because the sorted list of Yukawa couplings changes whenever another Yukawa pattern (3.11) exhibits a stronger hierarchy, i.e. a more minimal R_{23}. The occurring "kinks" of R_{23} are not differentiable any more, such that we cannot rely on further analytic evaluation. As a consequence, a fully numerical analysis has been chosen. The mentioned properties of R_{23} are helpful to shrink the parameter space of δ further, see (3.22). We already know that large values of $|z_I|$ lead to flavor-aligned Yukawa structures, where the matrix columns tend to equalize each other, which is used to separate flavor-unaligned from flavor-aligned parts of the valid parameter space. Although assumed to be unnaturally fine-tuned, we cannot exclude the flavor-aligned regions from our investigation. But explicit separation, $|z_I| \gg 1$ from $|z_I| \sim \mathcal{O}(1)$, helps to track which kind of Yukawa patterns rely on the assumption of an aligned flavor space. In the end, both parts have to be combined to represent the full parameter space without any further assumptions.

3.4.2. Advanced parameter space scan

In the following, we present the results of our numerical analysis of our model's full parameter space and comment on special findings.

The reduced parameter space of our framework consists only of both CP phases, δ and σ, which are directly connected by the assumption of maximal realizable hierarchies in the Yukawa matrix. This allows a straight forward prediction of the Majorana phase σ for a measured value of the Dirac phase δ, which is expected within the upcoming years. By simultaneously tracking, where the smallest entries in the Yukawa matrix appear, we can link the obtained hierarchies values to the underlying textures classes (3.11) as well, which helps to gain further knowledge about parameter space. We just classify them according to the location of their

smallest entries, irrespectively of the corresponding R_{23} value. Actual hierarchies that can be identified with, at least approximate, zero-textures have to exhibit appropriately small hierarchy values; for our analysis, we defined $R_{23} \leq \mathcal{O}(0.1)$ as a necessary condition to be referred as an actual Yukawa texture. The analysis consists of different parts that are summarized in the figures 3.3, 3.4, 3.5 and 3.6. Figure 3.3 shows the full parameter space H_{23} as a function of the CP phases δ and σ, minimized of the total complex z-plane for inverted and normal mass ordering, thus also including flavor-aligned textures. The separated scans of flavor-unaligned, $|z_I| \sim 1$, and flavor-aligned textures, $|z_I| \gg 1$, are presented in figures 3.4 and 3.5 for inverted and normal mass hierarchy respectively. A detailed scan of the minimized hierarchy parameter H_{23} in the vicinity around exact zero-textures, which is only possible in case of IH, is displayed in figure 3.6. In table 3.1, the whole investigation is summarized with an overview of all found local minima of H_{23} with corresponding Yukawa matrices. Now, the obtained results shall be commented individually for each mass ordering.

Inverted mass hierarchy

First of all, we recover the exact-zero texture points for the patterns $B_{1,4}$ and $B_{2,5}$, that were found by earlier studies in the case of inverted neutrino mass ordering [106, 112], which confirms the validity of our calculations. These originate as expected in the scan of flavor-unaligned regions, see upper panel of figure 3.4. By allowing for small perturbations, four additional textures can be found; A_1, A_2, A_3 and $C_{3,6}$. The textures $B_{1,4}$ and $\mathrm{B}_{2,5}$ are capable of realizing minimal H_{23}, corresponding to exact-zero textures with non-aligned flavor space. Yukawa matrices of texture $C_{3,6}$ can be obtained down to flat hierarchies and cover huge parts of the scanned (δ, σ)-plain. Further, they originate mostly from non-aligned flavor regions, see figure 3.3. A_1 structures are realized for $\sigma \sim \frac{\pi}{2}$ and small δ, but show almost no hierarchy since H_{23} exhibits a global maximum. The parameter scan of aligned Yukawa matrices, lower panel of figure 3.4, shows that all classes of texture A are realizable, whereas A_2 textures are minimal for small δ and A_3 structures for large δ respectively. Both regions span hierarchy values from their local minimum up to one, which corresponds to almost no hierarchy structure. Regions of A_1 Yukawa structure have no local minima and H_{23} indicates flat hierarchies among all entries. If we accept for flavor-aligned Yukawa matrices and combine both data sets, figure 3.3, we restore the characteristic points of both scans. The whole parameter scan exhibits a band of A textures at $\sigma \sim \frac{\pi}{2}$ and, within it, A_2 and A_3 structures show local minima, which clearly emerge from flavor-aligned regions.

Normal mass hierarchy

For exact-zero textures, no Yukawa matrix could be found that agrees with experimental measurements. This confirms the general wisdom that normal mass ordering is not consistent with two-zero texture in minimal seesaw models [106]. Scanning the available parameter space under relaxation of exact-zero textures and exclusion of flavor-aligned regions yields the possibility of three Yukawa textures;

	$(\delta, \sigma)\,/\pi$	Texture	H_{23}	z_I	Rescaled Yukawa matrix $\kappa \times 10^7$
NH-1	$(0.55, 0.96)$ $(1.45, 0.04)$	A1	0.11	$\ll -1$	$\begin{pmatrix} 0.41\, e^{1.02\, i\pi} & 0.41\, e^{1.52\, i\pi} \\ 3.85\, e^{1.38\, i\pi} & 3.85\, e^{1.88\, i\pi} \\ 3.90\, e^{1.60\, i\pi} & 3.90\, e^{0.10\, i\pi} \end{pmatrix} f\,(z)$
NH-2	$(1.00, 0.00)$	B1/B4	0.13	$\mathcal{O}(1)$	$\begin{pmatrix} -0.18 & 1.42 \\ 3.83 & -0.18 \\ 3.11 & -2.73 \end{pmatrix}$
NH-3	$(0.01, 0.00)$ $(1.99, 0.00)$	B2/B5	0.19	$\mathcal{O}(1)$	$\begin{pmatrix} 0.27\, e^{0.01\, i\pi} & 1.41\, e^{0.01\, i\pi} \\ 2.76 & 2.53 \\ 4.21 & 0.27 \end{pmatrix}$
IH-1	$(0.00, 0.50)$	A2	0.12	$\gg +1$	$\begin{pmatrix} 7.30 & -7.30\, i \\ 0.22 & -0.22\, i \\ -1.92 & 1.92\, i \end{pmatrix} f\,(z)$
IH-2	$(1.00, 0.50)$	A3	0.26	$\gg +1$	$\begin{pmatrix} 7.30 & -7.30\, i \\ 1.87 & -1.87\, i \\ -0.49 & 0.49\, i \end{pmatrix} f\,(z)$
IH-3	$(0.51, 0.94)$ $(1.49, 0.06)$	B1/B4	0.00	$\mathcal{O}(1)$	$\begin{pmatrix} 0 & 5.24\, e^{1.02\, i\pi} \\ 3.54\, e^{1.04\, i\pi} & 0 \\ 4.06\, e^{0.04\, i\pi} & 1.19\, e^{0.53\, i\pi} \end{pmatrix}$
IH-4	$(0.50, 0.04)$ $(1.50, 0.96)$	B2/B5	0.00	$\mathcal{O}(1)$	$\begin{pmatrix} 0 & 5.25\, e^{1.99\, i\pi} \\ 3.52\, e^{0.97\, i\pi} & 1.04\, e^{1.49\, i\pi} \\ 4.05\, e^{1.97\, i\pi} & 0 \end{pmatrix}$
IH-5	$(0.89, 0.78)$ $(1.11, 0.22)$	C3/C6	0.18	$\mathcal{O}(1)$	$\begin{pmatrix} 5.83\, e^{1.06\, i\pi} & 3.42\, e^{0.55\, i\pi} \\ 0.62\, e^{0.95\, i\pi} & 3.42\, e^{0.19\, i\pi} \\ 0.62\, e^{0.94\, i\pi} & 3.42\, e^{1.14\, i\pi} \end{pmatrix}$

Table 3.1.: Local minima of our minimized hierarchy parameter H_{23} in the (δ, σ) plane for IH and NH, see (3.2). The Assignment to the (approximate) textures follows (3.11). Large values of $|z_I|$ correspond to *flavor-aligned* neutrino Yukawa matrixes κ, while $\mathcal{O}(1)$ values $|z_I|$ do not exhibit any correlation among both Yukawa columns. At large $|z_I|$-values, all couplings scale with $f\,(z) = 1/2 \exp\left[\mathrm{sgn}\left\{z_I\right\}\left(z_I - i\, z_R\right)\right]$.

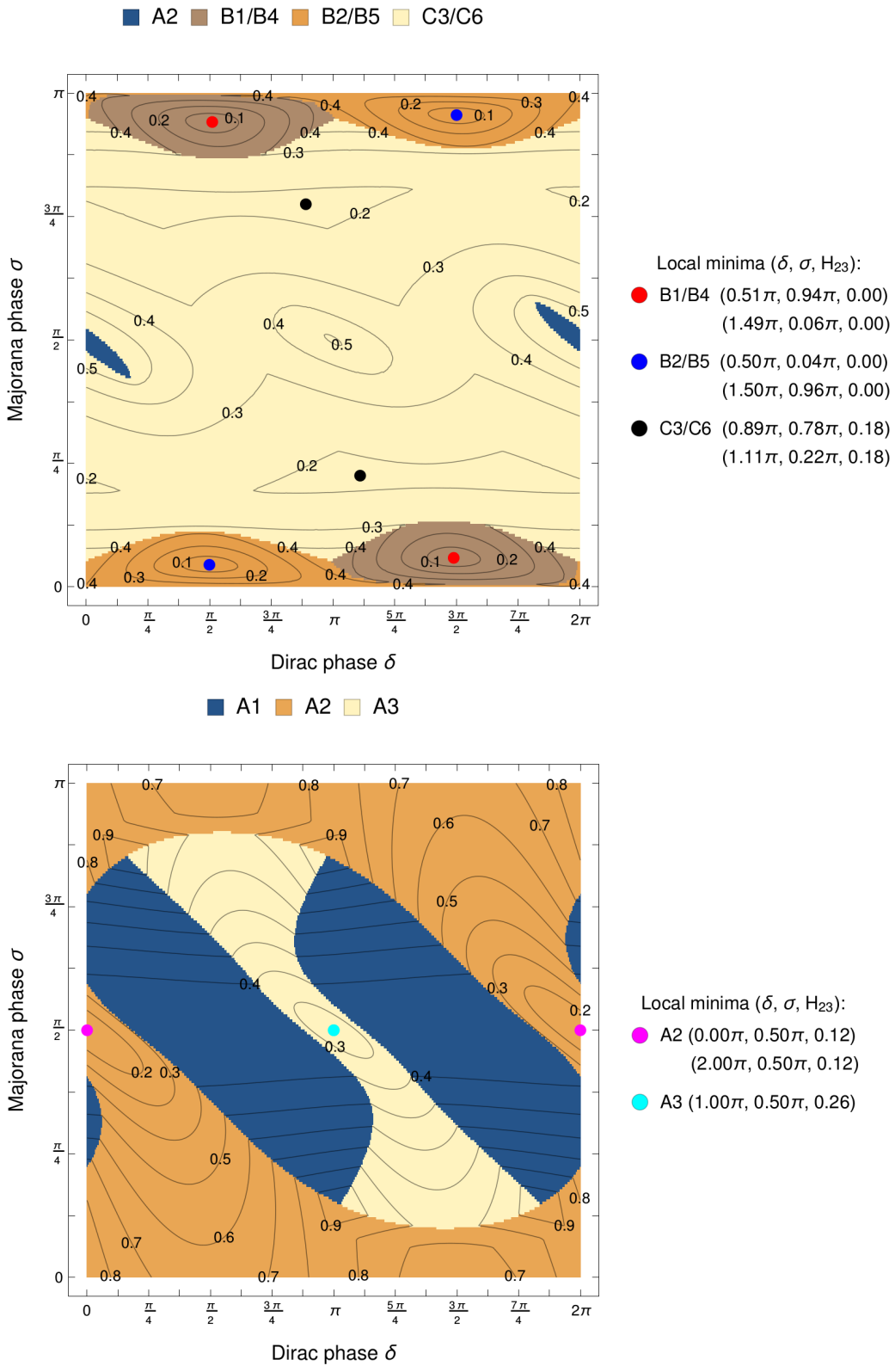

Figure 3.4.: Minimized hierarchy parameter H_{23} for IH. Flavor-unaligned parameter space, $|z_I| < 1$, **upper panel**, and flavor-aligned regions, $|z_I| >> 1$, **lower panel**, are depicted separately. Contours represent H_{23}-values and colors the underlying Yukawa texture class, listed in (3.11). Local H_{23}-minima are denoted by colored points.

A_1, $B_{1,4}$ and $B_{2,5}$, see upper panel of figure 3.5. In contrast to the inverted case, local minima for the textures $B_{1,4}$ and $B_{2,5}$ are obtained for $\sigma \sim \pi$ and $\delta \sim 0$ respectively, $\delta \sim \pi$ with hierarchy parameters allowing for moderate structure. Texture A_1 can only be realized with rather flat hierarchies. A special feature in contrast to the inverted mass ordering is, that this scan shows no direct contact between the two possible texture B regions. Considering the case of aligned flavor structure, see lower panel of figure 3.5, just one possible texture, A_1, can be realized. Its global minimum indicates a rather strong Yukawa hierarchy of $R_{23} \sim 0.1$ that is related to the CP phases $(\delta, \sigma) \simeq (0.55, 0.96)\pi$ or equivalently $(\delta, \sigma) \simeq (1.45, 0.04)\pi$, hence, being an approximate two-zero Yukawa texture according to our previous definition. Combining the separate scans of figure 3.5, we see that features of the un-aligned situation sustain, compare with lower panel of figure 3.3). The only difference is that B texture regions shrink and most of the $(\delta - \sigma)$-plain is now occupied by A_1 textures. The local minimum of the flavor-aligned case transmits allowing for stronger hierarchies.

Vicinity of exact-zero texture points and CP violation

In the end, we want to give a more qualitative statement about the performed parameter space scans. The whole investigations was motivated by the aim of finding points in our model's parameter space that yield strong hierarchies in the corresponding Yukawa matrix. Thus, the list of found minima, see table 3.1, summarizes our approach. On the other hand, we were also interested in quantifying the corrections an exact-zero texture is allowed to obtain, if some deviation from the predicted CP phases is measured.

Stated differently, we want to know how strong the underlying two-zero textures have to be relaxed for CP phases slightly differing from the generic predictions (3.14). For this, the vicinity of exact two-zero textures $B_{1,4}$ and $B_{2,5}$, which are only allowed for IH, is studied in more detail, see figure 3.6. For instance, if we allow a deviation of about 0.1π for the CP phases, δ and σ, a $\mathcal{O}(10\%)$ correction to the exact-zero texture is required. Hence, figure 3.6 is one of our main results since it corresponds to the theoretical error bars, we were searching for. It reflects a generalization ot the predictions in case of exact-zero textures (3.14) that can, in this context, be interpreted as "central values".

Conclusively, we want to comment on a special behavior of H_{23}. Our minimized hierarchy parameter seems to prefer small values close to CP-conserving phases,

$$\frac{(\delta, \sigma)}{\pi} = \left(m, \frac{n}{2}\right) \qquad \text{with } m, n \in \mathbb{Z}. \tag{3.28}$$

We already encountered a similar situation for exact-zero textures in section 3.2. Regarding the found minima of table 3.1, we can confirm that the maximal hierarchies of texture $B_{1,4}$ for NH and textures A_2 and A_3 associated with no $\not{CP}$. Texture $B_{2,5}$ in the case of NH is barely CP violating due to its small offset from integers in δ. Sizable effects of $\not{CP}$ can originate from the textures A_1 for NH and $C_{3,6}$ for IH. Remarkably, the local minimum of (approximate) A_1 texture for NH agrees with most recent data sets [8], compare tables 2.3 and 3.1.

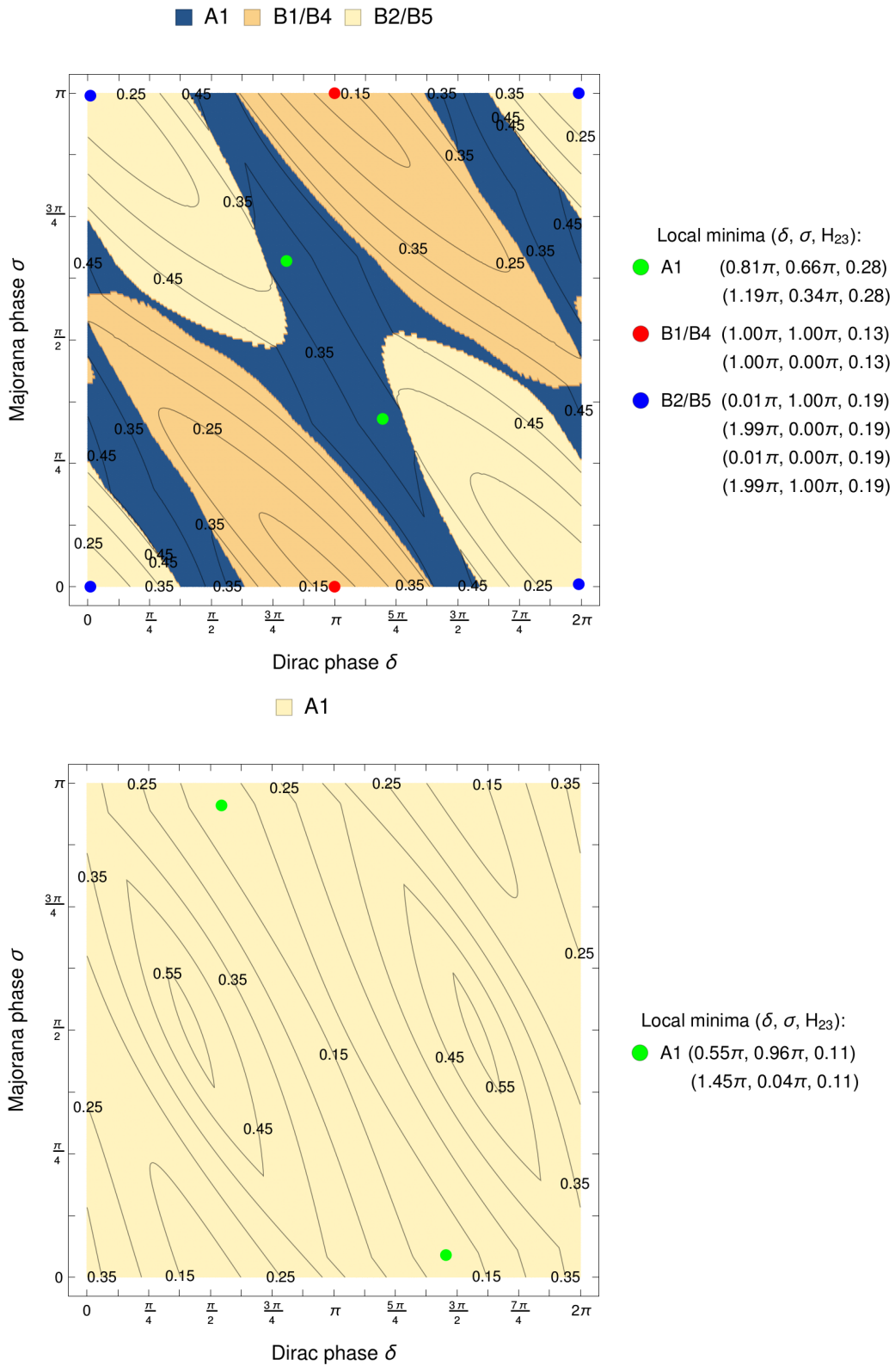

Figure 3.5.: Minimized hierarchy parameter H_{23} for NH. Flavor-unaligned parameter space, $|z_I| < 1$, **upper panel**, and flavor-aligned regions, $|z_I| >> 1$, **lower panel**, are depicted separately. Contours represent H_{23}-values and colors the underlying Yukawa texture class, listed in (3.11). Local H_{23}-minima are denoted by colored points.

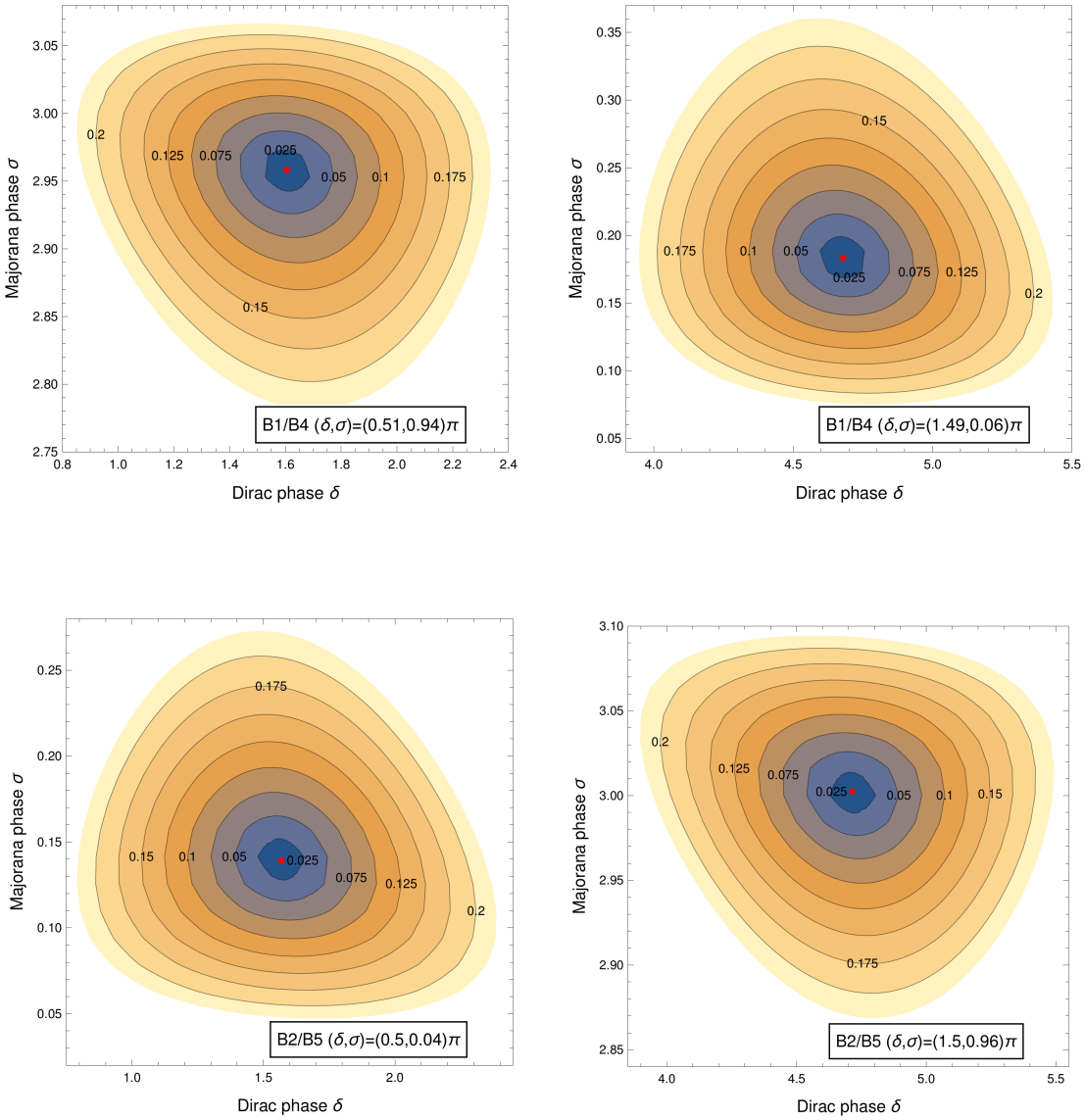

Figure 3.6.: Minimized hierarchy parameter H_{23} for IH as a function of the CP phases δ and σ in the vicinity of its exact zeros, see (3.14). We present both zero points of H_{23} for the two possible two-zero textures, $B_{1,4}$ and $B_{2,5}$, in the (δ, σ) plane, that are related by the reflection symmetry (3.22).

3.5. Experimental uncertainties and stability of zero textures

In the former numerical scan, experimental best fit values for mass differences and angles of the leptonic mixing matrix of an older data set were used, see table C.2. As experiments keep data-taking, we expect them to reach more statics and global fit results to change. Further, one naively expects some change of the obtained upper bounds on the Yukawa hierarchies, if the *actual* values differ from the obtained best-fit values. Both situations would result in some shift of the predictions for (δ, σ). Now, we want to check the stability of our results under variation of the five underlying input parameter; δm^2, Δm^2, $\sin^2\theta_{12}$, $\sin^2\theta_{13}$ and $\sin^2\theta_{23}$. To get a qualitative understanding of this issue, we investigate the stability of characteristic points, here, the predictions of exact-zero texture points possible for the textures $B_{1,4}$ and $B_{2,4}$ in case of IH. This is done by performing a simple χ^2 analysis. We vary these parameters within their experimental uncertainty regions and evaluate the change of exact zero-texture points in the (δ, σ)-plane by means of the corresponding χ^2-value defined as

$$\chi^2\left(\{\mathcal{O}_i\}\right) = \sum_{i=1}^{5} \frac{\left(\mathcal{O}_i - \mathcal{O}_i^{\text{exp}}\right)^2}{\left(\Delta\mathcal{O}_i^{\text{exp}}\right)^2}\,, \quad \{\mathcal{O}_i\} = \left\{\delta m^2, \Delta m^2, \sin^2\theta_{12}, \sin^2\theta_{13}, \sin^2\theta_{23}\right\}\,. \tag{3.29}$$

$\mathcal{O}_i^{\text{exp}}$ represents the best-fit value and $\Delta\mathcal{O}_i^{\text{exp}}$ the corresponding error of the listed quantities, which is obtained by tacking the full width of the $\pm 3\sigma$ ranges and dividing by six. Note that such kind of analysis assumes that fluctuations to follow a Gaussian distribution around their mean! However, this is not the case for given parameters and their experimental uncertainties; the detailed Likelihood function is given in [77]. Since we just want to promote some intuition, how the obtained texture plots might change under variation of their input parameters, our approach seems justified. For each variation of the five observables we obtain one χ^2 value that reflects the deviation from the best-fit set, which we use to group the corresponding parameter set into significance intervals. For five DOFs, the χ^2 values $(5.89, 11.31, 18.21)$ give upper limits on the $(1\sigma, 2\sigma, 3\sigma)$ confidence intervals.

In the following, we vary the experimental input parameter within their $\pm 3\sigma$ uncertainties, calculate the related CP phases according to (3.12) for either $B_{1,4}$ or $B_{2,5}$ texture and weight the resulting prediction for (δ, σ) with the corresponding χ^2 value obtained via (3.29). By grouping them into the mentioned χ^2 intervals, we are able to assign certain confidence regions the (δ, σ)-plane that are represented in figure 3.7 for both textures of interest.

This procedure proves that the phase shifts due to variations of experimental input are just at the order of $\mathcal{O}(0.1\%)\pi$ and can be considered as almost negligible, compare figure 3.7. Further, we see that the requirement of havening an exact two-zero texture within the neutrino Yukawa matrix is pretty strong, hence fixing the CP phases to very high precision.

All in all, the change of both texture zero points in the (δ, σ)-plane under variation of the underlying experimental parameters could be shown and leads to the

conclusion that characteristic points can safely be considered as stable. It is expected that the same behavior transmits to the numerical results of section 3.4. Again, we emphasize that this analysis just has qualitative character and a more sophisticated approach is needed, if one is interested in details, e.g. which kind of phase shift each individual parameter induces.

3.6. Summary and generalization

To conclude this chapter, the main aspects and results are now summarized and an outlook is given, how the developed method can be generalized. We have worked in a minimal type-I seesaw model with only two heavy RH neutrinos, which is capable of explaining all yet observed, low-energy neutrino quantities; namely two mass-squared differences and three mixing angles. One important feature of this model is that one light neutrino has to remain exactly massless. In contrast to the generic type-I seesaw framework of section 2.3, this model exhibits a smaller parameter space that can be parametrized by the CIP (3.8), which proved very convenient in our analysis. We investigated the minimal type-I seesaw model in light of future measurements of the Dirac phase δ through neutrino oscillations. We wanted to know what is inferable about the UV regions, if a certain degree of $\not{CP}$ is measured and to what extend the realization of (approximate) zero-texture structures can be achieved for given sets of (δ, σ). To answer this question, a data-driven approach was chosen and the scenarios of NH and IH have been checked individually. A new method has been developed to access maximal realizable hierarchies among Yukawa couplings for a given set of CP phases (δ, σ) by using our self-defined *hierarchy parameter* R_{23}, which is to be minimized over all inaccessible DOFs at low-energies.

By applying it to our minimal seesaw model, we find interesting results that generalizes knowledge gained by previous studies of exact-zero textures. After validating our approach by recovering the exact two-zero textures $B_{1,4}$ and $B_{2,5}$ for IH, we have studied the consequences of relaxing this assumption and instead allow for a small perturbation. As a result, maximal possible hierarchies in the neutrino Yukawa matrix have been found in dependence of the model's CP phases (δ, σ), see figures 3.3 and 3.4. Further, the vicinity of the above exact-zero textures has been investigated closer to give a qualitative statement for the cases, in which experimental measurements slightly deviate from predictions. Hence, figure 3.6 can be interpreted as theoretical error bars for the predictions of (3.14).

Another result is the resurrection of NH if we allow the correction to exact-zero textures to be of $\mathcal{O}(10\%)$. In addition, figures 3.3 and 3.5 clearly indicate the existence of a further approximate two-zero textures, i.e. texture A_1 at $(\delta, \sigma) = (0.55, 0.96)\pi$ or $(\delta, \sigma) = (1.45, 0.04)\pi$. Generally, we noticed that maximal hierarchies obtained by H_{23} tend to favor phase values that conserve CP. Table 3.1 divides the found local minima according to their CP property. Furthermore, the influence of flavor-aligned Yukawa texture on possible hierarchies has been studied as well, see figures 3.5 and 3.4. Although considered as theoretically unnatural, the general conclusion is that such regions cannot be excluded in the search of

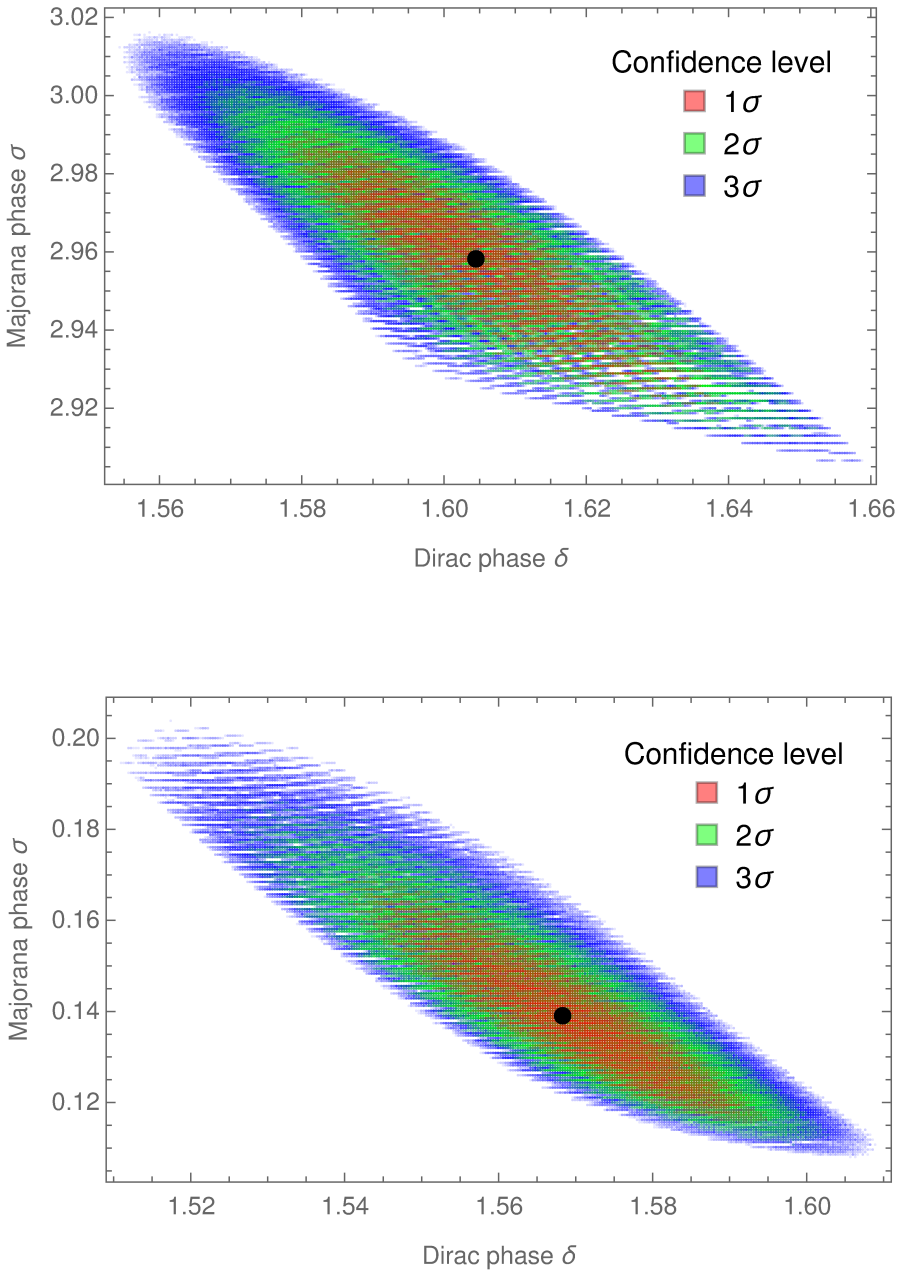

Figure 3.7.: Stability of exact two-zero prediction of textures $B_{1,4}$ (1.601, 2.958), **upper panel**, and $B_{2,5}$ (1.568, 2.958), **right panel**, under variation of the five experimental input parameters: δm^2, Δm^2, $\sin^2\theta_{12}$, $\sin^2\theta_{13}$ and $\sin^2\theta_{23}$. Confidence regions correspond to certain χ^2-values that are calculated with (3.29).

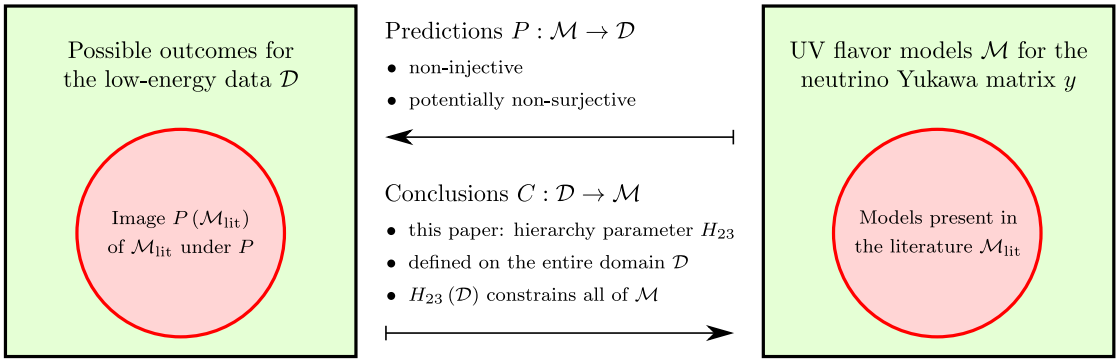

Figure 3.8.: Complementarity between conventional model building and the approach of this work. Top-down theory approaches make non-injective predictions on the set of all experimental outcomes, **right to left**. It is not clear, if there exists an appropriate UV flavor model, here in the context of our minimal type-I seesaw model, that can account for every possible measurement. Our bottom-up approach remains agnostic about the high-energy sector responsible for the resulting neutrino Yukawa matrix. A scan of the entire complex z plane, covers all possible Yukawa matrices within our framework and we can search for the strongest hierarchy that is consistent with experimental measurement.

maximal hierarchies since they give rise to further minimal realizations of R_{23}, e.g. A_1 textures in the case of NH. Interestingly enough, this coincides with recent neutrino-data, see table C.2. In the end, our results have been checked of their robustness against experimental uncertainties, see figure 3.7. These induce shift on the prediction for δ and σ (3.14) of order $\mathcal{O}(1\%)$ that can be considered as negligible.

In this context we want to comment on renormalization group equation (RGE) effects on neutrino parameters, which is expected due to radiative corrections [117–119]. Hence, our low-energy bounds obtained through H_23 should be evolved to the high-energy region to give certain statements about UV flavor theories. Since the induced RGE changes are negligibly small within our framework [109,117], we can safely neglect them and directly claim our results to be valid for UV regions.

Finally, the performed analysis shall be embedded into a broader context. The defined hierarchy R_{23} (3.17) and the corresponding minimization procedure (3.27) can easily be generalized for more complex studies and other Yukawa textures. For instance, in the generic type-I framework of section 2.3, we can investigate the m^{th} and n^{th} smallest Yukawa coupling by defining the corresponding ratio R_{mn} and subsequent minimization of inaccessible parameters. Here, they correspond to three complex rotation angles z_{12}, z_{13} and z_{23} in terms of the Casas-Ibarra notation. This yields a generalized form of the previously applied quantities

$$H_{mn}(\delta,\sigma) = \min_{\omega_{12}} \min_{\omega_{13}} \min_{\omega_{23}} R_{mn}(\delta,\sigma;\omega_{12},\omega_{13},\omega_{23}) \ , \tag{3.30}$$

which comes with growing complexity for more inaccessible parameters. Nevertheless, in principle the developed methods should be applicable for any model

and for any Yukawa structure, where the manifestation of certain internal hierarchies, consistent with experimental data, is subject of investigation. This again underlines the motivation of our entire work, see figure 3.8. Top-down approaches rely on some assumed model that leads to certain prediction at low-energy. Such predictions are typically non-injective, as for any possible realization of (δ, σ) an appropriate UV flavor seesaw model has to be built. It is unclear if there exists an appropriate UV flavor seesaw model for every possible experimental outcome. We tackle the problem from the opposite direction, bottom-up, and stay agnostic about potential UV completions of our minimal seesaw model. By scanning the whole z-plane, we take into account all possible high-energy flavor minimal seesaw models, as z represents some kind of labeling. As we do not know which z-value is realized, we tried to find the strongest Yukawa hierarchies, that are consistent with experimental data. This hierarchy can be interpreted as *upper bound* and especially in the vicinity of some prediction as theoretical error bar. In this sense, we have tried to "squeeze" out as much information as possible from recent experimental data; here in the sense of maximal realizable hierarchies in the neutrino Yukawa matrix. In this spirit, our approach complements typical theoretical approaches and is based on what experiments are expected to see in the near future.

4. Minimal UV seesaw model with a discrete exchange symmetry

In chapter 3 we used a bottom-up approach to investigate consequences of certain CP phase measurements for the type-I seesaw mechanism. Now, a top-down approach is chosen to embed this seesaw mechanism into a broader UV framework while simultaneously reducing its parameter space through certain exchange symmetries. In particular, we are interested in the emergence of an approximate A_1 Yukawa texture for NH, since the corresponding Dirac phase δ follows experimental trends, i.e. indicate close-to-maximal $\not{CP}$ through $\delta \simeq \frac{3\pi}{2}$ [8]. A model, capable of approximately reproducing this property, is developed and the consequences of other high-energy assumptions, e.g. electroweak naturalness and successful leptogenesis are presented. The building blocks underlying our model, the minimal $SU(5)$ GUT [49] and the FN mechanism [48], as well as a model which combines both [47], are introduced in the following sections. Appropriate modification leads to an embedding of the minimal type-I seesaw framework into a broader theoretical context. This chapter deals with the minimal seesaw model published in [51] and provides a broader introduction into the theoretical framework.

4.1. Motivation for a UV completion of the minimal type-I seesaw

Up to now, our work was motivated by the fact that upcoming experiments are on the edge of detecting leptonic $\not{CP}$ in neutrino oscillations. We have investigated the theoretical consequences of measured CP phases for a minimal type-I seesaw model with (approximate) two-zero texture. Due to its reduced parameter space, we have found realizations of certain exact and approximate Yukawa textures which coincide with experimental measurements. We could prove that the usually inconsistent NH is re-established, if small perturbations of exact-zeros are allowed.[1] Certain interesting points have been found that follow experimental trends, i.e. $\delta \simeq \frac{3\pi}{2}$ in a A_1 texture. Hence, to some degree, the following work is driven by the search of a possible UV flavor origin.

From a more general perspective, we are interested in finding a UV completion ot the minimal type-I seesaw mechanism, that is consistent with experiment and exhibits a minimal number of free parameters. Moreover, in the spirit of Ockham's razor we want to find a minimal UV realization of the type-I seesaw mechanism,

[1] See chapter 3 for a detailed motivation of this approach.

which is consistent with experimental data. Such models are always of great use as they represent valid benchmark scenarios.

Now, the most recent global fit results of table 2.3 are used, which exhibit more restricted regions for the Dirac phase δ than the ones table C.2. The starting point of our investigation is the already introduced minimal type-I seesaw model [41, 44–46, 120] presented is section 3.2. It demands one neutrino to be exactly massless, but is still consistent with all experimental observables. More recently, its conformity with several theoretical constraints, e.g. electroweak naturalness, lepton flavor violation, and leptogenesis, has been tested successfully [107, 109].

The embedding of the minimal type-I seesaw model in a FN GUT framework introduced by [47] connects the free seesaw parameters to other quantities and thus implies a reduction of the seesaw parameter space. By assuming additional (approximate) flavor exchange symmetries, we arrive at a minimal UV realization of the type-I seesaw model.[2] In this way, we perform a complementary approach to our previous track and address the minimal seesaw model from a top-down perspective.

4.2. $SU(5)$ GUT and Froggatt-Nielsen mechanism

Before diving into details, the most important facts about $SU(5)$ as a GUT example and the FN mechanism are presented. This allows to understand the neutrino mass generation from a high-energy perspective since RH neutrinos are needed for successful anomaly cancellation. The FN mechanism provides a useful tool in the suppression of certain flavor-sensitive interactions and will be of importance in the construction of our model.

4.2.1. Minimal $SU(5)$ as a GUT example

The $SU(5)$ gauge theory is the classic example of a GUT and the reference frame for the following UV embedding of our minimal type-I seesaw model. Before this is done, we want to introduce basic facts about GUT construction by following mainly [37, 57, 121].

GUT gauge group - $SU(5)$

The spirit behind GUTs is that at a certain energy scale all fundamental interactions unify to just one force, which accounts for all observed particle interactions in our Universe. Using the existing quantized theories of the electroweak and strong force, the usual GUT approach is to find a unifying theory for both. The corresponding unified force is expected to arise at energies of the order $\Lambda_{\text{GUT}} \sim 10^{15}$ GeV. If gravity is taken into account, one expects unification of all fundamental forces at least higher than the Planck scale $\Lambda_{\text{Planck}} \gtrsim 10^{19}$ GeV. To embed the SM gauge group $SU(3)_C \times SU(2)_L \times U(1)_Y$ into a larger group, one needs at least a

[2] "Minimal" is to be understood in terms of the valid neutrino sector. Of course, the embedding into a GUT framework comes with several additional DOFs.

group of rank[3] four since the SM group has this rank. Hence, the four diagonal generators are given by the diagonal Gell-Mann matrices λ^3 and λ^8, one generator of the weak isospin as well as one generator for the weak hypercharge, see appendices A and B. Among all possible groups of rank four, $SU(5)$ is the smallest groupcapable of accommodating for the SM's complex group representations ($SU(3)$ color triplets and $SU(2)$ isospin doublets), while at the same time providing a phenomenology in agreement with observations. We will see that $SU(5)$ clearly disagrees with current measurements of proton decay, but as it is the classic GUT example, we choose it to be our underlying framework. Of course, one could choose an even larger GUT group, which would exhibit more DOFs, and thus being in conflict with our spirit of finding the most minimal realization for the type-I seesaw model.

Now, that we motivated choosing $SU(5)$ as an appropriate gauge group, we repeat the basics of its construction. $SU(5)$ is the group of unitary (5×5) matrices with unit determinant and is spanned by 24 hermitian, traceless generators T^a, with $a = 1, ..., 24$, which are defined according to $\left[T^a, T^b\right] = if_{abc}T^c$ and specified by the structure constants f_{abc}. The usual normalization $tr(T^aT^b) = 2\delta^{\alpha\beta}$ is chosen. As usual, each generator is linked with a gauge field $A^a_\mu(x)$ transforming under the adjoint representation, such that the full gauge transformation and covariant derivative of $SU(5)$ are given by

$$\begin{aligned} U &= \exp\left(-i\sum_{a=1}^{24}\alpha^a_\mu(x)T^a\right), \\ D_\mu &= \partial_\mu + i\frac{g_5}{2}\sum_{a=1}^{24}A^a_\mu(x)T^a = \partial_\mu + i\frac{g_5}{\sqrt{2}}A_\mu\,, \end{aligned} \tag{4.1}$$

with gauge parameter α^a_μ and the "summed" gauge field $A_\mu(x) \equiv \frac{1}{\sqrt{2}}\sum_{a=1}^{24}A^a_\mu(x)T^a$. The covariant derivative invokes all particle interactions of the theory and its generators T^a have to be adjusted according to the (field-)representation, on which it acts. For reasons of convenience, the generators are chosen such that the SM's $SU(3)$ color group is located in the upper left corner and the $SU(2)$ isospin group in the lower right corner of the full $SU(5)$ transformation matrix. The corresponding generators of the fundamental $SU(5)$ representation can be found in appendix B. By doing so, the first eight vector fields $A^{1,...,8}_\mu(x)$ can be identified with the usual gluons of $SU(3)_C$. The charged weak gauge bosons are related to superpositions of A^9_μ, and A^{10}_μ. As the generators T^{11} and T^{12} are diagonal, we chose them to be proportional to the third component of the weak isospin and hypercharge, hence, relating them to W^3_μ and B_μ, respectively. The twelve additional generators $T^{13...24}$ are identified with twelve new gauge bosons, $X^i_\mu, i = 1, ..., 3$ with $SU(5)$-charge of $\frac{4}{3}$ and $Y^i_\mu, i = 1, ..., 3$ with charge $\frac{1}{3}$ and the corresponding charge-conjugated field. These are purely of $SU(5)$ type and reflect additional DOFs due to a larger gauge

[3] A group's rank is given by the number of simultaneously diagonalizable generators.

group. All vector fields can be represented by $A_\mu(x)$ defined according fo 4.1,

$$A_\mu(x) = \begin{pmatrix} G_1^1 - \frac{2}{\sqrt{30}}B & G_2^1 & G_3^1 & \bar{X}^1 & \bar{Y}^1 \\ G_1^2 & G_2^2 - \frac{2}{\sqrt{30}}B & G_3^2 & \bar{X}^2 & \bar{Y}^2 \\ G_1^3 & G_2^3 & G_3^3 - \frac{2}{\sqrt{30}}B & \bar{X}^3 & \bar{Y}^3 \\ X_1 & X_2 & X_3 & \frac{1}{\sqrt{2}}W^3 + \frac{3}{\sqrt{30}}B & W^+ \\ Y_1 & Y_2 & Y_3 & W^- & -\frac{1}{\sqrt{2}}W^3 + \frac{3}{\sqrt{30}}B \end{pmatrix}. \quad (4.2)$$

The corresponding gauge field Lagrangian has the typical form for a non-abelian gauge theory,

$$\mathcal{L}_{kin} = -\frac{1}{4}F^a_{\mu\nu}F^{\mu\nu,a} = -\frac{1}{2}tr(F_{\mu\nu}F^{\mu\nu}), \quad (4.3)$$

with $F^a_{\mu\nu} = \partial_\mu A^a_\nu(x) - \partial_\nu A^a_\mu(x) - \frac{g}{\sqrt{2}}f_{abc}\left[A^b_\mu(x), A^c_\nu(x)\right]$. At this point we want to emphasize that the non-abelian nature of $SU(5)$ leads to self-interactions among the gauge bosons, not only for the gluons and weak gauge bosons, but also for the new ones, X_μ and Y_μ.

Fermion representation

Although SM is conventionally defined in LH and RH chiral states, many BSM theories are equivalently formulated in one chiral state and the corresponding Lorentz-covariant charge-conjugate. We chose for LH fermions f_L and their LCC f_L^C as DOFs. In the GUT context, all fermions of same chirality transform in the same representation of the underlying gauge group. Equivalently to QCD [57], we start with the fundamental representation and construct further representations by products of the fundamental. For $SU(5)$, the fundamental representation is a five-dimensional vector $\psi_{\mathbf{5}}$. Since the upper left corner of the gauge field (4.2) is occupied by the $SU(3)$ vector bosons, we directly see that the first three entries of $\psi_{\mathbf{5}}$ have to carry color, thus forming a color triplet. As the lower right corner is identified with weak gauge bosons, we conclude that the last two entries of $\psi_{\mathbf{5}}$ have to form a doublet under $SU(2)$. If we define an appropriate charge operator and demand it to be traceless,[4] we obtain the condition $tr(Q) = 3\,Q_q + Q_{e^c} + Q_{\nu^c} \stackrel{!}{=} 0$, which directly identifies the quarks in the first three rows of $\psi_{\mathbf{5}}$ to be of down-type. This fixes the particle content of $\psi_{\mathbf{5}}$ as

$$\psi_{\mathbf{5}} = \begin{pmatrix} d^1 \\ d^2 \\ d^3 \\ e^c \\ \nu^c \end{pmatrix}_R = (3,1) + (1,2) \text{ under } SU(3) \times SU(2)\,. \quad (4.4)$$

[4] The used charge operator is defined according to $Q = \frac{1}{2}\left(T^{11} + \sqrt{\frac{5}{3}}T^{12}\right)$. The photon is a gauge boson of $SU(5)$ and must be related to one diagonal generator. Hence, Q has to be traceless.

With the help of the covariant derivative we directly write down the fermionic Lagrangian

$$\mathcal{L}^{\mathbf{5}}_{kin} = \bar{\psi}_{\mathbf{5}} i \not{D} \psi_{\mathbf{5}} = i \bar{\psi}_{\mathbf{5},i} \left(\partial_\mu \delta^i_j - i \frac{g_5}{\sqrt{2}} (V_\mu)^i_j \right) \psi^j_{\mathbf{5}} \, . \tag{4.5}$$

At this point, we already see one of the nice features the $SU(5)$ gauge group has t offer. Charges are naturally quantized and quarks carry a third of the electron's charge, $Q_q = \frac{e}{3}$. To built up $\psi_{\mathbf{5}}$, we had to group RH quarks with RH leptons, which forbids RH quarks to participate in weak interactions since they transform as $SU(2)$ singlets.

Up to now, we just incorporated RH down-quarks and RH leptons in the $SU(5)$ framework. If we also want to include the remaining SM particles, we have to find higher-dimensional representation. These can be obtained by products of the fundamental representation, such as $\mathbf{5}\times\mathbf{5} = \mathbf{10}+\mathbf{15}$. The decouplet $\mathbf{10}$ is identified with the antisymmetric product $X^{ij} = \frac{1}{\sqrt{2}} \left[a^i a'^j - a^j a'^i \right]$ with $i, j = 1, ..., 5$. It further contains the product of two $(3,1)$-representations, $\mathbf{3} \times \mathbf{3} = \mathbf{6} + \bar{\mathbf{3}}$, from which we have to take the antisymmetric part $\bar{\mathbf{3}}$. This is identified with the LH quark u^c_L. Hence, $X^{ij} = \epsilon^{ijk} (u^c_L)_k$ for $i, j, k = 1, 2, 3$. X^{i4} and X^{i5} correspond to a color triplet carrying weak isospin, hence being the product $(3,1) \times (1,2)$. For $i = 1, 2, 3$, one identifies them with LH up- and down- quarks, $X^{i4} = (u^i)_L$ and $X^{i5} = (d^i)_L$ respectively. X^{45} must be a singlet under $SU(3) \times SU(2)$ as it is the antisymmetric product of two $(1,2)$-representations, thus it is identified with e^c_L. Bringing all this together, we arrive at a ten-dimensional representation of $SU(5)$,

$$X = \begin{pmatrix} 0 & u^C_3 & -u^C_2 & -u^1 & -d^1 \\ -u^C_3 & 0 & u^C_1 & -u^2 & -d^2 \\ u^C_2 & -u^C_1 & 0 & -u^3 & -d^3 \\ u^1 & u^2 & u^3 & 0 & -e^+ \\ d^1 & d^2 & d^3 & e^+ & 0 \end{pmatrix}_L = (3,2) + (\bar{3},1) + (1,1) \, , \tag{4.6}$$

with the transformation properties under $SU(3) \times SU(2)$ on the right-hand side. To write down the corresponding Lagrangian, we have to find a ten-dimensional representation of $SU(5)$-generators, T_{10}. As we do not have to work with them, we just assume them as given, such that we can write down the corresponding Lagrangian,

$$\begin{aligned} \mathcal{L}^{\mathbf{10}}_{kin} &= \frac{i}{2} \left(\bar{X} \right)_{ac} \left(\partial_\mu \delta^a_b - \frac{2ig}{\sqrt{2}} (V_\mu)^a_b \right) \gamma^\mu X^{bc} \\ &= \left(\bar{X}_{\mathbf{10}} \right)_{ac} i \left(\partial_\mu \delta^a_b - \frac{2ig}{\sqrt{2}} (V_\mu)^a_b \right) \gamma^\mu X^{bc}_{\mathbf{10}} \, , \end{aligned} \tag{4.7}$$

where we used $X_{\mathbf{10}} \equiv \frac{1}{\sqrt{2}} X$ to obtain canonical normalization.

The traceless charge-condition for $X_{\mathbf{10}}$ again yields quantized charges with quarks carrying third integral electron charge, $tr(Q) = 3\, Q_d + Q_{e^c} = 0$. An important result is that one whole SM generation can be incorporated within one pair of $\psi_{\mathbf{5}}$ and $X_{\mathbf{10}}$ and, even further, anomalies arising from both representations, cancel each other.

With this definition, we are able to take a closer look at the underlying interactions of the minimal $SU(5)$ GUT, e.g. the couplings to neutral currents, which allow for important predictions. These are determined only by the generator T^{11} and T^{12}, associated with W^3_μ and B_μ respectively, such that we can neglect all other contributions at LO,

$$\begin{aligned} D_\mu &= \partial_\mu - \frac{ig}{2}(W^3_\mu T^{11} + B_\mu T^{12}) \\ &= \partial_\mu - \frac{ig}{2}\left[\left(\sin\theta T^{11} + \cos\theta T^{12}\right) A_\mu + \left(\cos\theta T^{11} - \sin\theta T^{12}\right) Z_\mu\right] \\ &\equiv \partial_\mu - i\left[QeA_\mu + Q_Z g_2 Z_\mu\right] , \end{aligned} \tag{4.8}$$

where we used the common SM relation to re-express it in terms of A_μ- and Z^μ-couplings. From this, we obtain a concrete value for the weak mixing angle and a relation between the $SU(5)$ and the electric charge to be valid at the GUT scale $\Lambda \sim m_X$,

$$\sin^2\theta_W = \frac{3}{8}, \qquad\qquad \frac{g_5}{2} = \sqrt{\frac{2}{3}}\, e. \tag{4.9}$$

After allowing for renormalization group evolution [122], the prediction of the weak mixing angle $\sin^2\theta_W$ agrees remarkably well with experimental measurements.

Another feature is the existence of new gauge bosons, X_μ and Y_μ, which can couple to quarks and leptons. They give rise to processes involving baryon and lepton number violation, but indicate the existence of a new quantum number $(B-L)$, under which they carry charge $\frac{2}{3}$. The baryon number violating part is described through the following effective Lagrangian,

$$\begin{aligned} \mathcal{L}_{\Delta B=1} = &\frac{g^2}{2m_X^2}\left(\epsilon_{ijk}(\bar{u}^c_L)^k\gamma_\mu u^j_L\right)\left(2\bar{e}^+_L\gamma^\mu d^i_L + \bar{e}^+_R\gamma^\mu d^i_R\right) \\ &+ \frac{g^2}{2m_Y^2}\left(\epsilon_{ijk}(\bar{u}^c_L)^k\gamma_\mu d^j_L\right)\left(\bar{\nu}^c_{eR}\gamma_\mu d^i_R\right) + h.c.\,, \end{aligned} \tag{4.10}$$

which introduces proton, $p \to e^+\pi^0$, and neutron, $n \to e^+\pi^-$ decay via dimension-6 operators, which, unfortunately, leads to the model's inconsistency with experimental data. Especially, measurements of the proton's lifetime are in clear disagreement with the model's predictions [37],

$$\tau(p \to \pi^0 e^+) \simeq 1.5 \cdot 10^{31}\left(\frac{m_X}{10^{15}\ \text{GeV}}\right)^4\left(\frac{0.15\ \text{GeV}}{|W|}\right)^2 \text{yrs}\ , \tag{4.11}$$

with the form factor of the $p \to \pi^0$ matrix element $W = W(k - q')$. The limits of the Super-Kamiokande experiment are with a value of$\tau(p \to \pi^0 e^+) = 8.2 \times 10^{33}$ yrs at 90% [123] more than two order of magnitude stronger and exclude the generic prediction of the minimal $SU(5)$ GUT. On the other hand, proton decay provides the opportunity to infer the typical GUT energy scale. For our minimal $SU(5)$ model, the scale of unification must be $\Lambda_{\text{GUT}} \gtrsim 10^{15}$ GeV.

Symmetry breaking of $SU(5)$

As we measure a different phenomenology at lowest energies, the $SU(5)$ GUT must be broken to the SM gauge group somewhere above the electroweak scale v_{EW} and further undergo usual symmetry breaking through the Higgs mechanism to agree with current experimental data. At each phase transition, the corresponding gauge bosons, X and Y as well as W and Z, receive their mass,

$$SU(5) \xrightarrow{m_X} SU(3)_C \times SU(2)_L \times U(1)_Y \xrightarrow{m_W} SU(3)_C \times U(1)_{EM} \,. \tag{4.12}$$

The $SU(5)$ breaking is arbitrary and can be realized discretely or even dynamically. However, as the existence of SSB through the Higgs is already confirmed, it is not to far-fetched to assume the same mechanism occurring at higher scales through another Higgs multiplet. Also breaking into intermediate groups, which finally results in the SM gauge group, is possible, but we restrict ourselves to the most minimal model. Breaking of $SU(5)$ gives mass to the X and Y bosons, while keeping the other twelve massless until the SM gauge group is broken by the usual Higgs. To obtain this, an additional scalar Σ_a is introduced, which transforms under the adjoint representation of $SU(5)$ and, hence, its properties are dictated by the Lagrangian,

$$\mathcal{L}^{\Sigma}_{kin} = \frac{1}{2}\sum_{a=1}^{24}\left[\left(D_\mu\Sigma\right)^\dagger_a \left(D^\mu\Sigma\right)_a\right], \tag{4.13}$$

with covariant derivative $\left(D_\mu\Sigma\right)_a = \left(\partial_\mu\delta^a_{a'} - \frac{ig}{2}V^k_\mu\left(F^k\right)_{aa'}\right)\Sigma_{a'}$ for $k, a, a' = 1, ..., 24$,. F^k are 24 (24×24) matrices corresponding the to 24-dimensional representation of the $SU(5)$ gauge group, which is obtained by the product $\mathbf{5}\times\bar{\mathbf{5}} = \mathbf{24}+\mathbf{1}$. The Σ_a can be represented by the components of a (5×5) matrix Σ, which transforms in the same way as the adjoint T^a_b, yielding a simplified Lagrangian,

$$\mathcal{L}^{\Sigma}_{kin} = tr\left[\left(D_\mu\Sigma\right)^\dagger\left(D^\mu\Sigma\right)\right], \tag{4.14}$$

with the covariant derivative acting as $D_\mu\Sigma = \partial_\mu\Sigma - ig\left[V^a_\mu\frac{L^a}{2},\Sigma\right]$. If Σ obtains a non-zero VEV,

$$\langle\Sigma\rangle = v_5\,\mathrm{diag}\left(1,1,1,-\frac{3}{2},-\frac{3}{2}\right) = -\frac{\sqrt{15}}{2}v_5T^{12}\,, \tag{4.15}$$

we generate gauge boson masses through the covariant derivative and since the commutator is exclusively non-zero for $T^{13,...24}$, only X and Y bosons receive mass,

$$\frac{g_5^2}{2}tr\left[V_\mu,\langle\Sigma\rangle\right]^2 \equiv m^2_{ab}V^a_\mu V^{\mu,b} \Longrightarrow m^2_X = m^2_Y = \frac{25}{8}g_5^2v_5^2\,. \tag{4.16}$$

With the VEV (4.15), $SU(5)$ is broken to the SM gauge group as desired. The potential which upon minimization yields such a VEV for Σ is given by

$$-\mathcal{L}_{int} = +V\left(\Sigma\right) = -\mu^2 tr\left(\Sigma^2\right) + \frac{a}{4}\left[tr\left(\Sigma^2\right)\right]^2 + \frac{b}{2}tr\left(\Sigma^4\right)\,, \tag{4.17}$$

where the cubic term is omitted by imposing a $\mathbb{Z}_2$-symmetry, $\Sigma \to -\Sigma$, by hand, which has no effects on the minimization procedure. For $b > 0$, $\mu^2 > 0$ and $a > \frac{7}{5}b$, the potential exhibits a minimum according to

$$\mu^2 = \frac{15}{2} a v_5^2 + \frac{7}{2} b v_5^2 \,. \tag{4.18}$$

As a next step we have to ensure that the SM gauge group is broken in a way consistent with observations. In the $SU(5)$ GUT framework, this is easily done by using a scalar fiveplet, $H_{\mathbf{5}}$, that contains the usual SM Higgs boson as well as a colored scalar triplet. It transforms in the fundamental representation and exhibits the usual scalar potential

$$H_{\mathbf{5}} = \begin{pmatrix} h^1 \\ h^2 \\ h^3 \\ h^+ \\ -h^0 \end{pmatrix} = (3,1) \times (1,2) \quad \Longrightarrow \quad V(H) = -\frac{1}{2}\mu^2 |H|^2 + \frac{1}{4}\lambda (|H|^2)^2 \,. \tag{4.19}$$

For $\nu^2 > 0$, $\lambda > 0$, $H_{\mathbf{5}}$ obtains a non-zero VEV, which induces the breaking of the SM gauge group. Without loss of generality, we can assume that the neutral component acquires the VEV $\langle H_5 \rangle = \langle -h^0 \rangle = v_{EW}$ with $v^2 = \frac{1}{2} v_{EW}^2 \lambda$. Hence, we end up with the usual ρ-parameter [54], with the weak boson masses obtained through EWSB $SU(2) \times U(1) \to U(1)_{EM}$,

$$\rho = \frac{m_W^2}{m_Z^2 \cos^2\theta} = \frac{g_2^2 v_{EW}^2}{4 m_Z^2 \cos^2\theta} \overset{!}{=} 1 \text{ in the SM.} \tag{4.20}$$

Unfortunately, there are two problems with this simple Higgs potential: The first problem is related to the masslessness of the Higgs color triplet h^i $i = 1,2,3$. It is achieved to radiative corrections of $\mathcal{O}(\frac{v_{EW}}{v_5})$. Through SSB of the SM gauge group, they receive a mass of $\mathcal{O}(m_W)$ and there is no way to absorb them by any gauge transformation. As a consequence, proton decay proceeds way to fast than it is observed. The second problem concerns possible cross terms between $H_{\mathbf{5}}$ and $\Sigma_{\mathbf{24}}$. Although both scalars have been treated independently,[5] interactions among them arise via radiative corrections and yield divergent diagrams that can only be regulated, if the full Lagrangian will contain all possible terms. As a partial solution, working with the full Lagrangian leads to Higgs triplet masses of $\mathcal{O}(v_5)$, which simultaneously solves the first problem. But unfortunately, also the Higgs doublet gets a mass contribution of $\mathcal{O}(v_5)$. In order to get a Higgs doublet mass of $\mathcal{O}(v_{EW})$, being twelve orders of magnitude smaller,[6] one has to assume very delicate cancellations in the potential.

[5] In the *minimal* $SU(5)$ approach, only as much terms as necessary are introduced. Hence, we rely in the minimal representations and interaction to obtain $SU(5) \to U(1)_{EM}$.

[6] The difference between the GUT scale and the electroweak scale is approximated by $\frac{v_{EW}}{v_5} \simeq \frac{m_W}{m_X} \simeq 10^{-12}$.

Yukawa sector

As already discussed in chapter 2, fermion masses have to be generated via Yukawa interaction of LH and RH fields since they violate the SM gauge symmetry. Equivalently, a LH/RH field and its corresponding LCC field can be used. As the LH fermions are now contained in a $(\overline{\mathbf{5}}+\mathbf{10})$ representation, the corresponding Yukawa terms include the product $(\overline{\mathbf{5}}+\mathbf{10})\times(\overline{\mathbf{5}}+\mathbf{10})$. This leads to the following fermionic products

$$\begin{aligned} \overline{\mathbf{5}} \times \mathbf{10} &= \mathbf{5} + \overline{\mathbf{45}} \\ \mathbf{10} \times \mathbf{10} &= \overline{\mathbf{5}} + \mathbf{45} + \mathbf{50} \\ \overline{\mathbf{5}} \times \overline{\mathbf{5}} &= \overline{\mathbf{10}} + \overline{\mathbf{15}}. \end{aligned} \tag{4.21}$$

Also in $SU(5)$, mass terms originate from couplings between the above terms and the Higgs scalar. The explicit form depends on the chosen representation for the Higgs scalar and, hence, produces different mass patterns at low-energy. In the *minimal* $SU(5)$ framework, one only uses the *minimal* scalar representation, that is needed to arive at $SU(3)_C \times U(1)_Y$, the $\mathbf{5}$ and $\mathbf{24}$. As the latter is not appearing in the fermionic products (4.21), it does not couple to any fermions. This sets the fermionic mass scale to $\mathcal{O}(v_{EW})$ through interactions with $H_{\mathbf{5}}$. Then, the possible Yukawa Lagrangian is given by

$$\mathcal{L}_{Yuk} = (\psi_R)^\dagger_{i\alpha}\, m^D_{ij} (X_L)^{\alpha\beta}_j H^\dagger_\beta - \frac{1}{4}\epsilon_{\alpha\beta\gamma\delta\epsilon}\left(X^T_L\right)^{\alpha\beta}_i \sigma^2 m^U_{ij} (X_L)^{\gamma\delta}_j H^\epsilon + h.c.\,, \tag{4.22}$$

where i, j correspond to generation and $\alpha, ..., \epsilon$ to $SU(5)$ indices. The representation labels are omitted to avoid clutter. If the neutral Higgs component develops a VEV, quark and lepton masses are generated and, after diagonalization of the corresponding mass matrices, the following LO mass relations are obtained

$$m_d = m_e = M^D_{11}\, v_{EW}\,, \quad m_s = m_\mu = M^D_{22}\, v_{EW}\,, \quad m_b = m_\tau = M^D_{33}\, v_{EW}\,. \tag{4.23}$$

For the minimal $SU(5)$ GUT with only $H_{\mathbf{5}}$ and $\Sigma_{\mathbf{24}}$, we generally arrive at $m_d = m_e$ and a symmetric up quark mass matrix, $m_u = m_u^T$. Radiative corrections lead to good agreement with experimental data for the bottom-quark, but unfortunately, with lowering generation index the conformity with experimental data gets worse. The up-quark masses do not exhibit any further mass relations since RH neutrinos are implemented in the generic model. As (4.21) indicates, the Higgs can also be chosen as a **10**-, **45**- or **50**-plet and would give different mass patterns or at least some modifications. By diagonalization of the mass matrices, one obtains a generalized form of the CKM matrix, see section 2.2. This procedure involves new rotation matrices for the new gauge bosons, X_μ and Y_μ, which could give rise to new CP violating processes.

Summary and final remark on neutrino masses

The minimal $SU(5)$ GUT is capable of providing a reasonable symmetry breaking pattern such that we arrive at the correct low-energy theory. The $(\bar{\mathbf{5}} + \mathbf{10})$-representations simplifies the SM family structure by grouping quarks and leptons

of the same generation, which results in certain mass relation. From a UV completion of the SM, we expect some answers to open questions, e.g. why there exist three particle generation, etc. Since the $SU(5)$ GUT seems to be a step in the right direction, we now discuss its strengths and weaknesses. Unfortunately, in the $SU(5)$ framework the number of generations or the connection between different representations of the Poincaré group remains unanswered. Its great success reveals itself in the prediction of third integral quark charges as well as the right prediction of the Weinberg angle θ_W. On the other hand, proton decay, a generic feature, is clearly in disagreement with observations. No progress is made in the scalar and Yukawa sector in comparison with the SM. Additional DOFs are needed to arrive at the SM gauge group, yielding more free parameters in the theory. The Yukawa interactions give some vague predictions on possible mass relations that are in clear tension with experiments.

The minimal $SU(5)$ GUT might not be the correct description of Nature, but it yields remarkable properties and already shows which kind of obstacles a real GUT has to overcome. However, in the pursuit of finding a UV completion of the minimal type-I seesaw model, it provides an elegant framework, because RH neutrino and, hence, a type-I seesaw mechanism can easily be implemented. A full embedding of RH neutrinos, ν_R, requires a group of rank 5, which $SU(5)$ is definitely not. The simplest way to accommodate their existence is to introduce an additional quantum number Y_5, called fiveness, which corresponds to an additional $U(1)_5$ symmetry. To guarantee cancellations of anomalies within $SU(5) \times U(1)_5$, an additional fermionic singlets $\mathbf{1}$ are needed to represent the RH neutrinos. An alternative is to chose another favored GUT group, e.g. $SO(10)$, that contains $SU(5) \times U(1)_5$ as a subgroup. There, the representations $\mathbf{10}$, $\bar{\mathbf{5}}$ and $\mathbf{1}$ are combined in the same multiplet. As the breaking-scheme of $SO(10)$ is tightly constrained, the minimal ansatz is just to start with $SU(5) \times U(1)$. Usually, the RH mass assignment is associated with breaking of fiveness, which is independent of $SU(5)$-breaking and hence not constrained by from low-energy phenomenology. If $SU(5)$ is broken before fiveness, one can combine $U(1)_5$ with the occurring $U(1)$ from $SU(5)$-breaking to $U(1)_Y \times U(1)_{B-L}$, hence obtaining finally the gauge group $SU(3)_C \times SU(2)_L \times U(1)_Y \times U(1)_{B-L}$. This not only establishes $(B-L)$ as another quantum number of the SM, but also links the RH Majorana mass term to the breaking of $U(1)_{B-L}$. Since the Majorana mass terms violate $(B-L)$, the corresponding $U(1)_{B-L}$ has to be broken before they are generated. Hence, the easiest way to obtain heavy Majorana masses, is to generate them directly through $(B-L)$-breaking, e.g. by some heavy scalar. In what follows, we simply assume the minimal realization of an $SU(5) \times U(1)_5$ symmetry and corresponding breaking in such a way that as to associate the occurring Majorana mass scale with $(B-L)$ breaking.

4.2.2. Froggatt-Nielsen flavor models

Since the FN mechanism [48] is an important ingredient of a broader framework [47], where we are working in, its basic principle and subsequent embedding in

the minimal $SU(5)$ GUT is explained in the following. Originally, Froggatt and Nielsen tried to tackle the SM's flavor problem by investigating how the large mass ratios between quarks and leptons can be achieved. Their main assumption was that effective particle masses are all of the same order of magnitude at some higher fundamental scale and large masses in the SM are generated by RGE from this fundamental scale down to observable scales. Although, both could proof RGE to induce large overall effects by many orders of magnitude for particular masses, e.g. top- and bottom-quark, the corresponding effect on mass ratios remained within the same order of magnitude. Hence, their main conclusion was that large renormalization of mass ratios is only possible if there exists a quantum number ensuring different treatment of up- and down-type quarks or some underlying physics that would allow for specific selection rules. In addition, they presented a mechanism capable of providing the desired mass ratios at least as an order of magnitude estimate, which is the subject of this section.

In the FN mechanism, the existence of a certain symmetry is assumed that forces particles to have zero mass. Finite particle masses are then generated at some order in interactions, where at some point symmetry breaking occurs. By choosing an almost conserved, global continuous symmetry and assuming the existence of heavy fermions F_i, with masses $m_F \gg v_{EW}$, charged under this new FN symmetry, one is able to generate arbitrary small masses for the known SM fermions. The simplest choice is an abelian $U(1)_{FN}$ symmetry with integrally quantized charges Q_{FN}. Furthermore, LH and RH components of SM fermion are allowed to couple differently to the new gauge bosons, which results in massless fermions for an exact $U(1)_{FN}$ conservation. Light fermion mass generation is basically obtained by SSB of a new scalar field Φ, that is commonly called flavon and charged under the new symmetry, $U(1)_{FN}$. The mechanism proceeds as follows:

At first, super-heavy fermion masses are generated through SSB by a non-zero VEV of a neutral scalar, $\langle\tilde{\Phi}\rangle \neq 0$ and $Q_{FN}(\tilde{\Phi}) = 0$, hence, giving $m_F \propto \langle\tilde{\phi}\rangle$. In common approaches, this step is skipped and only the existence of heavy fermionic particles is taken for granted.

In a second step, the masses of light fermions are generated by a non-zero VEV of the flavon field Φ, that carries $Q_{FN}(\Phi) = -1$. As this is usually assumed to happen at much lower scales, the heavy fermions can safely be integrated out, which leads to light fermion masses according to

$$m_f \propto \epsilon \equiv \frac{g_\Phi(\Lambda \sim \mathrm{GeV})}{g_{\tilde{\Phi}}(\Lambda_{FN})} \frac{\langle\Phi\rangle}{m_F} \simeq \frac{\langle\Phi\rangle}{\langle\tilde{\Phi}\rangle}\,, \tag{4.24}$$

with g_i representing the couplings to the corresponding scalars, $i = \tilde{\Phi}, \Phi$ being Λ_{FN} the fundamental scale of heavy fermion mass generation. Because of small changes in g_i, the resulting mass only depends on the ratio between both VEVs, which can be tuned arbitrarily.

In the last step, the usual Higgs boson ϕ is needed to break the electroweak symmetry group. It cannot generate light fermion masses alone since it is neutral under the FN symmetry. All Yukawa couplings are naturally assumed to be of $\mathcal{O}(1)$ at the fundamental scale Λ_{FN}. Hence, the light fermion masses are tuned by

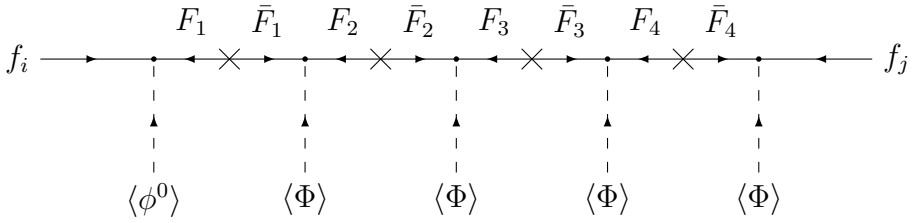

Figure 4.1.: Generation of mass hierarchies through the FN mechanism. The number of tadpoles corresponds to the difference in the FN quantum number between of RH and LH fermions, i.e. $\#(\Phi \text{ tadpoles}) = |Q_{FN}(L_j) - Q_{FN}(l_i)|$. The more interactions, the stronger suppression of the resulting Yukawa coupling due to different powers of ϵ.

appropriate choice of ϵ, which is given as the ratio of both VEVs, such that,

$$m_f = \mathcal{O}(1)\epsilon \langle\phi\rangle \ . \tag{4.25}$$

A certain hierarchy between different fermions can easily established via so-called "spaghetti" interactions, see figure 4.1.

In such interactions, light fermions acquire their mass through couplings to heavy fermions F_i and multiple tadpole interactions with $\langle\Phi\rangle$. The number of heavy fermion propagators or equivalently tadpoles depends on the Q_{FN}-assignment to the light fermions, $\#(\phi_1 \text{ tadpoles}) = |Q_{FN}(L_j) - Q_{FN}(l_i)|$. Each heavy fermion mediator contributes a factor of $\langle\tilde{\Phi}\rangle^{-1}$, while each tadpole-coupling yields a factor of $\langle\Phi\rangle$. The light fermion receives a total mass

$$(m_f)_{ij} \simeq h_{ij}\epsilon^{a_i+b_j} v_{EW} \equiv y_{ij} v_{EW} \ , \tag{4.26}$$

with the exponent originating from the difference in FN charges, $Q_{FN}(L_j) = c + b_j$ and $Q_{FN}(l_j) = c - a_j$, and h_{ij} being a matrix collecting all relevant couplings for each individual fermion. Usually each entry is assumed to be of $\mathcal{O}(1)$. To account for light fermions, an appropriately large FN charge difference has to be obtained, hence, assuming $a_i > 0$ and $b_j \geq 0$ with ordering $a_{i+1} \geq a_i$ and $b_{j+1} \geq b_j$. The explicit charge assignment depends on the specific value of ϵ, chosen to characterize the corresponding quark or lepton mass matrix, as we will see in the following. In this way, we are capable of generating the hierarchically structured Yukawa couplings of the SM.[7]

Finally, the whole mechanism yields a Yukawa term according to

$$\mathcal{L} = h_{ij} \left(\frac{\langle\Phi\rangle}{\Lambda}\right)^{Q_i+Q_j} \psi_i \psi_j \phi \ , \tag{4.27}$$

with coupling constants $h_{ij} \sim \mathcal{O}(1)$ and Λ_{FN} the scale of the introduced heavy fermions. Q_i correspond to the FN charges of fermion fields, whereas the usual SM Higgs ϕ remains neutral. For $\epsilon \ll 1$, assignment of FN charges is possible

[7] For the general proof that this mechanism is capable of reproducing appropriately large mass ratios, we refer to the original paper of Froggatt and Nielsen [48].

in a way that quark and lepton masses are recovered correctly, as shown in [47]. For details on the individual steps, see appendix B. Detection possibilities for the flavon field are investigated, e.g. in [124] in the context of the LHC and a future 100 TeV collider. Caution has to be taken in comparing different FN models as they are very sensitive to the chosen parametrization of quark and lepton mass matrices as well as the explicit value of ϵ.

$SU(5)$ Froggatt-Nielsen model

In the following, we present an embedding of the FN mechanism into the $SU(5) \times U(1)_5$ GUT, which is capable of reproducing the correct quark and lepton mass pattern, while further accommodating for RH neutrinos in $SU(5)$ singlet representations, $\psi_{\mathbf{1}}$ [37, 47]. This model will be our starting point in the next section, as we modify it appropriately for the minimal type-I seesaw model. The Yukawa sector of the usual $SU(5)$ GUT is modified, such that the corresponding Yukawa couplings are obtained through the FN mechanism. To avoid clutter, the $SU(5)$ Yukawa sector of equation (4.22) is stated in a more compact notion and RH neutrino terms are added, hence, yielding

$$\begin{aligned}\mathcal{L}^5_{Yuk} = {} & h^u_{ij}\epsilon^{Q^{\mathbf{10}}_i+Q^{\mathbf{10}}_j}(X_{\mathbf{10}})_i(X_{\mathbf{10}})_j H_{\mathbf{5}} + h^d_{ij}\epsilon^{Q^{\mathbf{5}}_i+Q^{\mathbf{10}}_j}(\psi_{\mathbf{5}})^*_i(X_{\mathbf{10}})_j H^*_{\mathbf{5}} \\ & + h^\nu_{ij}\epsilon^{Q^{\mathbf{5}}_i+Q^{\mathbf{1}}_j}(\psi_{\mathbf{5}})^*_i(\psi_{\mathbf{1}})_j H_{\mathbf{5}} + h^s_{ij}\epsilon^{Q^{\mathbf{1}}_i+Q^{\mathbf{1}}_j}(\psi_{\mathbf{1}})_i(\psi_{\mathbf{1}})_j S_{\mathbf{1}}\,,\end{aligned} \tag{4.28}$$

with generation indices $i, j = 1, 2, 3$, the FN parameter $\epsilon = \left(\frac{\langle\Phi\rangle}{\Lambda}\right)$ and the matrix h^α_{ij}, $\alpha = u, d, \nu, s$ that contains couplings of $\mathcal{O}(1)$. A non-zero VEV of the scalar singlet $S_{\mathbf{1}}$ is used to obtain RH Majorana masses. The GUT-scale masses of quarks and leptons are associated to the FN parameter ϵ according to,

$$\begin{aligned} m_t : m_c : m_u &\simeq 1 : \epsilon^2 : \epsilon^4 \\ m_b : m_s : m_d \simeq m_\tau : m_\mu : m_e &\simeq 1 : \epsilon : \epsilon^3\,, \end{aligned} \tag{4.29}$$

for an $\epsilon \sim \frac{1}{20} - \frac{1}{10}$. As the exponents of the small ϵ's reflect the difference in $U(1)_{FN}$ charges, we can directly infer the corresponding quantum numbers. Up-quark masses arise from the first term of (4.28) and the charges 2, 1, 0 for rising generation index of the decouplets $X_{\mathbf{10},i}$ have to be assigned to recover the mass relations of (4.29).[8] Equivalently, one can find the appropriate charges for the fiveplets $\psi_{\mathbf{5},i}$. As nothing can be said about the heavy neutrino masses, it is impossible to assign any concrete FN charge to them. By assuming a hierarchical generation structure, we are at least able to order these charges according to their magnitudes, $b \geq c \geq d$. An overview of the charge assignment is given in table 4.1.

Although the theoretical framework is already set, we want to address some phenomenological consequences of this model for the SM [37]. To account for the correct mass ratios between up- and down-type quarks, one has to set $a = 1$. In

[8] One obtains three conditions for the three individual charges. By setting $Q_{FN}(X_{\mathbf{10},3}) = 0$ minimal FN charges are guaranteed.

$SU(5)$ multiplet	$\mathbf{10}_1$	$\mathbf{10}_2$	$\mathbf{10}_3$	$\mathbf{5}^*_1$	$\mathbf{5}^*_2$	$\mathbf{5}^*_3$	$\mathbf{1}_1$	$\mathbf{1}_2$	$\mathbf{1}_3$	Φ
$SU(5)$ FN flavor model	2	1	0	$1+a$	a	a	b	c	d	-1
Minimal seesaw embedding	2	1	0	2	1	1	q	q	$\diagdown$	-1

Table 4.1.: FN charge assignment of SM fermions, RH neutrinos and the flavon field Φ of [47] and the constructed minimal type-I seesaw model. The multiplets are defined in (4.4) and (4.6) and carry a generation index. The singlets are needed to account for RH neutrinos and have undetermined charges in [47]. For the minimal seesaw embedding, just two RH neutrinos singlets are needed, whose charges are determined later through other theoretical constraints.

the basis where the up-quark mass matrix is diagonal, one obtains the following mass matrices,

$$m_u = \begin{pmatrix} \epsilon^4 & & \\ & \epsilon^2 & \\ & & 1 \end{pmatrix} \langle\phi\rangle\, y_t\,, \quad m_d = \begin{pmatrix} \epsilon^3 & \epsilon^2 & \epsilon \\ \epsilon^2 & \epsilon^1 & 1 \\ \epsilon^2 & \epsilon & 1 \end{pmatrix} \langle\phi\rangle\, y_b\,. \tag{4.30}$$

By further diagonalization, one achieves important predictions for the quark and lepton mixing. The quark mixing matrix exhibits small mixing angles, i.e. for the case of diagonal up-type matrix we get,

$$U_{12} =\simeq \mathcal{O}(\epsilon), \qquad U_{23} =\simeq \mathcal{O}(\epsilon), \qquad U_{13} = V^l_{13} \simeq \mathcal{O}(\epsilon^2)\,, \tag{4.31}$$

being in agreement with observations, if $\mathcal{O}(1)$ uncertainties of the matrix elements are taken into account. The leptonic mass matrix is given by $m_l = (m_d)^T$, leading to large mixing between the second and third element,

$$V^l_{23} \simeq \mathcal{O}(1), \qquad V^l_{12} \simeq \mathcal{O}(\epsilon), \qquad V^l_{13} \simeq \mathcal{O}(\epsilon), \tag{4.32}$$

which reflects the equal FN charge assignment of the corresponding fiveplets, see table 4.1. In contrast, the quark doublets contained in decouplets have different FN charges for each family, resulting in almost equally mixing.

If RH neutrinos are introduced, the corresponding mass matrix can be chosen to be diagonal,

$$M_{\nu_R} = \mathrm{diag}(\epsilon^{2b}, \epsilon^{2c}, \epsilon^{2d}) m_R\,. \tag{4.33}$$

The existence of RH neutrinos directly allows for neutrino Yukawa interactions

that result in Dirac masses through the usual Higgs mechanism,

$$m_{\nu,D} = \begin{pmatrix} \epsilon^{1+b} & \epsilon^b & \epsilon^b \\ \epsilon^{1+c} & \epsilon^c & \epsilon^c \\ \epsilon^{1+d} & \epsilon^b & \epsilon^b \end{pmatrix} \epsilon^2 \frac{\langle\phi\rangle}{m_R} \,. \tag{4.34}$$

Hence, the invoked seesaw mechanism will generate light neutrino masses according to (2.52), given by

$$m_\nu = \begin{pmatrix} \epsilon^2 & \epsilon & \epsilon \\ \epsilon & 1 & 1 \\ \epsilon & 1 & 1 \end{pmatrix} \epsilon^2 \frac{\langle\phi\rangle^2}{m_R} \,. \tag{4.35}$$

Remarkably, this does not depend on any RH neutrino FN charges, but only on the FN charges carried by lepton doublets.

In the end, we give one remark: From the last formula, the form of the Weinberg operator (2.42) in the context of our $SU(5)$ approach can directly be inferred as

$$\mathcal{L}_W = f_{ij} (\psi_{\mathbf{5}})^*_i (\psi_{\mathbf{5}})^*_j H_{\mathbf{5}} H_{\mathbf{5}} \,, \tag{4.36}$$

where f_{ij} are the generic neutrino couplings that are suppressed by the heavy RH neutrino mass scale.

4.3. High-energy embedding of the minimal type-I seesaw model

After the introduction of our framework and the underlying methods, we will present the actual flavor model that embeds the minimal type-I seesaw at high energies. By further assuming (approximate) exchange symmetries in the heavy neutrino sector, we are able to reduce this model's parameter space further, such that we arrive at a minimal UV completion of the type-I seesaw model.

4.3.1. Modified $SU(5)$ Froggatt-Nielsen framework

Without loss of generality, we assume to work in a basis, where the charged lepton, m_l, and the RH neutrino mass matrix, m_R, are diagonal and switch to index-notation. We begin by shortly reviewing the minimal type-I seesaw model of section 3.2 in a slightly different notation and link it to the presented $SU(5)$ FN flavor model of the last section. Hence, the Lagrangian of our minimal type-I seesaw model is given by[9]

$$\mathcal{L} = -y_{\alpha i} l_\alpha N_i \phi - \frac{1}{2} m_{R,i} N_i N_i + \text{h.c.} \,, \tag{4.37}$$

[9] For the following investigation we switch from chiral to two-component notation since it simplifies the formulation of the demanded exchange symmetries.

with the Yukawa coupling $y_{\alpha i}$ describing the interaction between RH neutrinos N_i $i = 1, 2$, the LH SM lepton doublets $l_\alpha = (\nu_\alpha, e_\alpha)^T$ and the Higgs doublet $\phi = (\phi^+, \phi^0)^T$. As already explained in chapter 3, the minimal type-I seesaw model has nine real DOFs, eleven if we do not absorb the heavy neutrino masses in the Yukawa coupling.

To further reduce the number of DOFs of the minimal seesaw framework, we chose to apply the FN mechanism to account for its Yukawa structure and embed it into the minimal $SU(5)$ GUT. Then the remaining free parameters can be interpreted in a broader theoretical context. For this, we take advantage of the previously introduced $SU(5)$ FN flavor model of [47] and modify it according to our purposes. Since we do not make any statement about the dynamics at scales much higher than the GUT scale, we omit the first step of the FN mechanism. As the heavy fermions are considered as non-propagating DOFs, they are integrated out[10] and subsequently lead to a suppression of the corresponding couplings according the FN energy scale Λ_{FN}. We assume that $SU(5)$ symmetry breaking proceeds as usual in the minimal $SU(5)$ GUT and does not affect the implemented FN mechanism, such that we can directly focus on the SM DOFs. As the FN charge is assigned to the GUT multiplets, all SM fermions within the same representation share equal FN charges as a relic of their unification. Hence, the most relevant part for the following procedure is

$$\mathcal{L}_{eff} \supset a_{ij} \left(\frac{\Phi}{\Lambda_{FN}} \right)^{p_{ij}} f_i \, f_j \, \phi \,, \tag{4.38}$$

for each SM fermion $f_i \in \{l_i \,, q_i\}$ with generation indices $i, j = 1, 2, 3$. a_{ij} represent arbitrary, dimensionless couplings of $\mathcal{O}(1)$ that incorporate all high-energy interactions, which are not subject of our interest. As usual, the flavon field Φ carries FN charge $Q_{FN} = -1$. Moreover, the FN charge assignment of the $SU(5)$ multiplets, see e.g. table 4.1, fixes the exponent of the ratio Φ/Λ_{FN} in (4.38), independently whether a global or local realization of $U(1)_{FN}$, is chosen $p_{ij} = Q_{FN}(f_i) + Q_{FN}(f_j)$.

Next we take the simplest way of breaking $U(1)_{FN}$ which is spontaneous breaking by a non-zero flavon VEV $\langle \Phi \rangle$, slightly below the effective theory's cut-off, Λ_{FN}. Having fixed the ratio Φ/Λ_{FN}, which can occur in various powers depending on the previously chosen FN charges Q_{FN}. By doing so, we convert the problem of certain hierarchies among SM Yukawa couplings into an explicit charge assignment within the context of a minimal $SU(5)$ GUT, extended with a RH neutrino sector. Hence, the SM Yukawa matrices can easily be parametrized by the parameter ϵ_0 and the fermionic charge under the broken FN symmetry $U(1)_{FN}$,

$$\Phi \to \langle \Phi \rangle \Longrightarrow \mathcal{L}_{eff} \to y_{ij} f_i \, f_j \, \phi, \qquad y_{ij} = a_{ij} \epsilon_0^{p_{ij}}, \qquad \epsilon_0 = \frac{\langle \Phi \rangle}{\Lambda_{FN}} \,. \tag{4.39}$$

This does not solve SM flavor puzzle at all! The resulting Yukawa hierarchies are now originating from an explicit $U(1)_{FN}$ charge assignment, which has to be put

[10] We assume their masses to be of the same order as the FN scale, $m_F \propto \Lambda_{FN}$. Integrating out contributes a factor of Λ_{FN}^{-1}.

in by hand. Moreover, we have to guarantee a very fine-tuned value of the ratio $\langle\Phi\rangle/\Lambda_{FN}$ to account for the observed quark and lepton mass patterns. However, the flavor puzzle is exchanged with a mechanism that is already realized in Nature, the Higgs mechanism, and the occurring Yukawa couplings arise from a theoretical more favored origin; a symmetry with its corresponding charges. In our pursuit of finding a minimal UV flavor embedding of the minimal seesaw, this mechanism seems justified due to its simplicity and known behavior.

Now, we can rely on the findings of [47] and use the postulated charge assignment according to table 4.1. By setting $\epsilon_0 \simeq 0.17$, the correct quark and lepton mass matrices are recovered, up to $\mathcal{O}(1)$ coefficients. The only remaining task is to modify the heavy neutrino sector. In contrast to [47], we only introduce two RH neutrinos with FN charges q_i. To account for light neutrino masses coming from the seesaw mechanism, we introduce a (2×2) Majorana mass matrix. At this stage, we assume that the hierarchy among the heavy neutrinos is also generated through the FN mechanism, yielding

$$m_R = \begin{pmatrix} b_1\epsilon_0^{q_1} & 0 \\ 0 & b_2\epsilon_0^{q_2} \end{pmatrix} m_0 \qquad \text{with } q_i = 2\,Q_{FN}(N_i)\ , \tag{4.40}$$

where b_i is again a dimensionless coefficient of $\mathcal{O}(1)$ and m_0 refers to the generic mass scale of heavy neutrinos, which is usually generated by some $U(1)_{B-L}$ breaking. Driven by the aim of minimality, we charge both RH neutrinos equally, $Q_{FN}(N_2) = Q_{FN}(N_1) \equiv q \geq 0$. Another motivation is that approximate mass degeneracy between both RH neutrinos, $m_{R,1} \sim m_{R,2}$ can yield successful leptogenesis scenarios [40, 109]. According to (4.39), equation (4.37) becomes

$$y_{\alpha I} = a_{\alpha I}\epsilon_0^{p_{\alpha I}} \qquad \text{with} \quad p_{\alpha I} = Q_{FN}(l_\alpha) + Q_{FN}(N_i)\,. \tag{4.41}$$

The full charge assignment of our framework can be seen in table 4.1 and its application leads to the following structure in the neutrino Yukawa coupling matrix (4.41),

$$y_{\alpha I} \sim \begin{pmatrix} \epsilon_0 & \epsilon_0 \\ 1 & 1 \\ 1 & 1 \end{pmatrix} y_0, \qquad y_0 \equiv \epsilon_0^q\ , \tag{4.42}$$

where y_0 corresponds to the universal suppression of all Yukawa couplings due to the RH neutrino charge q. All entries exhibit $\mathcal{O}(1)$ uncertainties, as does the hierarchy structure.

In this way, we have obtained a generic Yukawa structure produced by the simple FN mechanism through explicit charge assignments to multiplets of the minimal $SU(5)$ GUT. Hence, we arrive at a high-energy embedding of the minimal type-I seesaw model, now derived as a well-motivated top-down approach.

4.3.2. Exchange symmetries in the heavy neutrino sector

Now, that we have modified the $SU(5)$ FN model according to the minimal seesaw framework, we want to dive further into parameter space considerations in order to

continue reducing the number of free parameters. We have already seen that the FN mechanism can easily produce hierarchies within the neutrino Yukawa matrix (4.42) up to coefficients of $\mathcal{O}(1)$. To get a handle on this, we apply a "self-made" parametrization of the seesaw Yukawa matrix according to

$$y_{\alpha I} = \begin{pmatrix} \epsilon \cos\theta_e e^{i\phi_e} & \epsilon \sin\theta_e e^{i\phi_e + \Delta\phi_e} \\ \cos\theta_\mu e^{i\phi_\mu} & \sin\theta_\mu e^{i\phi_\mu + \Delta\phi_\mu} \\ c_{\mu\tau} \cos\theta_\tau e^{i\phi_\tau} & c_{\mu\tau} \sin\theta_\tau e^{i\phi_\tau + \Delta\phi_\tau} \end{pmatrix} y_0 \ , \tag{4.43}$$

that will proof very useful in what follows. Since we assigned explicit variables to each $\mathcal{O}(1)$-uncertainty, we can study their behavior, e.g. in the transition to flavor-aligned texture regions. The three mixing angles are defined in the interval $\theta_\alpha \in \left[-\frac{\pi}{2}, \frac{\pi}{2}\right]$ and the phases $\varphi_\alpha \in [0, 2\pi]$. The phase shifts $\Delta\varphi_\alpha \in [0, 2\pi]$ are introduced to account for some relative phase between both matrix columns. Further, $c_{\mu\tau}$ is a dimensionless quantity of $\mathcal{O}(1)$ and $\epsilon \simeq \epsilon_0 \simeq 0.17$ is defined in close connection to [47], while we also allow for small deviations. The quantity y_0 is the same as in (4.42) and reflects the universal suppression through heavy neutrinos FN charges. If we do not apply any further assumptions or constraints, (4.43) exhibits the same number of parameters as a general complex (3×2) matrix; six absolute values, y_0, ϵ, $c_{\mu\tau}$ and $\theta_{e,\mu,\tau}$, and three phases as well as three phase shifts, φ_α and $\Delta\varphi_\alpha$.

We can further reduce them by making the following observations:
The Yukawa pattern of (4.42) exhibits equal Yukawa couplings for both matrix columns up to correction of $\mathcal{O}(1)$, suggesting an approximate exchange symmetry between both columns. Motivated by the fact that nearly-degenerate heavy neutrino masses are capable of yielding successful leptogenesis [109], we already assigned equal FN charges according to table 4.1. This reflects a further (approximate) exchange symmetry, now in terms of heavy neutrino masses. The application of both approximate exchange symmetries, exchange of Yukawa columns and heavy neurino masses,

$$|y_{\alpha 1}| \sim |y_{\alpha 2}|, \qquad\qquad m_{R,1} \sim m_{R,2} \tag{4.44}$$

puts constraints on all mixing angles of (4.43), which have to satisfy $\sin\theta_\alpha \approx \cos\theta_\alpha$ or equivalently $\tan\theta_\alpha \approx 1$. Therefore, the number of independent parameters is reduced from twelve to nine, leaving us with all undetermined phases and shifts, but just three absolute values, y_0, ϵ and $c_{\mu\tau}$. As already discussed in chapter 3, too strong reduction of free parameters, e.g. assuming exact-zero textures, would lead to inconsistencies with experimental measurements. This also applies here, where the assumption of an exact exchange symmetry reflects such a situation, i.e. forcing some mixing angles to be exactly zero. We already encountered such a kind of exact exchange symmetry in chapter 3 in the discussion of flavor-aligned texture regions. There, both Yukawa columns are equalized, such that both heavy neutrinos couple equally to one lepton flavor. This gives us a first indication that we are on the right track of describing the origin of flavor-aligned texture regions, which was one of our motivations to study a top-down realization of our model. If we assume an approximate exchange symmetry, e.g. $|y_{\alpha 1}| = |y_{\alpha 2} + \delta y_\alpha|$ for $|\delta y_\alpha| \ll |y_{\alpha I}|$, we can in principle realize both, consistency with experimental

measurements and the order of magnitude estimates originating from our FN flavor model (4.42).

To get a better understanding of the transition towards flavor-alignment in the Yukawa matrix $y_{\alpha i}$, we apply the CIP [85] as it provides a successful separation between low- and high-energy parameters. For this purpose, we use the equations (3.8), (3.7) and (3.24), with $\kappa_{\alpha i}$ and $V_{\alpha i}$ as rescaled and dimensionless versions of the Yukawa and PMNS matrix respectively. Slight modifications lead to even more compact expressions, e.g. with $V_\alpha^\pm = \frac{1}{\sqrt{2}}\left(V_{\alpha k} \pm V_{\alpha l}\right)$ and $z = \frac{1}{\sqrt{2}}\left(z_R + i z_I\right)$, one arrives at

$$\kappa_{\alpha 1} = \frac{1}{\sqrt{2}}\left(V_\alpha^+ e^{-iz} + V_\alpha^- e^{+iz}\right), \quad \kappa_{\alpha 2} = \frac{i}{\sqrt{2}}\left(V_\alpha^- e^{+iz} - V_\alpha^+ e^{-iz}\right), \tag{4.45}$$

again with indices $(k,l) = (2,3)$ for NH and $(k,l) = (1,2)$ for IH. As we already know, the regions where an alignment of Yukawa columns is achieved, i.e. $|\kappa_{\alpha 1}| \simeq |\kappa_{\alpha 2}|$, exhibit large imaginary parts of the complex rotation angle, $|z_I| \gg 1$. For completeness, the compact expressions for flavor-aligned Yukawa matrices are given:

$$\begin{aligned} z_I \gg 1 \quad &\Longrightarrow \quad \kappa_{\alpha 1} \simeq i\kappa_{\alpha 2} \simeq \frac{1}{\sqrt{2}} V_\alpha^+ e^{-iz}\,, \\ z_I \ll 1 \quad &\Longrightarrow \quad \kappa_{\alpha 1} \simeq -i\kappa_{\alpha 2} \simeq \frac{1}{\sqrt{2}} V_\alpha^- e^{+iz}\,. \end{aligned} \tag{4.46}$$

So far, we just claimed that we transit into flavor-aligned texture regions, if $|z_I|$ is large enough, see chapter 3. To quantify what z_I value is actually enough, we now study the general behavior of mixing angles θ_α, or more precisely $\tan\theta_\alpha$, in dependence of the imaginary part of z and investigate at which values flavor-alignment occurs. After this analysis, we can specify this statement and give a certain value for z_I. We obtain the desired results by setting (4.46) equal to the dimensionless version of the introduced Yukawa parametrization (4.43). For each value of z_I, we vary the remaining free parameter of our model, the real part of the rotation angle z_R and both CP phases δ and σ, over their entire domain, while fixing the already measured neutrino observables to the values presented in table 2.3. As we have no knowledge about the realized neutrino mass hierarchy, the analysis is performed for both possible mass orderings, NH and IH. As we tested the influence of slight variation within the experimental input parameters in section 3.5, we know that our results of chapter 3 remain unaffected by this more recent data set.

We obtain distributions of the mixing angles $\tan\theta_\alpha$, where we group them according to certain quantiles Q_p analogous to a Gaussian distribution. The applied quantiles Q_p are shown in table 4.2 and the obtained mixing angle distributions can be viewed in figure 4.2.

After this investigation, we come to the following results: While for $|z_I| \leq 1$, the mixing angles can occupy various values, each leading to a slightly different neutrino Yukawa matrix with no exchange symmetry at all. For $|z_I| \gtrsim 2$, all mixing angles converge to unity, such that our assumption of approximate exchange symmetry among the Yukawa columns is almost realized and we approach flavor-alignment.

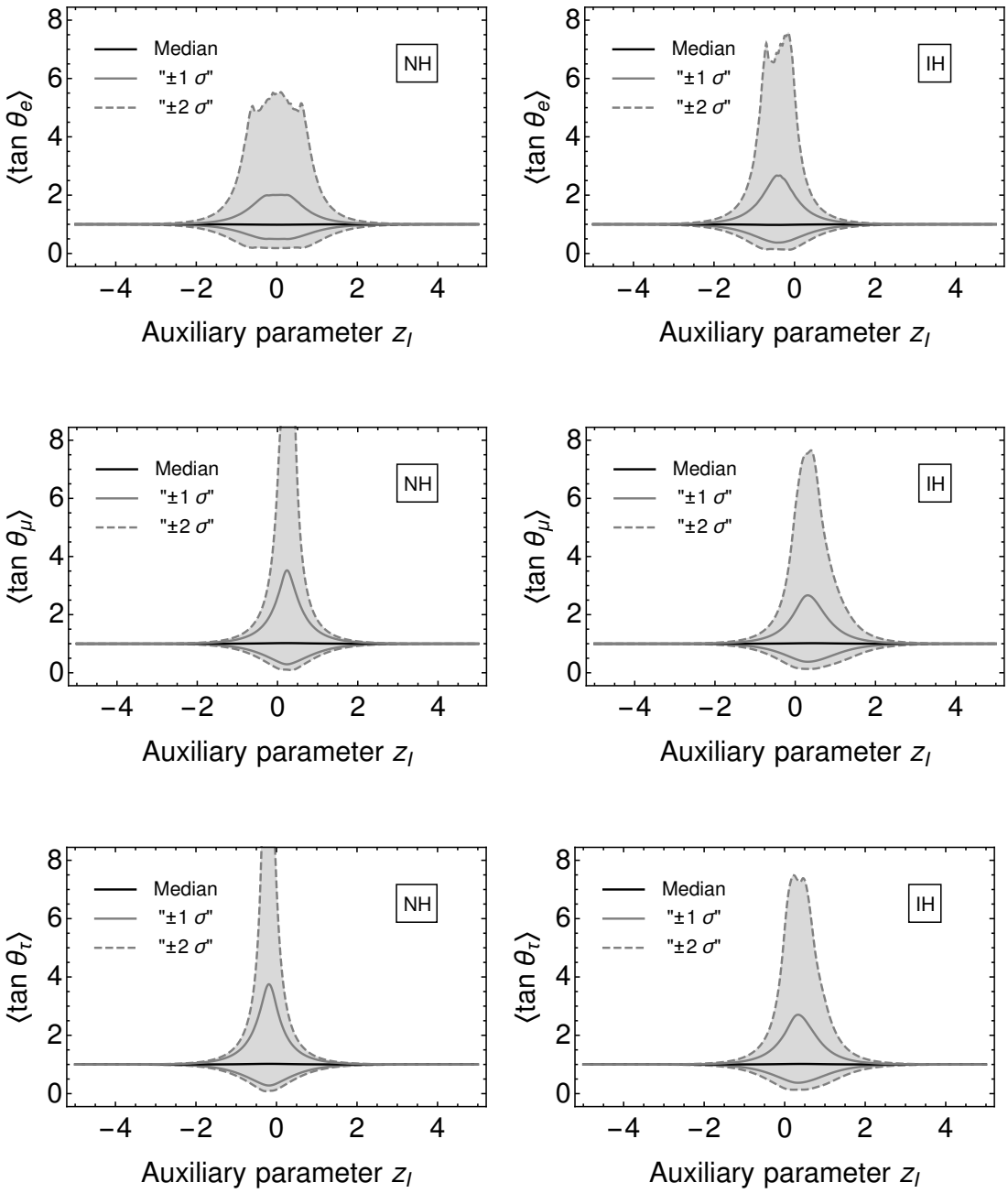

Figure 4.2.: Expectation values of the three mixing angles $\tan\theta_\alpha$ as functions of the imaginary component of the rotation angle z for both NH, **right panel**, and IH, **left panel**. The mixing angles are defined via equation (4.43) and z is defined according to (4.45). The distributions are generated by varying the undetermined parameters z_R, δ and σ, while applying the most recent neutrino data, see table 2.3 The curves indicate quantiles Q_p in analogy to a Gaussian distribution. The assigned value can be seen in table 4.2.

quantile Q_p	$-2\,\sigma$	$-1\,\sigma$	median	$+1\,\sigma$	$+2\,\sigma$
probability $p\,[\%]$	2.28	15.87	50.00	84.13	97.72

Table 4.2.: Quantiles of a Gaussian distribution that are applied to the distributions of mixing angles $\tan\theta_\alpha$ in figure 4.2.

Another result from (4.46) is that we are only able to achieve full flavor-alignment, if we allow for a specific phase relation between both Yukawa columns,

$$y_{\alpha 1} \simeq i\,\mathrm{sign}\{z_I\}\,y_{\alpha 2}\,, \tag{4.47}$$

that immediately determines the phase shifts in (4.43), up to a sign, as $\Delta\varphi_\alpha \simeq \pm\frac{\pi}{2} \simeq \mathrm{sign}\{y_i\}\frac{\pi}{2}$.

This means, the assumption of an (approximate) exchange symmetry between the Yukawa columns eliminates six parameters: all three mixing angles θ_α as well as the three phase shifts $\Delta\varphi_\alpha$. Moreover, the remaining tree phases φ_α can always be absorbed by an appropriate redefinition of the charged lepton fields. As a result, the transition to an exact exchange symmetry yields a tremendous decrease of model parameters, such that we only have to deal with three remaining parameters real values; y_0, ϵ and $c_{\mu\tau}$. The first two can be derived in the context of the previously constructed flavor model, *only* $c_{\mu\tau}$ remains as the last undetermined parameter of $\mathcal{O}(1)$. Without any further theoretical assumption, there is no possibility of linking $c_{\mu\tau}$ to other quantities. Conclusively, we arrive at a minimal top-down realization of the type-I seesaw model with only two RH heavy neutrinos, which is characterized by the following LO Lagrangian,

$$\begin{aligned}\mathcal{L}_{min} \sim &- y_0\,(\epsilon l_e + l_\mu + c_{\mu\tau} l_\tau)\,(N_1 - i\,\mathrm{sign}\{z_I\}\,N_2)\,\phi \\ &- \frac{1}{2} M (N_1 N_1 + N_2 N_2) + \text{h.c.}\,,\end{aligned} \tag{4.48}$$

with $M = \frac{1}{2}\,(m_{R,1} + m_{R,2}) \simeq m_{R,1} \simeq m_{R,2}$ due to the assumed exchange symmetry in the RH neutrino mass term. Of course, one has to take care of perturbations that arise from the approximate exchange symmetry. Viewed from a top-down perspective, at first we are interested in exact realization of some symmetry at some high scale. In this naive approach, we do not care about mechanisms that could lead to such small perturbations.

After we arrived at the minimal Lagrangian (4.48), we want to justify why it can safely be considered as a minimal realization of the seesaw mechanism with only two RH neutrinos. First, our model exhibits only two instead of the three heavy neutrinos. With this assumption, the parameter space can be reduced much and further restrictions enable us to make predictions of neutrino observables. If,

for instance, successful leptogenesis is assumed as another constraint [109], nearly-degenerate neutrino masses are required, which further shrinks the applicable parameter space. Both neutrinos than form a pair of pseudo-Dirac neutrinos, that share a common Dirac mass M, compare section 2.2.

Secondly, the underlying neutrino Yukawa matrix $y_{\alpha i}$ exhibits flavor-alignment, up to small deviations due to only approximate symmetry realization. If taken exact, the corresponding Yukawa interactions only rely on three parameters, y_0, ϵ and $c_{\mu\tau}$ and are further invariant under the exchange symmetry $N_1 \to -i\,\mathrm{sign}\{z_I\}\,N_2$. In contrast, the neutrino mass term is invariant under the exchange of both RH neutrinos $N_1 \to N_2$ as both are nearly-degenerate in mass. One has to keep in mind, that the postulated symmetries only hold for their associated terms. As we want to stay agnostic, we do not further investigate their origin.

Finally, the high-energy FN mechanism, leads to a natural suppression of the coupling between heavy neutrinos and the electron, $\epsilon \ll 1$. This results in an approximate two-zero texture that has been the subject of chapter 3. As this structure represents the strongest reduction of parameters that is consistent with observations, we also arrive at a minimal theoretical realization of experimental observables at high energies. As discussed in section 3.6, we can safely neglect RGE effects within the context of the minimal type one seesaw model [109] and directly infer properties of high-energy parameters from low-energy neutrino observables, as done in figure 4.3.

In this sense, we actually arrive at a minimal realization of the type-I seesaw mechanism. The only assumptions are the FN symmetry with a certain $SU(5)$-multiplet assignment, see table 4.1, and the approximate exchange symmetries in the heavy neutrino Yukawa interaction and mass matrix, see (4.44). As the Lagrangian (4.48) also matches the large $|z_I|$-limit of the applied CIP [85], we have shown that it can accommodate for all currently observed low-energy neutrino data, see table 2.3.

4.4. Phenomenological aspects

Since the minimal type-I seesaw model is embedded in a $SU(5)$ FN flavor model and restricted to a minimal number of free parameters, we are now interested in the model's phenomenological consequences. We investigate the available parameter space in terms of its CP phases, δ and σ, as at least one of them, δ, is expected to be determined in the near future. To be more specific, the consequences for the free model parameters are considered. In this way, we tie in with the analysis performed in chapter 3 and complement it from the high-energy point of view. Further, we confront our model with additional theoretical constraints, e.g. electroweak naturalness and leptogenesis, that have recently been investigated in the framework of this model.

4.4.1. Normal ordering and maximal CP violation

One of the main features of our FN flavor model is that, due to explicit charge assignment, some hierarchy between certain entries of the neutrino Yukawa matrix $y_{\alpha i}$ is invoked. Through the parametrization (4.43), this hierarchy can be described by relations among the Yukawa coupling, e.g.

$$\frac{|y_{e1}|^2 + |y_{e2}|^2}{|y_{\mu 1}|^2 + |y_{\mu 2}|^2} = \epsilon^2\,, \qquad \frac{|y_{\tau 1}|^2 + |y_{\tau 2}|^2}{|y_{\mu 1}|^2 + |y_{\mu 2}|^2} = c_{\mu\tau}^2\,. \tag{4.49}$$

By postulating the approximate exchange symmetry (4.44), these terms simplify to

$$\frac{|y_{ei}|}{|y_{\mu j}|} \sim \epsilon, \qquad \frac{|y_{\tau i}|}{|y_{\mu j}|} \simeq c_{\mu\tau}, \qquad \text{with } i,j = 1,2\,. \tag{4.50}$$

This gives a prediction, at least in terms of magnitudes, on the ratios of Yukawa couplings between two flavors that allows a consistency check with experimental data. Or we reverse the approach and test which kind of hierarchies are allowed by experimental data. For this approach, we apply the CIP (4.45), that has already proven very useful. If we go to the limit of exact exchange symmetry, i.e. $|z_I| \gg 1$, we obtain exact flavor-alignment between both Yukawa columns and can rely on the knowledge gained in section 3.3. From (4.46), one obtains simplified expressions that directly relate the high-energy Yukawa couplings to the observable low-energy neutrino parameters,

$$|z_I| \gg 1 \quad \Rightarrow \quad \frac{|y_{ei}|}{|y_{\mu j}|} \simeq \left|\frac{V_e^{\pm}}{V_\mu^{\pm}}\right|, \qquad |z_I| \gg 1 \quad \Rightarrow \quad \frac{|y_{\tau i}|}{|y_{\mu j}|} \simeq \left|\frac{V_\tau^{\pm}}{V_\mu^{\pm}}\right|\,, \tag{4.51}$$

with $V_\alpha^{\pm}$ as the linear combination between different rescaled Yukawa couplings, see (4.45). Equivalently to chapter 3, the flavor-aligned regions become independent of any auxiliary rotation parameter z. Hence, the ratios in (4.51) depend only on the low-energy observables, see table 2.3, and can be calculated in terms of the yet undetermined CP phases δ and σ. In contrast, we check the consistency of the high-energy parameters ϵ and $c_{\mu\tau}$ with measured low-energy neutrino observables as well, since they help us to infer any hierarchy within the neutrino Yukawa matrix. To be precise, we calculate the ratios of (4.50) in terms of the CP phases, δ and σ, while applying the measured neutrino data of table 2.3. In our model, these ratios are related to the high-energy parameters ϵ and $c_{\mu\tau}$, such that we can interpret the results as predictions for both parameters. These predictions can be viewed in figure 4.3, where we calculated the ratios given by (4.50) for both mass ordering, NH and NH, and both possible signs of z_I. The actual ratios are independent of z_I, but the sign is important as it indicates which definition of $V_\alpha^{\pm} \to V_\alpha^{\mathrm{sign}\{z_I\}}$ is used. We have found a similar situation for the asymptotic hierarchy parameter R_{23} in (3.25).

These numerical scans reveal several important results, which we will comment on in the following:

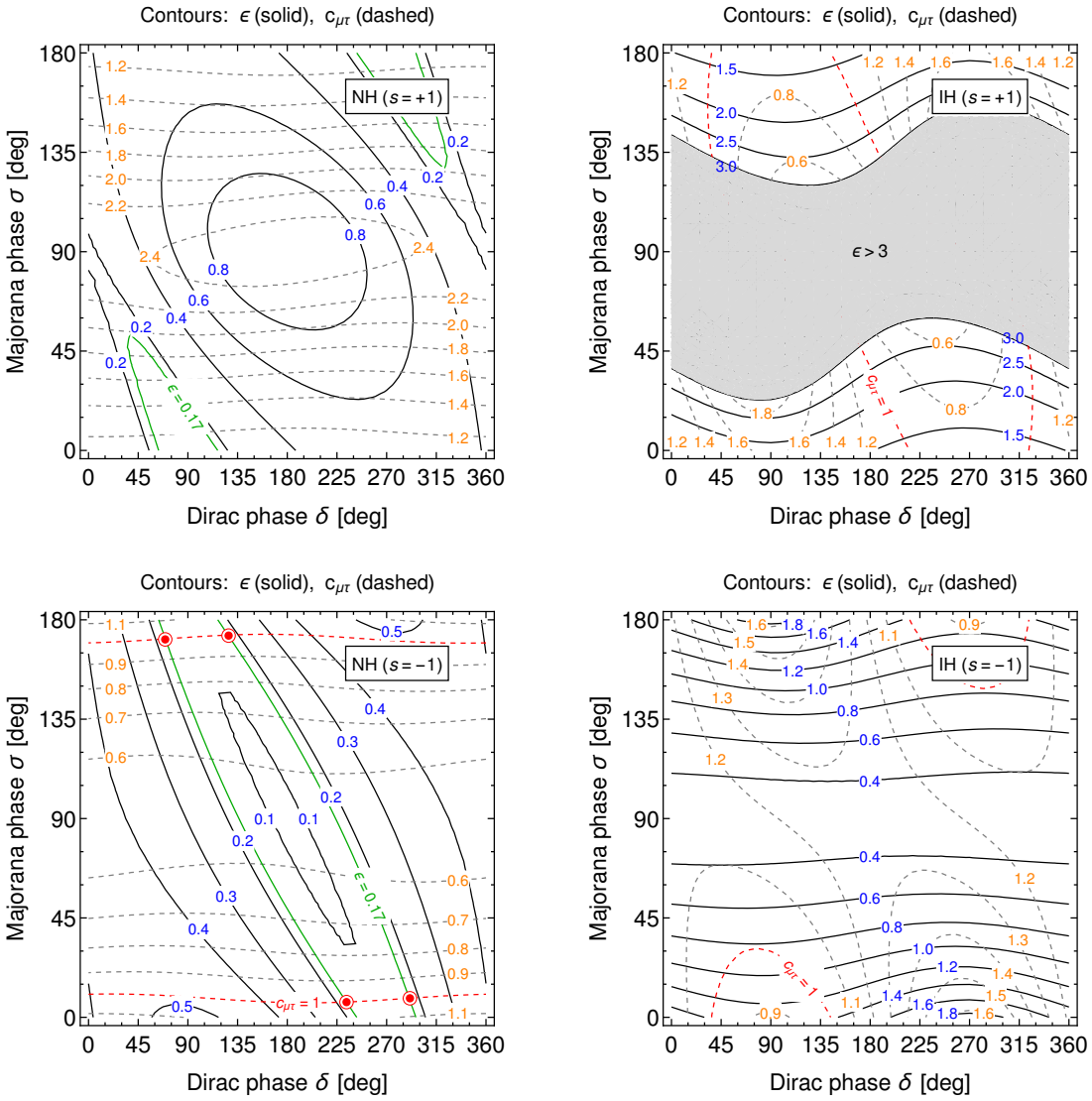

Figure 4.3.: Ratios of Yukawa couplings $|y_{eI}| / |y_{\mu J}|$ (black solid contours, blue labels) and $|y_{\tau I}| / |y_{\mu J}|$ (gray dashed contours, orange labels) as functions of the CP violating phases (δ, σ) in the flavor-aligned limit. Ratios are presented for both mass orderings, NH in the **left panels** and IH in the **right panels**, as well as for both possible signs of z_I in the CIP, $\text{sign}\{z_I\} = +1$, **upper panels** and $\text{sign}\{z_I\} = -1$, **lower panels**. All ratios are calculated according to (4.50) with the recent low-energy neutrino data, see table 2.3. The ratios $|y_{eI}| / |y_{\mu J}|$ and $|y_{\tau I}| / |y_{\mu J}|$ are controlled by the parameters ϵ and $c_{\mu\tau}$, see (4.51), the above plots can be understood as predictions for (δ, σ). The theoretical expected values for ϵ and $c_{\mu\tau}$ correspond to $\epsilon \simeq \epsilon_0 \simeq 0.17$ (green solid line) and $c_{\mu\tau} \simeq 1$ (red dashed line).

Inverted mass hierarchy The ratio between electron and muon Yukawa coupling, indicated by the black solid lines, is bounded from below, yielding values according to $|y_{ei}|/|y_{\mu j}| \gtrsim 0.30$. This is inconsistent with our general assumption of $|y_{ei}|/|y_{\mu j}| \simeq \epsilon \simeq \epsilon_0 \simeq 0.17$, which is needed to produce the right quark and lepton mass patterns that originate from (4.28) with the explicit charge assignment of table 4.1. Deviations would lead to different fermion mass patterns and necessary corrections would make things even more complicated. This would be in clear disagreement to Ockham's razor, our guiding principle in the search for a minimal seesaw realization. In this sense, we have to accept that the $SU(5)$ FN flavor model is not able to account for inverted neutrino mass ordering.

Normal mass hierarchy The corresponding plots for NH indicate that the theoretically favored ratio between electron and muon Yukawa coupling of $|y_{ei}|/|y_{\mu j}| \simeq 0.17$ can be achieved for both, positive and negative, signs of z_I. The solid green contour lines show, where the experimental data match the model's expectations. Hence, the flavor model uniquely predicts the existence of NH! Moreover, it leads to an approximate two-zero texture in the Yukawa coupling matrix and provides the missing high-energy link to the investigation performed in chapter 3. There, we already proved that NH can be in agreement with experimental data, if one allows an approximate two-zero texture and can now give an explicit high-energy model predicting its origin.

Variation of $c_{\mu\tau}$ As we also have plotted the ratio between tau and muon Yukawa coupling, gray and red dashed lines within figure 4.3, we see the prediction of certain $c_{\mu\tau}$-values. In general, various combinations of (δ, σ) are allowed by the experimental input parameters. Taking $c_{\mu\tau} \in [0.5, 2]$, for NH all possible values of the Dirac phase δ can be occupied, while some small regions of the Majorana phase σ are spared. For IH, we obtain values for every CP phase within its corresponding domain, if we assume $c_{\mu\tau}$ to be in the same regions. Assuming a certain value of $c_{\mu\tau}$ leads to strong correlation between both CP phases.

Generic prediction for CP phases Of course, we are interested in some precise predictions of our $SU(5)$ FN flavor model, to probe it with future experimental measurements. Since $c_{\mu\tau}$ is introduced as a parameter of $\mathcal{O}(1)$ in our Yukawa parametrization (4.43), we expect some predictions by fixing it to its generic value. As $c_{\mu\tau}$ already implies a strong correlation between the CP phases δ and σ, we obtain a strong reduction of possible values by assuming it close to its generic unity, $c_{\mu\tau} \simeq 1$, as indicated by the red dashed line. Only four valid combinations of δ and σ remain for NH (red dots) and a negative sign of z_I, if we simultaneously assume ϵ to take its generic value, $\epsilon \simeq 0.17$,

$$\frac{(\delta, \sigma)}{\text{deg}} \simeq \begin{cases} (234, 7) & \text{(I)} \\ (291, 9) & \text{(II)} \\ (69, 171) & \text{(III)} \\ (126, 173) & \text{(IV)} \end{cases} . \tag{4.52}$$

All solution favor phase values δ that correspond to maximal $\not{CP}$, e.g. $\delta = 90°$ or $\delta = 270°$, and moreover, the first two solutions remarkably coincide with current best-fit values of δ for NH, see table 2.3. For positive z_I and both signs in the case of IH, we do not find any predictions, consistent with the assumptions of our model. Equivalent, to the investigations of chapter 3, we can safely neglect RGE effects in the context of the minimal type-I seesaw model as their contribution are much smaller than the $\mathcal{O}(1)$ uncertainties of the applied FN mechanism [109].

By assuming $c_{\mu\tau} \simeq 1$, we absorb the last free parameter of our $SU(5)$ FN flavor model, which is justified as a naive expectation from (4.43). By doing so, we are not only able to obtain precise predictions for both CP phases at low-energies, but can also rely on more theoretical reasons since a $c_{\mu\tau}$-value close to unity implies an approximate $\mu - \tau$ symmetry [125] of the Lagrangian (4.48).

We end up with the heavy neutrino's FN charge q and their fundamental mass scale m_0 as only remaining free parameter. This is a remarkable result, as (4.48) exhibits the potential of realizing all currently measured low-energy neutrino observable as a UV completion of the type-I seesaw mechanism with only two RH neutrinos. Further, the SM's quark and lepton mass patterns are recovered, at least within their order of magnitude, originating from a well-motivated high-energy flavor model [47]. The remaining two free parameters, q and m_0, are connected to the yet unknown heavy neutrino sector and are far from being directly detected.

4.4.2. Heavy neutrino mass scale and theoretical constraints

In the following, we try to constrain the model's remaining parameter with two theoretical assumptions, that are related to the high-energy region. Hence, we expect to get some intuition about their actual values as both are also connected to high-energy regions. The authors of [109] have already checked the minimal type-I seesaw model with respect to its agreement with several theoretical constraints. This means, we can take advantage of their knowledge and simply have to apply them to our model. We only apply the strongest bounds, which are electroweak naturalness and the potential to realize successful leptogenesis. At first, we estimate the absolute RH neutrino mass scale within the context of our model by combining equations (4.40), (4.46) and (4.50), such that we obtain, in the limit of exact flavor-alignment, the following expression,

$$m_0 e^{-2z_I} \simeq 2\epsilon_0^2 |V_e^-|^{-2} \simeq 2|V_\mu^-|^{-2} v_{EW} \simeq 4.6 \times 10^{15}\ \text{GeV}. \tag{4.53}$$

Hence, the heavy neutrino (pseudo-) Dirac mass M is obtained as a function of q and z_I,

$$M \simeq 4.6\, \epsilon_0^{-2q} e^{2z_I} 10^{15}\,\text{GeV}\,. \tag{4.54}$$

As the heavy neutrinos participate in Yukawa interactions with SM leptons and the SM Higgs doublet, they can contribute radiative corrections to the SM Higgs mass-squared parameter μ^2, according to [109]

$$\delta\mu^2 \approx \frac{M^3}{4\pi^2 v^2} \cosh(2z_I) \sum_i m_i\ . \tag{4.55}$$

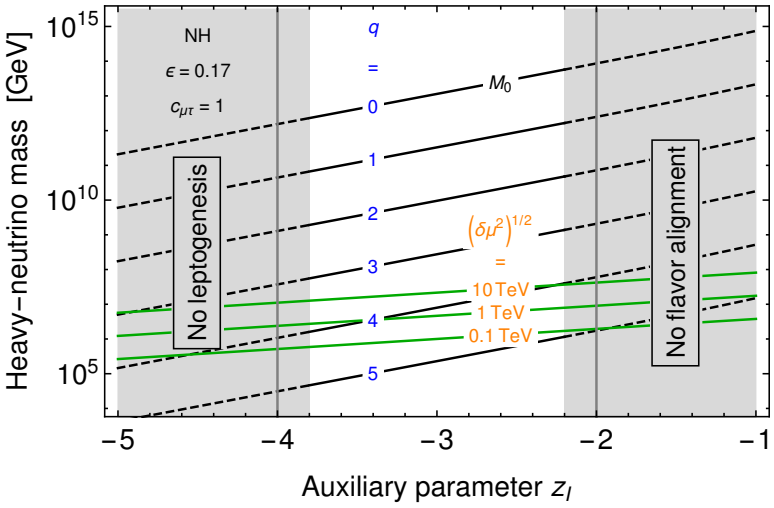

Figure 4.4.: Heavy neutrino (pseudo-) Dirac mass M as a function of the FN charge q and the imaginary part of z, black lines, given by (4.54). The corresponding masses are plotted within the range $-4 \lesssim z_I \lesssim -2$. For larger values of z_I, i.e. smaller $|z_I|$, the Yukawa matrix does no longer exhibit flavor-alignment, compare with figure 4.2. Smaller values,i.e. larger $|z_I|$, on the other hand, do not allow successful leptogenesis, as discussed [109]. In addition, the upper bound on the heavy neutrino mass scale M is given by the condition of electroweak naturalness (4.56), for three characteristic values of $\delta\mu^2_{\text{max}}$, green lines.

If such corrections exceed the Higgs VEV v_{EW}, they drive corresponding particle mass away from its measured value of $m_\phi \approx 125$ GeV. Additional terms, introduced to compensate for such contributions, are usually considered as fine-tuning. Therefore, a general assumption is that radiative contributions to the Higgs mass m_ϕ must not exceed $\mathcal{O}(\text{TeV}^2)$ to avoid such cancellations. This general statement is referred to as electroweak naturalness. In our case, this requirement gives strong bounds on the heavy neutrino mass M, given by

$$M \lesssim M_{max} \simeq \left[\left(\cosh(2z_I) \sum_i m_i \right)^{-1} 4\pi^2 v^2 \delta\mu^2_{max} \right]^{\frac{1}{3}} . \tag{4.56}$$

The possibility of accounting for the observed BAU has been checked in the framework of this minimal model. As the standard thermal leptogenesis scenario requires heavy neutrino masses that are in clear disagreement with bounds from naturalness, see e.g. for the three flavor case [126, 127], we have to rely on a different mechanism. Fortunately, resonant leptogenesis [98, 99, 108] provides a circumvention by allowing for lighter RH neutrino masses, if they are assumed to be almost degenerate. The authors of [109] found that the minimal type-I seesaw is indeed capable of realizing this scenario, assuming that $|z_I|$ does not take too large values, e.g. $|z_I| \lesssim 4$ for $M \gtrsim 1$ TeV. As other bounds from vacuum metastability, perturbativity and LNV are less constraining [109], we do not apply them in the following. Taking into account electroweak naturalness and successful leptogenesis, we plot the possible heavy neutrino masses given by (4.54) in figure 4.4. We immediately see that the imaginary z-part is restricted by requirements of having flavor-alignment on the one hand, $|z_I| \lesssim 2$, and successful leptogenesis on the other hand, $|z_I| \gtrsim 4$. The requirement of electroweak naturalness excludes all FN charges $Q_{FN}(N_i) < 4$, as the corresponding RH neutrino masses lead to strong radiative corrections contributing to μ^2. Neutrinos with FN charges $Q_{FN}(N_i) = 4$ are allowed depending on the corresponding z_I-value, whereas all heavy neutrino masses corresponding to FN charges larger than four are in perfect agreement with electroweak naturalness. Hence, we have proven that the constructed model exhibits parameter regions that are in agreement with constraints from electroweak naturalness and can lead to baryogenesis via leptogenesis. For this, FN charges larger than three have to be assigned while the fundamental RH neutrino mass scale m_0 has to be fixed to $\mathcal{O}(10^{12\ldots14})$ GeV.

4.4.3. Deeper connections to other theories

Before closing this investigation with a conclusion, we want to comment on some interesting parallels to another model, that exhibits similar properties. Some manipulations have to be performed to emphasize this point. We perform a basis transformation of the heavy neutrino sector,

$$\tilde{N}_1 = \frac{1}{\sqrt{2}} (N_1 + i\, N_2) \ , \quad \tilde{N}_2 = \frac{1}{\sqrt{2}} (N_1 - i\, N_2) \ , \tag{4.57}$$

to obtain a Lagrangian, in which the pseudo-Dirac nature of the heavy neutrino fields is evident,

$$\mathcal{L}_{\text{seesaw}} \sim -\sqrt{2}\,\epsilon_0^q\,(\epsilon_0\,\ell_e + \ell_\mu + \ell_\tau)\,\tilde{N}_1\,H - \epsilon_0^{2q}\,M_0\,\tilde{N}_1\tilde{N}_2 + \text{h.c.}\,. \tag{4.58}$$

The important exchange symmetries applied in this chapter are then given by

$$\begin{aligned} N_1 &\leftrightarrow i\,N_2 \quad \Leftrightarrow \quad \tilde{N}_{1,2} \leftrightarrow \pm\ \tilde{N}_{1,2}\,, \\ N_1 &\leftrightarrow\ \ N_2 \quad \Leftrightarrow \quad \tilde{N}_{1,2} \leftrightarrow \pm i\,\tilde{N}_{2,1}\,, \end{aligned} \tag{4.59}$$

while the first one corresponds to the approximate symmetry assumed to be present in the Yukawa interactions and the second one to the symmetry of the heavy neutrino mass term. Remarkably, the Lagrangian (4.58) receives special attention in the models of [40, 128, 129], where its supersymmetric version is responsible for the exponential expansion during the inflationary epoch of the Universe. For this type of models the super-partners of $\tilde{N}_2$ and $\tilde{N}_1$ act as inflation and a corresponding stabilizer field, such that a successful inflation epoch is established by a sufficient suppression of couplings within the corresponding Yukawa matrix. While in [128] an approximate shift symmetry in a certain field direction is used, our model relies on an approximate discrete symmetry. As both models exhibit some parallels, a deeper investigation of the supersymmetric version of our model could be useful, although it is way beyond the scope of this thesis. More importantly, a deeper investigation of the small corrections to the model's Lagrangian and (4.58) is needed, as there arise some inconsistencies between the exact LO Lagrangian and non-zero neutrino masses. The reason is expression (4.58), which clearly exhibits some lepton number symmetry under which $\tilde{N}_1$ and $\tilde{N}_2$ carry opposite charges. Light-neutrino masses are forbidden in the case of an exact symmetry, such that some symmetry-breaking terms have to be introduced. These are expected to occur in the missing corrections.

4.5. Summary and remarks

Finally, we summarize this chapter and comment on open issues. After a detailed introduction into the simplest $SU(5)$ GUT [49, 121] and the FN mechanism [48], a model combining both has been presented [47]. It was the starting point in the construction of a high-energy theory that embeds the minimal type-I seesaw framework with only two RH neutrinos [41, 44–46, 120]. By the assumption of approximate exchange symmetries, $N_1 \leftrightarrow i\,N_2$ for the Yukawa coupling matrix and $N_1 \leftrightarrow N_2$ for the heavy neutrino mass term respectively, the model's parameter space is strongly reduced and leaves us with only three parameters, y_0, ϵ and $c_{\mu\tau}$, if the symmetry is exact at LO. A cross check of the obtained Yukawa structures (4.50) with low-energy neutrino observables revealed that the generic assumption $c_{\mu\tau} \simeq 1$ is justified, see figure 4.3. The resulting $\mu - \tau$ symmetry [125] leads to the

elimination of $c_{\mu\tau}$ and gives a Lagrangian with minimal number of free parameters,

$$\mathcal{L}_{min} \sim -\epsilon_0^q \left(\epsilon_0 \ell_e + \ell_\mu + \ell_\tau\right)\left(N_1 + i\, N_2\right)\phi \tag{4.60}$$

$$-\frac{\epsilon_0^{2q}}{2} M_0 \left(N_1 N_1 + N_2 N_2\right) + \text{h.c.}\,, \tag{4.61}$$

with the FN hierarchy parameter $\epsilon_0 \simeq 0.17$, that is required for consistency with observed quark and lepton mass patterns [47]. This represents a minimal realization of the type-I seesaw mechanism with a well-motivated UV origin. We only assumed an approximate exchange symmetry such that the Lagrangian of (4.60) has to be considered as LO expression with small corrections coming from non-exact realization. The heavy neutrinos' FN charge q and their fundamental mass scale $m_0 \sim \mathcal{O}(10^{12...14})\,\text{GeV}$ are then the only free parameters of our minimal model. Although q remains generally unconstrained, further theoretical requirements like electroweak naturalness and leptogenesis restrict its value to be $q \geq 4$, indicated by figure 4.4. As desired, we arrive at an important benchmark scenario that relies on a UV framework and provides agreement with experimental observations. Its strongly reduced parameter space is caused by three ingredients:

At first, it contains only a pair of pseudo-Dirac neutrinos, which span a smaller parameter space than the generic three flavor case. Furthermore, the neutrino Yukawa matrix exhibits an approximate flavor-alignment such that the SM charged lepton flavors can be viewed as coupling only to one linear combination of neutrino fields, i.e. $N_1 + iN_2$. And finally, an approximate two-zero texture is obtained within the Yukawa matrix, which is the most minimal structure for the case of NH to be consistent with experimental data.

In the end, the eleven parameters of the generic two heavy neutrino seesaw are reduced to only five. The following properties invoke this reduction: Two DOFs are absorbed due to the constraints from (4.50), only one DOF is needed to describe the heavy neutrinos' degenerate mass spectrum, equation (4.54) connects M and q and exact flavor-alignment leads to independence of the auxiliary parameter z_R and z_I.

We obtain precise predictions for the Dirac phase δ for NH (4.52), $\delta \pm \frac{\pi}{2}$, which remarkable agree with experimental trends, see table 2.3.

As we only focused on LO terms in this first approach, of course further work is needed to understand deviations from the exact symmetry case, which is necessary to ensure the model's conformity with experiments.

In addition, the origin of structures, emerging in figure 4.3, should also be examined analytically, since this would allow a study of stability under variation of experimental input parameters, equivalently to the one performed in section 3.5.

Although we motivated the formulation of our high-energy approach by a GUT, there still exist unanswered questions. The connection between the heavy neutrino mass scale m_0 and the GUT scale Λ_{GUT} should be clarified, at least in the context of some $U(1)_{B-L}$ breaking, which is a common realization to explain the Majorana mass term. An important fact is that the minimal $SU(5)$ GUT itself suffers from problems like too fast proton decay and mismatches between mass predictions for heavier quarks and leptons [37, 121]. Regarding the postulated symmetries, (4.44)

as well as (4.59), their origin is far from clear and has to be explained in a broader context. One possibility is that they are related to certain boundary conditions in extra-dimensional orbifolds [130–133].

All in all, we have formulated a minimal UV realization of the type-I seesaw which is consistent with important theoretical constraints, electroweak naturalness and leptogenesis. It predicts NH in the light neutrino sector with certain values for the Dirac phase δ, see (4.52). Hence, it is a justified benchmark scenario as it is capable of reproducing the current experimental data sets. We motivated our approach by a minimal GUT framework, but to stay agnostic, one can always assume some framework-independent realization of the FN mechanism according to (4.39) with an equivalent SM fermion charge assignment as in table 4.1.

We remark that our results, i.e. the prediction of $\delta \simeq \frac{\pi}{2}$, are consistent with a FN model that assumes a flavor-independent condition on the neutrino mass matrix, $\det(m_\nu) = 0$ [134]. Moreover, the authors find that their prediction on the Dirac phase δ does not necessarily rely on the assumption of two heavy RH neutrinos as long as the lightest neutrino mass does not exceed a value of 10^{-4}.

5. Conclusion and Outlook

Finally, the main results of the previous chapters are shortly summarized with concluding remarks. Subject of the present thesis is the minimal type-I seesaw mechanism with only two RH neutrinos [41–46], which has been studied from two different directions; a bottom-up approach, that tried to investigate consequences of certain CP phase measurements, and top-down model building, which was motivated by a high-energy embedding of the seesaw mechanism and minimality arguments.

In chapter 2, we introduced the theory and phenomenology of massive neutrinos. It was tried to develop an intuition of the seesaw mechanism from basic principles, e.g. the difference between Dirac and Majorana fermions. A short excursion to neutrino oscillations and absolute mass measurements has been given to provide some understanding of future experiments, which try to uncover missing low-energy parameters like the Dirac CP phase δ. This should enable the reader to interpret the following investigations in an experimental context. The type-I seesaw mechanism has been introduced in detail, as it is the starting point for the performed bottom-up approach. In the end, an overview of different neutrino mass models has been given and the scenario of leptogenesis has slightly been introduced.

Chapter 3 dealt with the data-driven investigation of the minimal seesaw mechanism. After an introduction of the two heavy neutrino realization, which demands one neutrino to be exactly massless, a short summary of the so-called zero-texture ansatz [45, 106, 112, 116] with its phenomenological consequences has been given, see section 3.2. As our approach was motivated by relaxation of the conventional exact zero-texture ansatz, we developed a method to investigate certain hierarchies within the neutrino Yukawa matrix, which is mainly based on the self-defined hierarchy parameter R_{23}, see equation (3.17). Detailed investigation of its properties led to useful simplification for later purposes, see section 3.3. Furthermore, the developed method has been applied to the parameter space of the minimal type-I seesaw model and confirmed useful for investigation of approximate zero-texture Yukawa matrices, see section 3.4. This can be understood as a first proof of principle. The whole bottom-up approach has been completed with studying the robustness of obtained results, i.e. under variation of the experimental input parameters, see section 3.5.

The main result of this investigation is that application of R_{23} under the assumption of approximate zero-textures revealed the NH to be still consistent with experimental parameters if one allows for small perturbations of exact zero Yukawa entries. Further, an approximate Yukawa texture, A_1, has been found that is in line with recent experimental trends, see figure 3.5. The vicinity around the model's

prediction in case of exact two-zero texture, see (3.14), has been studied in detail and can be interpreted as theoretical error bars, assignable to the predictions of $B_{1,4}$ and $B_{2,5}$ texture, see figure 3.6. The detailed summary of the whole approach is given in section 3.6.

We also approached the minimal seesaw model in context of a possible high-energy origin in chapter 4. After an introduction into the topics of the minimal $SU(5)$ GUT [49] as well as the Froggatt-Nielsen mechanism [48], a combined model [47] has been presented that served as building block for our constructed model, see section 4.2. Its appropriate modification has led to a well-motivated UV embedding of the minimal seesaw model, where some of its free parameter can be understood in a broader context, i.e. Yukawa couplings generated by the FN mechanism. By assuming certain (approximate) exchange symmetries, see equation (4.44), further DOFs could be eliminated. The transition to flavor-aligned parameter space region, that we already encountered in chapter 3, has been studied in detail as it directly results from the assumed symmetries at LO, see figure 4.2. Checking the model's consistency with current experimental data, led to clear predictions, i.e. NH and an approximate A_1 Yukawa texture, see figure 4.3. The procedure has been presented step by step in section 4.3. Finally, by demanding theoretical constraints like electroweak naturalness and successful leptogenesis, the last free parameters could be constrained and a minimal UV embedding of the minimal type-I seesaw could be obtained, see section 4.4. Hence, the Lagrangian (4.60) describes a valid benchmark scenario, consistent with current experimental data and only depending on parameters associated to the unknown heavy neutrino sector, see section 4.5. Moreover, the prediction of our model are confirmed by an independent FN flavor model [134]. In the end, some remarks beyond the scope of this thesis shall be given:
The procedure to investigate the manifestation of certain hierarchies in the neutrino Yukawa matrix, can be generalized to study the characteristic of arbitrary couplings. This can be done by appropriate redefinition of our hierarchy parameter, see equation (3.30), according to the individual purposes. Unfortunately, we have to scan over all unaccessible parameters, such that the complexity of our procedure can grow rapidly. Regarding the most minimal Lagrangian (4.60), we have to point out that our naive approach just covered UV terms, which come from exact exchange symmetry. The origin of such symmetries remains unknown and has to be clarified. Furthermore, as the symmetries must not be realized exactly, a deeper investigation of perturbative terms seems necessary, i.e. their detailed structure as well as generation mechanisms.

Conclusively there remains only one thing to say: In times, where neutrino experiments are reaching better sensitivities and will penetrating yet unknown parameter space regions, as much information as possible has to be extracted from current data sets; may it be in terms of new "observables", i.e. hierarchy structures within a coupling matrix, or benchmark scenarios that cover all current knowledge. For theorists, it is easy to hide from experimental constraints, but after all, it remains as Richard Feynman once said [135], 'Experiment is the sole judge of scientific "truth".'

Bibliography

[1] W. Pauli, "Dear radioactive ladies and gentlemen," *Phys.Today*, vol. 31N9, p. 27, 1978.

[2] "All nobel prizes in physics," 2017. [Online; accessed 18-February-2017].

[3] "The 2015 nobel prize in physics - press release," 2015. [Online; accessed 18-February-2017].

[4] Q. R. Ahmad *et al.*, "Direct evidence for neutrino flavor transformation from neutral current interactions in the Sudbury Neutrino Observatory," *Phys. Rev. Lett.*, vol. 89, p. 011301, 2002.

[5] S. Fukuda *et al.*, "Solar B-8 and hep neutrino measurements from 1258 days of Super-Kamiokande data," *Phys. Rev. Lett.*, vol. 86, pp. 5651–5655, 2001.

[6] B. Pontecorvo, "Mesonium and anti-mesonium," *Sov. Phys. JETP*, vol. 6, p. 429, 1957. [Zh. Eksp. Teor. Fiz.33,549(1957)].

[7] K. N. Abazajian *et al.*, "Cosmological and Astrophysical Neutrino Mass Measurements," *Astropart. Phys.*, vol. 35, pp. 177–184, 2011.

[8] I. Esteban, M. C. Gonzalez-Garcia, M. Maltoni, I. Martinez-Soler, and T. Schwetz, "Updated fit to three neutrino mixing: exploring the accelerator-reactor complementarity," *JHEP*, vol. 01, p. 087, 2017.

[9] C. Weinheimer and K. Zuber, "Neutrino Masses," *Annalen Phys.*, vol. 525, no. 8-9, pp. 565–575, 2013.

[10] R. B. Patterson, "Prospects for Measurement of the Neutrino Mass Hierarchy," *Ann. Rev. Nucl. Part. Sci.*, vol. 65, pp. 177–192, 2015.

[11] M. Agostini *et al.*, "Results on Neutrinoless Double-β Decay of ^{76}Ge from Phase I of the GERDA Experiment," *Phys.Rev.Lett.*, vol. 111, no. 12, p. 122503, 2013.

[12] A. Osipowicz *et al.*, "KATRIN: A Next generation tritium beta decay experiment with sub-eV sensitivity for the electron neutrino mass. Letter of intent," 2001.

[13] D. S. Ayres *et al.*, "NOvA: Proposal to build a 30 kiloton off-axis detector to study nu(mu) —¿ nu(e) oscillations in the NuMI beamline," 2004.

[14] K. Abe *et al.*, "Indication of Electron Neutrino Appearance from an Accelerator-produced Off-axis Muon Neutrino Beam," *Phys. Rev. Lett.*, vol. 107, p. 041801, 2011.

[15] F. Reines and C. L. Cowan, "The Neutrino," *Nature*, vol. 178, pp. 446–449, Sept. 1956.

[16] Y. Fukuda *et al.*, "Measurements of the solar neutrino flux from Super-Kamiokande's first 300 days," *Phys. Rev. Lett.*, vol. 81, pp. 1158–1162, 1998. [Erratum: Phys. Rev. Lett.81,4279(1998)].

[17] C. Arpesella *et al.*, "Direct Measurement of the Be-7 Solar Neutrino Flux with 192 Days of Borexino Data," *Phys.Rev.Lett.*, vol. 101, p. 091302, 2008.

[18] S. Geer, "Neutrino beams from muon storage rings: Characteristics and physics potential," *Phys. Rev.*, vol. D57, pp. 6989–6997, 1998. [Erratum: Phys. Rev.D59,039903(1999)].

[19] P. Minkowski, "$\mu \to e\gamma$ at a Rate of One Out of 10^9 Muon Decays?," *Phys. Lett.*, vol. B67, pp. 421–428, 1977.

[20] T. Yanagida, "Horizontal Symmetry and Masses of Neutrinos," *Prog. Theor. Phys.*, vol. 64, p. 1103, 1980.

[21] M. Gell-Mann, P. Ramond, and R. Slansky, "Complex Spinors and Unified Theories," *Conf. Proc.*, vol. C790927, pp. 315–321, 1979.

[22] R. N. Mohapatra and G. Senjanovic, "Neutrino Masses and Mixings in Gauge Models with Spontaneous Parity Violation," *Phys. Rev.*, vol. D23, p. 165, 1981.

[23] T. Yanagida, "HORIZONTAL SYMMETRY AND MASSES OF NEUTRINOS," *Conf. Proc.*, vol. C7902131, pp. 95–99, 1979.

[24] M. Magg and C. Wetterich, "Neutrino Mass Problem and Gauge Hierarchy," *Phys. Lett.*, vol. B94, pp. 61–64, 1980.

[25] J. Schechter and J. W. F. Valle, "Neutrino Masses in SU(2) x U(1) Theories," *Phys. Rev.*, vol. D22, p. 2227, 1980.

[26] C. Wetterich, "Neutrino Masses and the Scale of B-L Violation," *Nucl. Phys.*, vol. B187, pp. 343–375, 1981.

[27] G. Lazarides, Q. Shafi, and C. Wetterich, "Proton Lifetime and Fermion Masses in an SO(10) Model," *Nucl. Phys.*, vol. B181, pp. 287–300, 1981.

[28] R. Foot, H. Lew, X. G. He, and G. C. Joshi, "Seesaw Neutrino Masses Induced by a Triplet of Leptons," *Z. Phys.*, vol. C44, p. 441, 1989.

[29] E. Ma, "Pathways to naturally small neutrino masses," *Phys. Rev. Lett.*, vol. 81, pp. 1171–1174, 1998.

[30] E. Ma and D. P. Roy, "Heavy triplet leptons and new gauge boson," *Nucl. Phys.*, vol. B644, pp. 290–302, 2002.

[31] H. Georgi and S. L. Glashow, "Spontaneously broken gauge symmetry and elementary particle masses," *Phys. Rev.*, vol. D6, pp. 2977–2982, 1972.

[32] A. Zee, "A Theory of Lepton Number Violation, Neutrino Majorana Mass, and Oscillation," *Phys. Lett.*, vol. B93, p. 389, 1980. [Erratum: Phys. Lett.B95,461(1980)].

[33] L. Wolfenstein, "A Theoretical Pattern for Neutrino Oscillations," *Nucl. Phys.*, vol. B175, pp. 93–96, 1980.

[34] K. S. Babu and E. Ma, "Radiative Mechanisms for Generating Quark and Lepton Masses: Some Recent Developments," *Mod. Phys. Lett.*, vol. A4, p. 1975, 1989.

[35] E. Ma, "Verifiable radiative seesaw mechanism of neutrino mass and dark matter," *Phys. Rev.*, vol. D73, p. 077301, 2006.

[36] S. F. King, A. Merle, and L. Panizzi, "Effective theory of a doubly charged singlet scalar: complementarity of neutrino physics and the LHC," *JHEP*, vol. 11, p. 124, 2014.

[37] M. Fukugita and T. Yanagida, *Physics of neutrinos.* Texts and monographs in physics, Berlin ; Heidelberg [u.a.]: Springer, 2003. Includes bibliographical references and index.

[38] M. Fukugita and T. Yanagida, "Baryogenesis Without Grand Unification," *Phys. Lett.*, vol. B174, pp. 45–47, 1986.

[39] S. Davidson, E. Nardi, and Y. Nir, "Leptogenesis," *Phys. Rept.*, vol. 466, pp. 105–177, 2008.

[40] F. Björkeroth, S. F. King, K. Schmitz, and T. T. Yanagida, "Leptogenesis after Chaotic Sneutrino Inflation and the Supersymmetry Breaking Scale," 2016.

[41] S. F. King, "Atmospheric and solar neutrinos with a heavy singlet," *Phys. Lett.*, vol. B439, pp. 350–356, 1998.

[42] S. F. King, "Atmospheric and solar neutrinos from single right-handed neutrino dominance and U(1) family symmetry," *Nucl. Phys.*, vol. B562, pp. 57–77, 1999.

[43] S. F. King, "Large mixing angle MSW and atmospheric neutrinos from single right-handed neutrino dominance and U(1) family symmetry," *Nucl. Phys.*, vol. B576, pp. 85–105, 2000.

[44] S. F. King, "Constructing the large mixing angle MNS matrix in seesaw models with right-handed neutrino dominance," *JHEP*, vol. 09, p. 011, 2002.

[45] P. H. Frampton, S. L. Glashow, and T. Yanagida, "Cosmological sign of neutrino CP violation," *Phys. Lett.*, vol. B548, pp. 119–121, 2002.

[46] A. Ibarra and G. G. Ross, "Neutrino phenomenology: The Case of two right-handed neutrinos," *Phys. Lett.*, vol. B591, pp. 285–296, 2004.

[47] W. Buchmuller and T. Yanagida, "Quark lepton mass hierarchies and the baryon asymmetry," *Phys. Lett.*, vol. B445, pp. 399–402, 1999.

[48] C. D. Froggatt and H. B. Nielsen, "Hierarchy of Quark Masses, Cabibbo Angles and CP Violation," *Nucl. Phys.*, vol. B147, pp. 277–298, 1979.

[49] H. Georgi and S. L. Glashow, "Unity of All Elementary Particle Forces," *Phys. Rev. Lett.*, vol. 32, pp. 438–441, 1974.

[50] T. Rink and K. Schmitz, "From CP Phases to Yukawa Textures: Maximal Yukawa Hierarchies in Minimal Seesaw Models," 2016.

[51] T. Rink, K. Schmitz, and T. T. Yanagida, "Minimal Seesaw Model with a Discrete Heavy-Neutrino Exchange Symmetry," 2016.

[52] W. Buchmuller, P. Di Bari, and M. Plumacher, "Leptogenesis for pedestrians," *Annals Phys.*, vol. 315, pp. 305–351, 2005.

[53] E. Majorana, "Teoria simmetrica dell'elettrone e del positrone," *Nuovo Cim.*, vol. 14, pp. 171–184, 1937.

[54] M. D. Schwartz, *Quantum field theory and the standard model*. Cambridge [u.a.]: Cambridge University Press, 2014.

[55] A. Aste, "A direct road to Majorana fields," *Symmetry*, vol. 2, pp. 1776–1809, 2010.

[56] M. E. Peskin and D. V. Schroeder, *An introduction to quantum field theory*. The advanced book program, Boulder, Colo. [u.a.]: Westview Pr., [nachdr.] ed., 2006.

[57] P. Langacker, *The standard model and beyond*. Series in high energy physics, cosmology, and gravitation, Boca Raton [u.a.]: CRC Press, 2010. Includes bibliographical references and index.

[58] P. B. Pal, "Dirac, Majorana and Weyl fermions," *Am. J. Phys.*, vol. 79, pp. 485–498, 2011.

[59] B. Pontecorvo, "Inverse beta processes and nonconservation of lepton charge," *Sov. Phys. JETP*, vol. 7, pp. 172–173, 1958. [Zh. Eksp. Teor. Fiz.34,247(1957)].

[60] W. Rodejohann, "Neutrino-less Double Beta Decay and Particle Physics," *Int. J. Mod. Phys.*, vol. E20, pp. 1833–1930, 2011.

[61] M. Kobayashi and T. Maskawa, "CP Violation in the Renormalizable Theory of Weak Interaction," *Prog. Theor. Phys.*, vol. 49, pp. 652–657, 1973.

[62] C. Patrignani *et al.*, "Review of Particle Physics," *Chin. Phys.*, vol. C40, no. 10, p. 100001, 2016.

[63] Z. Maki, M. Nakagawa, and S. Sakata, "Remarks on the unified model of elementary particles," *Prog. Theor. Phys.*, vol. 28, pp. 870–880, 1962.

[64] C. Giunti and C. W. Kim, *Fundamentals of neutrino physics and astrophysics*. Oxford [u.a.]: Oxford Univ. Press, 1. publ. ed., 2007.

[65] J. Schechter and J. W. F. Valle, "Neutrino Oscillation Thought Experiment," *Phys. Rev.*, vol. D23, p. 1666, 1981.

[66] H. Fritzsch and Z.-z. Xing, "How to describe neutrino mixing and CP violation," *Phys. Lett.*, vol. B517, pp. 363–368, 2001.

[67] E. K. Akhmedov, "Neutrino physics," pp. 103–164, 1999.

[68] M. Gell-Mann and A. Pais, "Behavior of neutral particles under charge conjugation," *Phys. Rev.*, vol. 97, pp. 1387–1389, 1955.

[69] S. M. Bilenky, C. Giunti, and W. Grimus, "Phenomenology of neutrino oscillations," *Prog. Part. Nucl. Phys.*, vol. 43, pp. 1–86, 1999.

[70] L. Wolfenstein, "Neutrino Oscillations in Matter," *Phys. Rev.*, vol. D17, pp. 2369–2374, 1978.

[71] S. P. Mikheyev and A. Yu. Smirnov, "Resonant neutrino oscillations in matter," *Prog. Part. Nucl. Phys.*, vol. 23, pp. 41–136, 1989.

[72] K. Dick, M. Freund, M. Lindner, and A. Romanino, "CP violation in neutrino oscillations," *Nucl. Phys.*, vol. B562, pp. 29–56, 1999.

[73] G. C. Branco, R. G. Felipe, and F. R. Joaquim, "Leptonic CP Violation," *Rev. Mod. Phys.*, vol. 84, pp. 515–565, 2012.

[74] C. Giunti and A. Studenikin, "Neutrino electromagnetic interactions: a window to new physics," 2014.

[75] D. V. Forero, M. Tortola, and J. W. F. Valle, "Neutrino oscillations refitted," *Phys. Rev.*, vol. D90, no. 9, p. 093006, 2014.

[76] M. C. Gonzalez-Garcia, M. Maltoni, and T. Schwetz, "Global Analyses of Neutrino Oscillation Experiments," *Nucl. Phys.*, vol. B908, pp. 199–217, 2016.

[77] F. Capozzi, E. Lisi, A. Marrone, D. Montanino, and A. Palazzo, "Neutrino masses and mixings: Status of known and unknown 3ν parameters," *Nucl. Phys.*, vol. B908, pp. 218–234, 2016.

[78] G. Pagliaroli, F. Rossi-Torres, and F. Vissani, "Neutrino mass bound in the standard scenario for supernova electronic antineutrino emission," *Astropart. Phys.*, vol. 33, pp. 287–291, 2010.

[79] M. Thomson, *Modern particle physics*. Cambridge, U.K.: Cambridge University Press, 2013.

[80] C. Jarlskog, "Commutator of the Quark Mass Matrices in the Standard Electroweak Model and a Measure of Maximal CP Violation," *Phys. Rev. Lett.*, vol. 55, p. 1039, 1985.

[81] C. S. Wu, E. Ambler, R. W. Hayward, D. D. Hoppes, and R. P. Hudson, "Experimental test of parity conservation in beta decay," *Phys. Rev.*, vol. 105, pp. 1413–1415, Feb 1957.

[82] M. Goldhaber, L. Grodzins, and A. W. Sunyar, "Helicity of neutrinos," *Phys. Rev.*, vol. 109, pp. 1015–1017, Feb 1958.

[83] S. Weinberg, "Baryon and Lepton Nonconserving Processes," *Phys. Rev. Lett.*, vol. 43, pp. 1566–1570, 1979.

[84] A. Merle, "keV Neutrino Model Building," *Int. J. Mod. Phys.*, vol. D22, p. 1330020, 2013.

[85] J. A. Casas and A. Ibarra, "Oscillating neutrinos and muon —¿ e, gamma," *Nucl. Phys.*, vol. B618, pp. 171–204, 2001.

[86] S. Kanemura and K. Yagyu, "Radiative corrections to electroweak parameters in the Higgs triplet model and implication with the recent Higgs boson searches," *Phys. Rev.*, vol. D85, p. 115009, 2012.

[87] M. Platschter, "Renormalisation of radiative neutrino masses," Master's thesis, Ludwig-Maximilians-Universität Munich.

[88] R. N. Mohapatra and J. W. F. Valle, "Neutrino Mass and Baryon Number Nonconservation in Superstring Models," *Phys. Rev.*, vol. D34, p. 1642, 1986.

[89] N. Arkani-Hamed, S. Dimopoulos, and G. R. Dvali, "The Hierarchy problem and new dimensions at a millimeter," *Phys. Lett.*, vol. B429, pp. 263–272, 1998.

[90] N. Arkani-Hamed, S. Dimopoulos, G. R. Dvali, and J. March-Russell, "Neutrino masses from large extra dimensions," *Phys. Rev.*, vol. D65, p. 024032, 2001.

[91] Y. Grossman and M. Neubert, "Neutrino masses and mixings in nonfactorizable geometry," *Phys. Lett.*, vol. B474, pp. 361–371, 2000.

[92] A. D. Sakharov, "Violation of CP Invariance, c Asymmetry, and Baryon Asymmetry of the Universe," *Pisma Zh. Eksp. Teor. Fiz.*, vol. 5, pp. 32–35, 1967. [Usp. Fiz. Nauk161,61(1991)].

[93] F. R. Klinkhamer and N. S. Manton, "A Saddle Point Solution in the Weinberg-Salam Theory," *Phys. Rev.*, vol. D30, p. 2212, 1984.

[94] P. B. Arnold and L. D. McLerran, "Sphalerons, Small Fluctuations and Baryon Number Violation in Electroweak Theory," *Phys. Rev.*, vol. D36, p. 581, 1987.

[95] P. B. Arnold and L. D. McLerran, "The Sphaleron Strikes Back," *Phys. Rev.*, vol. D37, p. 1020, 1988.

[96] G. 't Hooft, "Naturalness, chiral symmetry, and spontaneous chiral symmetry breaking," *NATO Sci. Ser. B*, vol. 59, pp. 135–157, 1980.

[97] K. Schmitz, *The B-L Phase Transition: Implications for Cosmology and Neutrinos*. PhD thesis, Hamburg U., 2012.

[98] A. Pilaftsis, "CP violation and baryogenesis due to heavy Majorana neutrinos," *Phys. Rev.*, vol. D56, pp. 5431–5451, 1997.

[99] A. Pilaftsis and T. E. J. Underwood, "Resonant leptogenesis," *Nucl. Phys.*, vol. B692, pp. 303–345, 2004.

[100] A. Pilaftsis, "The Little Review on Leptogenesis," *J.Phys.Conf.Ser.*, vol. 171, p. 012017, 2009.

[101] C. Patrignani *et al.*, "Review of Particle Physics," *Chin. Phys.*, vol. C40, no. 10, p. 100001, 2016.

[102] N. Cabibbo, "Time Reversal Violation in Neutrino Oscillation," *Phys. Lett.*, vol. B72, pp. 333–335, 1978.

[103] R. Acciarri *et al.*, "Long-Baseline Neutrino Facility (LBNF) and Deep Underground Neutrino Experiment (DUNE)," 2015.

[104] G. Altarelli and F. Feruglio, "Discrete Flavor Symmetries and Models of Neutrino Mixing," *Rev. Mod. Phys.*, vol. 82, pp. 2701–2729, 2010.

[105] S. F. King and C. Luhn, "Neutrino Mass and Mixing with Discrete Symmetry," *Rept. Prog. Phys.*, vol. 76, p. 056201, 2013.

[106] K. Harigaya, M. Ibe, and T. T. Yanagida, "Seesaw Mechanism with Occam's Razor," *Phys. Rev.*, vol. D86, p. 013002, 2012.

[107] T. Endoh, S. Kaneko, S. K. Kang, T. Morozumi, and M. Tanimoto, "CP violation in neutrino oscillation and leptogenesis," *Phys. Rev. Lett.*, vol. 89, p. 231601, 2002.

[108] M. Flanz, E. A. Paschos, U. Sarkar, and J. Weiss, "Baryogenesis through mixing of heavy Majorana neutrinos," *Phys. Lett.*, vol. B389, pp. 693–699, 1996.

[109] G. Bambhaniya, P. S. B. Dev, S. Goswami, S. Khan, and W. Rodejohann, "Naturalness, Vacuum Stability and Leptogenesis in the Minimal Seesaw Model," 2016.

[110] M. Raidal and A. Strumia, "Predictions of the most minimal seesaw model," *Phys. Lett.*, vol. B553, pp. 72–78, 2003.

[111] S. F. King, "Minimal predictive see-saw model with normal neutrino mass hierarchy," *JHEP*, vol. 07, p. 137, 2013.

[112] J. Zhang and S. Zhou, "A Further Study of the Frampton-Glashow-Yanagida Model for Neutrino Masses, Flavor Mixing and Baryon Number Asymmetry," *JHEP*, vol. 09, p. 065, 2015.

[113] S. Weinberg, "The Problem of Mass," *Trans. New York Acad. Sci.*, vol. 38, pp. 185–201, 1977.

[114] T. Banks and N. Seiberg, "Symmetries and Strings in Field Theory and Gravity," *Phys. Rev.*, vol. D83, p. 084019, 2011.

[115] K. S. Babu, "TASI Lectures on Flavor Physics," in *Proceedings of Theoretical Advanced Study Institute in Elementary Particle Physics on The dawn of the LHC era (TASI 2008): Boulder, USA, June 2-27, 2008*, pp. 49–123, 2010.

[116] F. Björkeroth, F. J. de Anda, I. de Medeiros Varzielas, and S. F. King, "Leptogenesis in minimal predictive seesaw models," *JHEP*, vol. 10, p. 104, 2015.

[117] J.-w. Mei and Z.-z. Xing, "Radiative corrections to neutrino mixing and CP violation in the minimal seesaw model with leptogenesis," *Phys. Rev.*, vol. D69, p. 073003, 2004.

[118] C. Hagedorn, J. Kersten, and M. Lindner, "Stability of texture zeros under radiative corrections in see-saw models," *Phys. Lett.*, vol. B597, pp. 63–72, 2004.

[119] T. Ohlsson and S. Zhou, "Renormalization group running of neutrino parameters," *Nature Commun.*, vol. 5, p. 5153, 2014.

[120] A. Yu. Smirnov, "Seesaw enhancement of lepton mixing," *Phys. Rev.*, vol. D48, pp. 3264–3270, 1993.

[121] G. G. Ross, *Grand Unified Theories*. Frontiers in Physics, Menlo Park, CA: Benjamin-Cummings, 1984.

[122] H. Georgi, H. R. Quinn, and S. Weinberg, "Hierarchy of Interactions in Unified Gauge Theories," *Phys. Rev. Lett.*, vol. 33, pp. 451–454, 1974.

[123] H. Nishino *et al.*, "Search for Proton Decay via p —¿ e+ pi0 and p —¿ mu+ pi0 in a Large Water Cherenkov Detector," *Phys. Rev. Lett.*, vol. 102, p. 141801, 2009.

[124] M. Bauer, T. Schell, and T. Plehn, "Hunting the Flavon," *Phys. Rev.*, vol. D94, no. 5, p. 056003, 2016.

[125] Z.-z. Xing and Z.-h. Zhao, "A review of mu-tau flavor symmetry in neutrino physics," *Rept. Prog. Phys.*, vol. 79, no. 7, p. 076201, 2016.

[126] J. D. Clarke, "How to avoid unnatural hierarchical thermal leptogenesis," *PoS*, vol. PLANCK2015, p. 026, 2015.

[127] J. D. Clarke, R. Foot, and R. R. Volkas, "Electroweak naturalness in the three-flavor type I seesaw model and implications for leptogenesis," *Phys. Rev.*, vol. D91, no. 7, p. 073009, 2015.

[128] K. Nakayama, F. Takahashi, and T. T. Yanagida, "Viable Chaotic Inflation as a Source of Neutrino Masses and Leptogenesis," *Phys. Lett.*, vol. B757, pp. 32–38, 2016.

[129] R. Kallosh, A. Linde, D. Roest, and T. Wrase, "Sneutrino inflation with α-attractors," *JCAP*, vol. 1611, p. 046, 2016.

[130] W. Buchmuller, L. Covi, D. Emmanuel-Costa, and S. Wiesenfeldt, "Flavour structure and proton decay in 6D orbifold GUTs," *JHEP*, vol. 09, p. 004, 2004.

[131] T. Kobayashi, Y. Omura, and K. Yoshioka, "Flavor Symmetry Breaking and Vacuum Alignment on Orbifolds," *Phys. Rev.*, vol. D78, p. 115006, 2008.

[132] L. J. Hall, J. March-Russell, T. Okui, and D. Tucker-Smith, "Towards a theory of flavor from orbifold GUTs," *JHEP*, vol. 09, p. 026, 2004.

[133] A. Hebecker and J. March-Russell, "The Flavor hierarchy and seesaw neutrinos from bulk masses in 5-d orbifold GUTs," *Phys. Lett.*, vol. B541, pp. 338–345, 2002.

[134] Y. Kaneta, M. Tanimoto, and T. T. Yanagida, "Dirac CP phase in the neutrino mixing matrix and the Froggatt-Nielsen mechanism with $\mathbf{det}[\mathbf{M}_\nu] = \mathbf{0}$," 2017.

[135] R. P. Feynman, R. B. Leighton, and M. Sands, *The Feynman lectures on physics, Vol. I: The new millennium edition: mainly mechanics, radiation, and heat*, vol. 1. Basic Books, 2015.

[136] E. P. Wigner, "On Unitary Representations of the Inhomogeneous Lorentz Group," *Annals Math.*, vol. 40, pp. 149–204, 1939. [Reprint: Nucl. Phys. Proc. Suppl.6,9(1989)].

[137] A. Nucciotti, "The use of low temperature detectors for direct measurements of the mass of the electron neutrino," *Adv. High Energy Phys.*, vol. 2016, p. 9153024, 2016.

A. Clifford algebra and chiral projections

Particles generally transform under irreducible representations of the Poincaré group and are characterized by two quantum numbers m and j as indicated by Wigner's theorem [136]. The spin representation, $j = \frac{1}{2}$, can be deduced from the Clifford algebra $\mathbb{Cl}_{1,3}(\mathbb{R})$.

General properties of the Clifford algebra

We motivated the spinor space as vector room, from whose solutions the Dirac equation,

$$\left(i\partial\!\!\!/ - m\right)\psi = 0\,, \tag{A.1}$$

can be constructed as superposition of so-called spinors. This spinor space can have arbitrary dimension d and is spanned by any set of ($\gamma-$)matrices that fulfills the Clifford algebra $\mathbb{Cl}_{1,3}(\mathbb{R})$,

$$\{\gamma^\mu, \gamma^\nu\} = 2g^{\mu\nu}\,, \tag{A.2}$$

with the metric tensor $g_{\mu\nu}g^{\mu\nu} = d$. Usually, we want to describe motion in a flat four-dimensional space, such that $d \to 4$ and $g^{\mu\nu} \to \eta^{\mu\nu} = \mathrm{diag}\,(1, -1, -1, -1)$.

We know that the proper Lorentz algebra $\mathfrak{so}(1,3)$ is isomorphic to $SU(2) \times SU(2)$, such that the Pauli-matrices, which are associated with the generators of $SU(2)$, can construct representations of the Clifford algebra. With this representation the proper action of the Lorentz transformation on the spinor space can be formulated. That means, under an infinitesimal Lorentz transformation $x^\mu \longrightarrow x'^\mu = x^\mu + \omega^{\mu\nu}$ a fermionic field transforms as

$$\psi \longrightarrow \psi' = e^{-\frac{i}{4}\omega^{\mu\nu}\sigma_{\mu\nu}}\psi\,, \tag{A.3}$$

with $\sigma_{\mu\nu} = \frac{i}{2}\left[\gamma_m u, \gamma_\nu\right]$.

Pauli matrices

The Pauli-Matrices are a set of three complex 2×2 matrices exhibiting the following structure:

$$\sigma_1 = \begin{pmatrix} 0 & 1 \\ 1 & 0 \end{pmatrix}\,, \quad \sigma_2 = \begin{pmatrix} 0 & -i \\ i & 0 \end{pmatrix}\,, \quad \sigma_3 = \begin{pmatrix} 1 & 0 \\ 0 & -1 \end{pmatrix}\,. \tag{A.4}$$

Since they are hermitian and unitary, $(\sigma_i)^\dagger = (\sigma_i)$ and fulfill $\sigma_i^2 = \mathbb{1}_2$, they have eigenvalues ± 1. Further, they have a negative determinant, $\det(\sigma_i) = -1$, and are traceless, $\mathrm{tr}(\sigma_i) = 0$, For practical purpose, their commutation and anti-commutation relation is useful,

$$[\sigma_i, \sigma_j] = 2i\epsilon_{ijk}\sigma_k \qquad \{\sigma_i, \sigma_j\} = 2\delta_{ij}\mathbb{1}_2\,, \tag{A.5}$$

such that their combination yields

$$\sigma_i\sigma_j = \delta_{ij}\mathbb{1}_2 + i\epsilon_{ijk}\sigma_k \tag{A.6}$$

Chirality and chiral projections

For an even number of dimensions, it is always possible to construct another γ-matrix,

$$\gamma^5 \equiv \frac{i}{4!}\epsilon_{\alpha\beta\gamma\delta}\gamma^\alpha\gamma^\beta\gamma^\gamma\gamma^\delta \overset{d\to 4}{=} i\gamma^0\gamma^1\gamma^2\gamma^3 = \begin{cases} \begin{pmatrix} 0_2 & \mathbb{1}_2 \\ \mathbb{1}_2 & 0_2 \end{pmatrix} & \text{Dirac} \\ \\ \begin{pmatrix} \sigma^2 & 0 \\ 0 & -\sigma^2 \end{pmatrix} & \text{Majorana} \end{cases}. \tag{A.7}$$

It is hermitian, $(\gamma^5)^\dagger = \gamma^5$, has eigenvalues ± 1, originating from $(\gamma^5)^2 = \mathbb{1}_4$, and commutes with all other γ-matrices,$\{\gamma^5, \gamma^\mu\} = 0$. In the SM it receives special attention as is defines *chirality*, which refers to its two eigenvalues ± 1. A fermion field's chirality is then defined under application of the appropriate projection operators,

$$\mathcal{P}_L = \frac{1}{2}(1-\gamma^5) = \begin{pmatrix} \mathbb{1}_2 & 0 \\ 0 & 0 \end{pmatrix}, \quad \mathcal{P}_R = \frac{1}{2}(1+\gamma^5) = \begin{pmatrix} 0 & 0 \\ 0 & \mathbb{1}_2 \end{pmatrix}, \tag{A.8}$$

which exhibit the properties

$$\mathcal{P}_{L/R}^2 = \mathcal{P}_{L/R} \qquad \mathcal{P}_L\mathcal{P}_R = \mathcal{P}_R\mathcal{P}_L = 0\,. \tag{A.9}$$

When dealing with Majorana fermions, we have to know, how charge conjugation C affects the chiral components of fermion field. For this, we need to know the properties of the charge conjugation operator C (in the Dirac representation): $C^\dagger = C^{-1} = C^T = -C$. It allowed us to construct the so-called Lorentz-covariant conjugate by $\psi^C \equiv \gamma_0 C\psi^*$. A further ingredient is that fermion fields anti-commute. Now, we calculate how the LCC of a chiral field looks like.

$$\begin{aligned} (\psi_L)^C &= \gamma_0 C\,(\psi_L)^* = \gamma_0 C\mathcal{P}_L^*\psi^* = \gamma_0 C\mathcal{P}_L\psi^* = \mathcal{P}_R\gamma_0 C\psi^* = \mathcal{P}_R\psi^C \\ &= \left(\psi^C\right)_R \end{aligned} \tag{A.10}$$

Hence, the LCC of a left-chiral field corresponds to the right-chiral component of the field's LCC and vice versa.

B. $SU(5)$ GUT and Froggatt-Nielsen mechanism

In chapter 4 we skipped all mathematical details in the presented steps. Now, the underlying generators of $SU(5)$ are presented to allow the reader to reconstruct the performed steps. For this, we introduce the Gell-Mann matrices λ_i with $i = 1, ..., 8$.

Gell-Mann matrices

As generators of the $SU(3)$ group the Gell-Mann matrices receive special attention in QCD. They are traceless and unitary matrices, which fulfill the Lie algebra $[T^i, T^j] = i\, f_{ijk}\, T^{ijk}$, with $T^i \equiv \frac{1}{2}\lambda_i$, $i = 1, ..., 8$ and the structure constants f_{ijk}. The corresponding matrices are given by

$$\lambda^1 = \begin{pmatrix} & & 0 \\ & \sigma_1 & 0 \\ 0 & 0 & 0 \end{pmatrix}, \quad \lambda^2 = \begin{pmatrix} & & 0 \\ & \sigma_2 & 0 \\ 0 & 0 & 0 \end{pmatrix}, \quad \lambda^3 = \begin{pmatrix} & & 0 \\ & \sigma_3 & 0 \\ 0 & 0 & 0 \end{pmatrix},$$

$$\lambda^4 = \begin{pmatrix} 0 & 0 & 1 \\ 0 & 0 & 0 \\ 1 & 0 & 0 \end{pmatrix}, \quad \lambda^5 = \begin{pmatrix} 0 & 0 & -i \\ 0 & 0 & 0 \\ i & 0 & 0 \end{pmatrix}, \tag{B.1}$$

$$\lambda^6 = \begin{pmatrix} 0 & 0 & 0 \\ 0 & & \\ 0 & \sigma_1 & \end{pmatrix}, \quad \lambda^7 = \begin{pmatrix} 0 & 0 & 0 \\ 0 & & \\ 0 & \sigma_2 & \end{pmatrix}, \quad \lambda^8 = \frac{1}{\sqrt{3}} \begin{pmatrix} 1 & 0 & 0 \\ 0 & 1 & 0 \\ 0 & 0 & -2 \end{pmatrix}.$$

The structure constants of $\mathfrak{su}(3)$ are totally anti-symmetric and exhibit the following values

$$\begin{aligned} f^{123} &= 1\,, \\ f^{458} = f^{678} &= \frac{\sqrt{3}}{2}\,, \\ f^{147} = f^{165} = f^{246} = f^{257} = f^{345} = f^{376} &= \frac{1}{2}\,. \end{aligned} \tag{B.2}$$

$SU(5)$ generators and gauge bosons

With the Pauli- and Gell-Mann matrices at hand, we are now ready to construct the generators of $SU(5)$

$$T^i = \begin{pmatrix} & & & 0 & 0 \\ & \lambda^i & & 0 & 0 \\ & & & 0 & 0 \\ 0 & 0 & 0 & 0 & 0 \\ 0 & 0 & 0 & 0 & 0 \end{pmatrix}, \qquad T^{9,10} = \begin{pmatrix} 0 & 0 & 0 & 0 & 0 \\ 0 & 0 & 0 & 0 & 0 \\ 0 & 0 & 0 & 0 & 0 \\ 0 & 0 & 0 & & \\ 0 & 0 & 0 & \sigma_{1,2} & \end{pmatrix},$$

$$T^{11} = \mathrm{diag}(0,0,0,1,-1)\,, \qquad T^{12} = \frac{1}{\sqrt{15}}\mathrm{diag}(-2,-2,-2,3,3)\,,$$

$$T^{13} = \begin{pmatrix} & & & 1 & 0 \\ & 0 & & 0 & 0 \\ & & & 0 & 0 \\ 1 & 0 & 0 & & \\ 0 & 0 & 0 & 0 & \end{pmatrix}, \qquad T^{14} = \begin{pmatrix} & & & i & 0 \\ & 0 & & 0 & 0 \\ & & & 0 & 0 \\ -i & 0 & 0 & & \\ 0 & 0 & 0 & 0 & \end{pmatrix}, \tag{B.3}$$

$$T^{19} = \begin{pmatrix} & & & 1 & 0 \\ & 0 & & 0 & 0 \\ & & & 0 & 0 \\ 1 & 0 & 0 & & \\ 0 & 0 & 0 & 0 & \end{pmatrix}, \qquad T^{20} = \begin{pmatrix} & & & i & 0 \\ & 0 & & 0 & 0 \\ & & & 0 & 0 \\ -i & 0 & 0 & & \\ 0 & 0 & 0 & 0 & \end{pmatrix},$$

with $i = 1, ..., 8$. The left generators are $T^{13...18}$ and $T^{19...24}$ and are obtained by putting 1 and $\pm i$ in the same position. Hence, all $SU(5)$ generators are obtained and the existing gauge bosons are linked to them in the following way:

gauge boson	A^a_μ	generator T^a
gluons $G^{1...8}_\mu$	$A^{1...8}_\mu$	$T^{1...8}$
charged weak bosons $W^\pm_\mu$	$\frac{1}{\sqrt{2}}\left(A^9_\mu \pm iA^{10}_\mu\right)$	$T^9 \pm iT^{10}$
neutral weak boson W^3_μ	A^{11}_μ	T^{11}
hypercharge boson B_μ	A^{12}_μ	T^{12}
SU(5) bosons $X^{1..3}_\mu$ + LCC	$A^{13...18}_\mu$	$T^{13...18}$
SU(5) bosons $Y^{1..3}_\mu$ + LCC	$A^{19...24}_\mu$	$T^{19...24}$

Table B.1.: $SU(5)$ gauge bosons and their identification with the corresponding $SU(5)$ generators.

Froggatt-Nielsen procedure in details

In chapter 4, the Froggatt-Nielsen mechanism was used as possibility to dynamically generate small Yukawa couplings. Although we mentioned the mains step, we will present them now in detail with corresponding diagrams and Lagrangians illustrating the procedure. The existence of some globally or locally conserved charge Q_{FN} is required, to restrict certain Yukawa interactions among light and heavy fermions. The corresponding charge assignment has to be individually done for each "spaghetti", but in the end only the difference in FN quantum number are relevant for low-energy phenomenology, i.e. the generation of SM Yukawa coupling.

0. Heavy fermion mass generation at Λ_{FN}
   The first ingredient of the mechanism is the assumption of some heavy fermions. Usually one takes their existence as massive particle for granted, but without difficulty we can generate their masses through Yukawa interactions with a scalar $\tilde{\phi}$ that obtains a non-zero VEV $\langle\tilde{\Phi}\rangle \neq 0$; equivalent to the Higgs mechanism. This comes with the advantage of relating all masses to a common scale $M_{ij} = a_{ij}\langle\tilde{\Phi}\rangle$. In our approach, we defined $\Lambda_{FN} = \langle\tilde{\Phi}\rangle$

1. "Spaghetti"-interaction at a high scale
   The important point of the entire mechanism is the existence of another scalar field Φ, commonly called flavon, which has Yukawa interaction with the SM fermion and the heavy ones, such that the relevant part of the Lagrangian is given by,

$$\mathcal{L} \supset b_{ij}\Phi f_i F_j + c_{ij}\Phi F_i F_j + d_{ij}\phi f_i F_j + M_{ij} F_i F_j + \text{h.c.}\,, \tag{B.4}$$

   wheres the corresponding interactions are depicted in figure B.1.

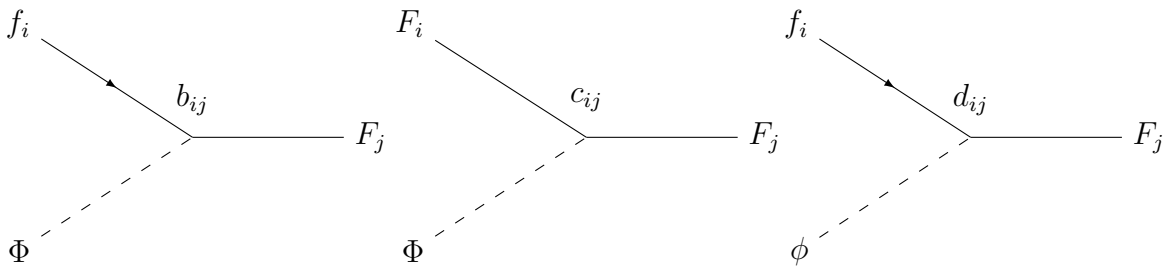

Figure B.1.: Tree-level interactions (B.4) that needed for the construction of "spaghetti"-interactions.

By using tree-level interaction, a chain of reactions can be constructed, that is referred to as "spaghetti"-interaction. The FN charge assignment to light and heavy fermions depends on the suppression factor one needs to achieve. The number of flavon interactions as well as the number of heavy fermion mediators is given by the difference in FN quantum numbers of the external fermions; this also corresponds to the exponent of the small FN parameter ϵ.

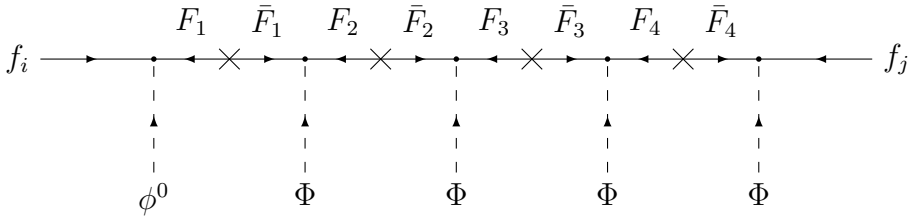

Figure B.2.: Interaction chain of the FN mechanism. To each fermion, an appropriate FN charge hast to be assigned, giving rise to a certain interaction "length".

2. Integrating out heavy fermions F_i
   Since the introduced heavy fermions are assumed to be non-propagating, we can easily integrate them out. To safely guarantee this, we have to be at an energy scale much lower than their mass scale $\Lambda \leq \Lambda_{FN}$. This gives rise to an effective dimension-4 operator that corresponds to the usual SM Yukawa interaction,

$$\mathcal{L}_{eff} \subset e_{ij} \left(\frac{\Phi}{\Lambda_{FN}}\right)^p f_i f_j \phi \,, \tag{B.5}$$

   where e_{ij} are new coefficient incorporating all former pre-factors and are usually assumed to be of $\mathcal{O}(1)$. Again, exponent p just on the light fermions' difference in FN charge $p \equiv Q_{FN}(f_i) - Q_{FN}(f_j)$. The corresponding effective interaction is given in figure B.3. As non-propagating DOFs, the heavy fermion are not relevant anymore, but lead to a suppression according to their mass scale Λ_{FN}.

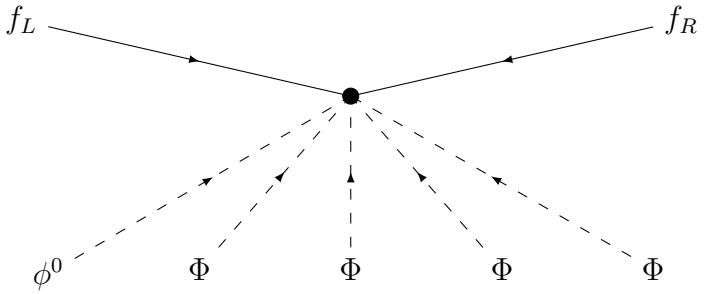

Figure B.3.: Effective scalar interaction in the FN mechanism. As the heavy fermion mass scale Λ_{FN} is much higher than the energy region of interest, they can safely be integrated out.

3. SSB of the FN symmetry: $\Phi \longrightarrow \langle\Phi\rangle$
   In the last step, the flavon field Φ acquires a non-zero VEV $\langle\Phi\rangle \neq 0$, which leads to the generation of usual SM Yukawa couplings suppressed by a small parameter, ϵ.

$$\mathcal{L}_{eff} \supset e_{ij} \left(\frac{\Phi}{\Lambda_{FN}}\right)^p f_i f_j \phi \equiv e_{ij}\, \epsilon^p\, f_i f_j \phi \tag{B.6}$$

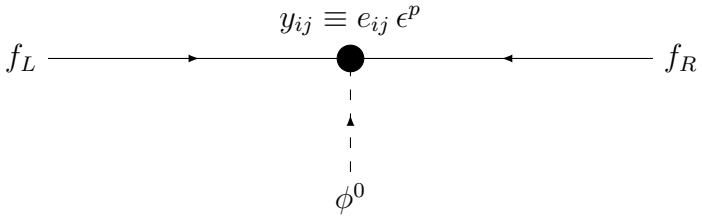

Figure B.4.: SM Yukawa interaction viewed from the FN perspective.

By appropriate choice of ϵ and FN charge assignment, a huge parameter space of possible Yukawa interactions can be spanned. Hence, couplings that are of $\mathcal{O}(1)$ at some fundamental scale, can now be suppressed by FN charge assignment to certain flavors, while the familiar SM Yukawa interaction is retained, see figure B.4.

C. Massive neutrino phenomenology

In this chapter, we summarize some outstanding points that we have met in the context of mass.

Symmetry of Majorana mass matrix

In the context of Majorana neutrino mixing, see section 2.2, we stated without proof that the Majorana mass matrix in (2.18) has to be symmetric. This shall now be proven by using fermionic anti-commutation and properties of the charge conjugation and switching to index notation. The prove is a simple one-line calculation:

$$\begin{aligned}\sum_{\alpha,\beta} \nu_L^{\alpha T} C^{-1} m_{\alpha\beta} \nu_L^{\beta} &= -\sum_{\alpha,\beta} \nu_L^{\beta T} m_{\beta\alpha} (C^{-1})^T \nu_L^{\alpha} = \sum_{\alpha,\beta} \nu_L^{\alpha T} C^{-1} m_{\beta\alpha} \nu_L^{\beta} \\ &= \sum_{\alpha,\beta} \nu_L^{\alpha T} C^{-1} m_{\alpha\beta}^T \nu_L^{\beta} \,.\end{aligned} \tag{C.1}$$

In the first step, we transposed the expression and had to applied fermionic anti-commutation, which gives an additional minus sign. As the charge conjugation operator exhibits $(C^{-1})^T = -C^{-1}$, this minus sign is again eliminated in the second step. The charge conjugation operator can be shifted to the left since the mass is just a usual number and we obtained the same structure as in the beginning. This becomes obvious by renaming the used indices $\alpha \leftrightarrows \beta$. Thus, we end up with

$$m_{\alpha\beta} = m_{\beta\alpha} \quad \Longleftrightarrow m = m^T \tag{C.2}$$

which proves the symmetry of the Majorana mass matrix.

BSM models incorporating massive neutrinos

In the section 2.3 and 4.2, we mentioned that the RH neutrino mass, which is needed for an successful type-I scenario, has to originate from some higher scale. In this context, we referred to the case of local $(B-L)$ breaking as option. The following table gives an overview of different possibilities to generate heavy Majorana masses, with their corresponding energy scale Λ.

		Symmetry	Energy scale Λ
(1)	$U(1)_{B-L}$	Local	> 1000 GeV
(2)	Left-right symmetry	Local	> 1000 GeV
(3)	$SO(10)$	Local	$10^4 - 10^{14}$ GeV
(4)	Horizontal symmetry	Local	$> 10^6$ GeV
(5)	Horizontal symmetry	Global	$> 10^{10}$ GeV
(6)	Peccei-Quinn symmetry	Global	$10^{10} - 10^{12}$ GeV
(7)	Lepton number	Global	no bound

Table C.1.: Classification of neutrino mass models according to the underlying symmetry and corresponding energy scale Λ [37].

Former oscillation data

The whole investigation of chapter 3, has been performed with an older data set [77]. To guarantee reproducibility, we list the applied best-fit values and corresponding uncertainty regions below. From the robustness study of section 3.5, we know that all result of chapter 3 are stable under small variations, i.e. more recent data sets like [8] or experimental fluctuations.

Observable	Units	Hierarchy	Best-fit value	$3\,\sigma$ confidence interval
δm^2	$\left[10^{-5}\,\mathrm{eV}^2\right]$	both	$+7.37$	$[+6.93, +7.97]$
Δm^2	$\left[10^{-3}\,\mathrm{eV}^2\right]$	NH IH	$+2.50$ -2.46	$[+2.37, +2.63]$ $[-2.33, -2.60]$
$\sin^2\theta_{12}$	$[10^{-1}]$	both	$+2.97$	$[+2.50, +3.54]$
$\sin^2\theta_{13}$	$[10^{-2}]$	NH IH	$+2.14$ $+2.18$	$[+1.85, +2.46]$ $[+1.86, +2.48]$
$\sin^2\theta_{23}$	$[10^{-1}]$	NH IH	$+4.37$ $+5.69$	$[+3.79, +6.16]$ $[+3.83, +6.37]$
δ	$[\pi]$	NH IH	$+1.35$ $+1.32$	$[+0.00, +2.00]$ $[+0.00, +2.00]$

Table C.2.: Best-fit values and $3\,\sigma$ confidence intervals for the five low-energy observables that are currently accessible in experiments and for the CP violating phase δ [77]. Due to the large uncertainty, δ can vary over its full range $[0, 2\pi)$.

Investigation of the neutrino mass hierarchy

In chapter 2, we mentioned that the current investigation of new neutrino parameters, i.e. the measurement of CP phases is limited due to the ambiguity in neutrino mass ordering. As the sign of the atmospheric mass-squared difference is unknown, we can construct two different mass orderings, which are illustrated in the following figure.

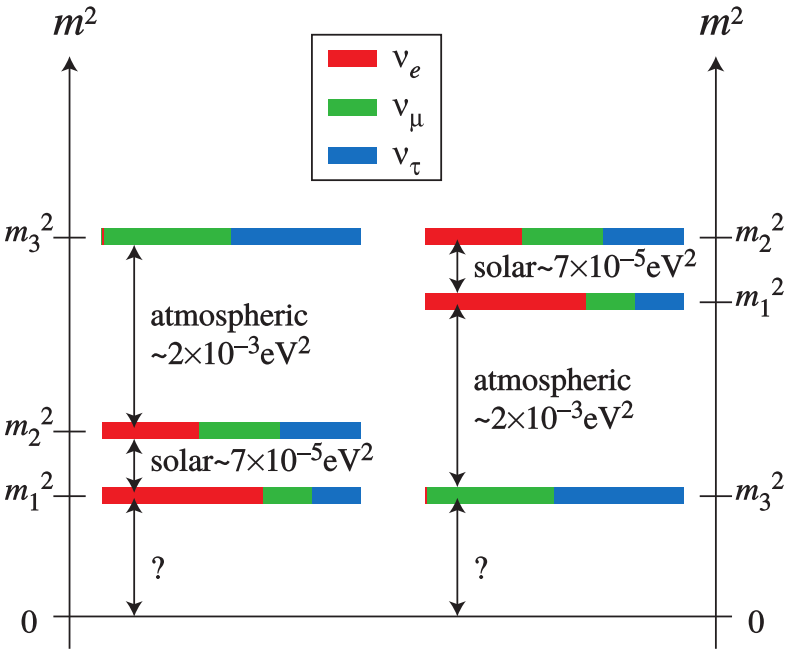

Figure C.1.: Possible neutrino mass hierarchies with their corresponding composition in flavor eigenstates. NH corresponds to the **right-hand side**, wheres IH refers to the **left-hand side**. The corresponding mass values are given via (2.35). Picture is taken from [137]

In addition, we discussed certain possibilities to resolve this problem and referred to future experiments. The table below shall give an overview of current and planned experiments listed according to their targeted timescale and sensitivity in measuring the neutrino mass hierarchy.

Experiment	Sensitivity	Approx. timescale
Noνa	1-3 σ	2020
T2K	1-3 σ	2020
PINGU	3-6 σ	2025
DUNE	3-6 σ	2030
Hyper-K	3-6 σ	2030
ORCA	3-6 σ	-
JUNO	$\sim 4\sigma$	2027
Cosmology	0-4σ	2027
ICAL	2-4σ	2030
RENO-50	$\sim 3\sigma$	-

Table C.3.: List of planned neutrino experiments with their prospects of investigating the neutrino mass hierarchy. The list is taken from [10].

Statement Of Authorship

I assure, that this work was written independently and no other than the quoted references and tools were used.

Heidelberg, 1st March, 2017 .....

Ich versichere, dass ich diese Arbeit selbstständig verfasst habe und keine anderen als die angegebenen Quellen und Hilfsmittel benutzt habe.

Heidelberg, den 1. März 2017 .....